UNIVERSITÀ DEGLI STUDI DI PADOVA

DEPARTMENT OF INDUSTRIAL ENGINEERING
Master Degree in Mechanical Engineering

Structural analysis and functional behaviour of Running Specific Prosthesis during in-vivo field tests and laboratory bench tests

Supervisor: **Prof. Nicola Petrone**
Co-supervisors: **Ing. Andrea G. Cutti**
T.O. Gianluca Migliore

Graduand: **Gianmario Foscan**
Student number: **1153778**

Academic years: 2017-2018

“Don't wait for luck
Dedicate yourself and you can find yourself”

The Script-Hall of Fame

SUMMARY

Carbon fiber Running Specific Prostheses (RSPs) emulate the spring like behavior of biological limbs during running, allowing people with amputation to compete at their maximum level of performance.

Amputations could be transtibial, if it is under the knee joint, or transfemoral, if it is above the knee. In both case, the stump of the athlete goes into the socket, and the prosthesis is fixed to it with different types of attachment, depends by the type of the prosthetic foot. In this study are evaluated two typologies of RSP, the J-shaped named Cheetah Xtreme (Össur) and the C-shaped, Runner 1E91 (ottobock).
The J-shaped is attached to the posterior segment of the socket by means two screws, on the contrary, the C-shaped is attached by means the pyramid attachment developed by ottobock. It is a pyramidal short beam fixed by four screws to the pyramid receiver, and by these screws is possible to perform the same adjustment to the inclination and orientation of the prosthetic foot.

The athletes involved in this study have unilateral amputation, that is interesting because their affected leg (AL) can be compared with the unaffected leg (UL). The first athlete has a transtibial amputation and run with the Cheetah prosthesis (J-shaped), the second one, is a transfemoral amputee, that wear a mechanical knee joint with one axis of rotation and run with the Runner prosthesis (C-shaped).

Figure 1: On Left: Cheetah RSP (J-shaped) for a transtibial amputee, on Right: Runner RSP (C-shaped) for a transfemoral amputee, with the mechanical knee.

The first step of the thesis was to design a measurement system that allow to measure the forces acting on the foot clamp of the athlete during running, without introducing external components. For this reason, a strain gauge system was applied to the prosthesis.
The in-vitro calibration was performed with a test bench designed for testing the prosthesis, for three type of RSPs, one J-shaped and two C-shaped, one category 3 and one cat.4. The category of the blade indicates the relative stiffness, bigger is the number and stiffer is the prosthetic foot.

The further step was to validate the system during in-vitro and in-vivo tests.
The in-vitro validation is performed again with the test bench, instead, for the in-vivo validation, data were collected with the SoMat acquisition system, carried in a backpack, while the athlete runs.
The data read by the SoMat refer to the Foot Reference System and for comparison with the forceplate data, it was necessary to rotate the frame into the Foot-Global Reference System, that is the Ground Reaction Forces Reference Frame. In this way it is possible to see how good the strain gauge acquisition system was, in relation to the loads collected by a single step on the ground.
Also, during in-vivo test, the datasets of the runs are used for an evaluation of the loads acting at the foot clamp of the prosthetic foot, in that way is possible to understand which forces are transmitted between the socket and the RSP. No one analyze this reference point yet.
Another comparison, that was possible to made, is between the step load of the affected leg (AL) with the unaffected leg (UL) for the transfemoral amputee.

On the test bench was performed a pilot drop test, for evaluate the energy dissipation on the prosthetic foot at different inclination between the fall axis and the ground. The angles were selected from a video analysis of the stance phase of the athletes runs, so that to replicate the same conditions.

INDEX

CHAPTER 1: INTRODUCTION

For many years, people are searching for a mechanical solution for amputees, with the aim of enabling the amputees to walk with two legs. Across the years, different solutions were thought, form the first peg leg to the actual Carbon Fibers Running Specific Prostheses.
The first prototype of prosthesis, the peg leg, was a wooden stick attached to a stump and tight, but it was focused only to connecting the stump with the ground and not on ergonomic aspects. It was uncomfortable for the amputees and it may cause chafing or muscle and bone aches.
Along the time, the designers tried to build prosthesis that resembles a human limb, that imitating a leg and even a foot, for hide the missing leg.

In the Figure 1.1 is possible to see the evolution of the prosthesis along the time, with their improvement compared to the older ones:

Figure 1.1: A mixture of simple function and mimesis of the human leg in different eras. (Ventura and Shvo, 2017) [1]

There are many prosthetic feet designed over time. The Federal Government's Artificial Limb program converted various designs into one standard manufactured production model: The Solid Ankle and Cushioned Heel (SACH) foot. In 1957 this model was approved for male amputees. The SACH foot has a simple design and gives amputees many foot and ankle functions that are required. Therefore, it is and will be a valuable product for patients. [2].

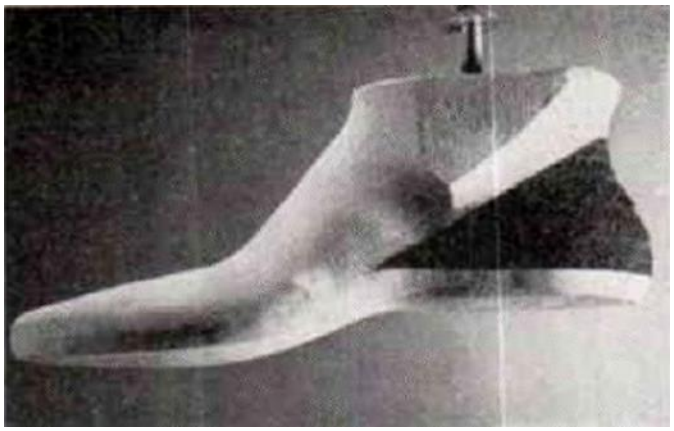

Figure 1.2: SACH Foot [2]

A special mention goes to the Canadian Terry Fox, which ran the Marathon of Hope in 1980, a cross-country run dedicated to raising awareness and money for cancer research. Fox, whose right leg had been amputated in 1977, performed this incredible feat using a prosthesis designed primarily for walking. His accomplishment inspired Canadians across the country as well as amputees and para-athletes around the world.
It also motivated researchers to develop prostheses better suited for running. Since 1980, developments in materials manufacturing and computer/bionic technology have led to more comfortable, stable and responsive prostheses, both for recreational and elite athletes. [3]

Figure 1.3: Terry Fox

Prosthetic foot designs and materials changed little for approximately 20-30 years after the invention of SACH foot (Ohio Willow Wood, Ohio, USA) in the late 1950s.
The big innovation and research improvements in the lower limb prostheses happened in the ‘80s, when new materials flooded the prosthetics industry. Carbon composite materials brought lightness, durability, and strength to the design of prosthetic feet, pylons, and sockets.

In 1984, Van Phillips, an American inventor of prostheses, created the "Flex-Foot®" made of carbon graphite. The innovative artificial foot allowed users to store and then return elastic energy during the ground-contact phase of gait. [4]

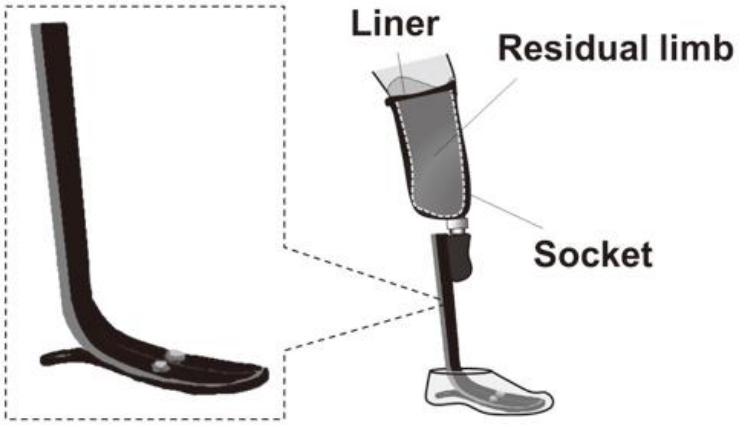

Figure 1.4: Schematic representation of "Flex-Foot®" and prosthetic components (socket and liner) with representation of a residual limb. The schema is based on transtibial (below-knee) amputees. (Hobara, 2014) [4]

That was the first Running Specific Prosthesis (RSP) used at the 1988 Paralympic Games. Four years later, the prosthetic heel was absent in some athlete's configuration, and this created the first running prosthesis.

The first specialized RSP was developed by eliminating the prosthetic heel from the Flex-Foot®, also, the stiffness configuration was altered with the layup sequence of carbon fibres while still maintaining the J-shape outline of the carbon forefoot. That was called Flex Sprinter I, manufactured by Össur (Reykjavik, Iceland), and nowadays there are several different sprint foot designs available, all with a similar basic shape (Figure 5).

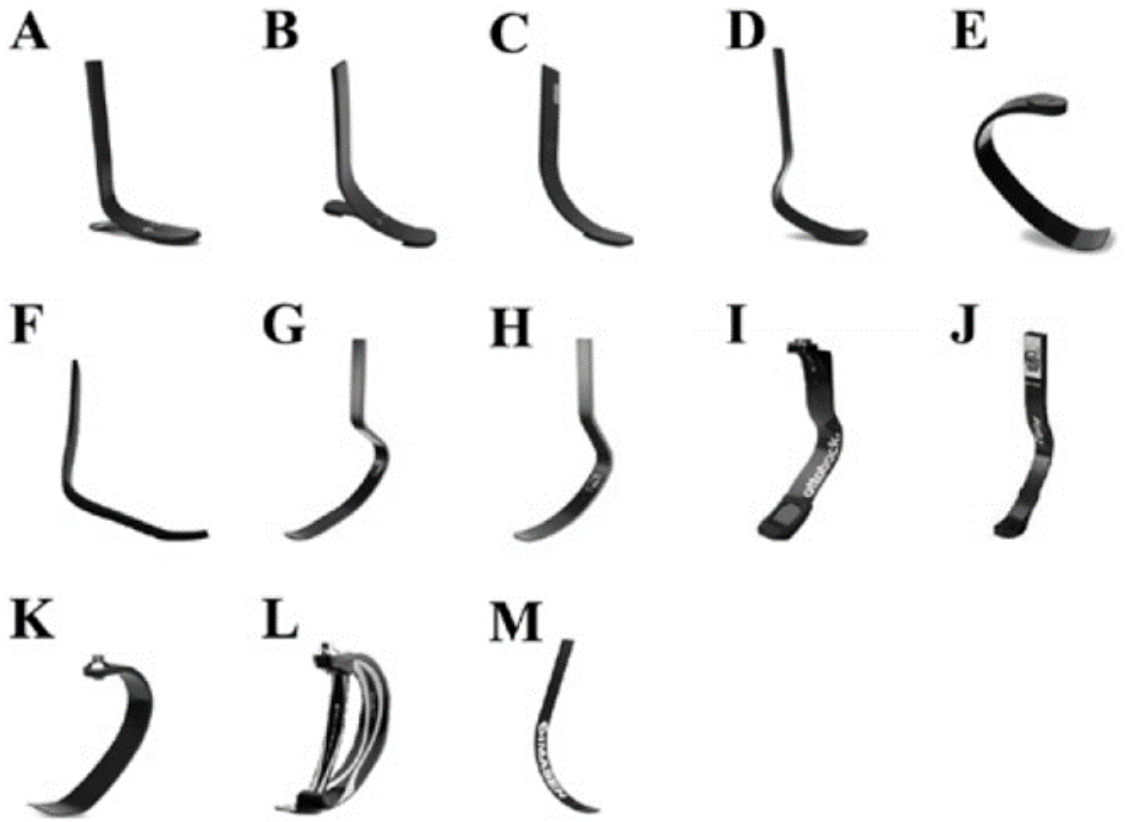

Figure 1.5: A: Flex-Foot® (Modular III; Össur), B: Flex-Sprint II (Össur), C: Flex-Sprint I (Össur), D: Flex-Sprint III® (Cheetah; Össur), E: Flex-RunTM (Össur), F: Symes-Sprint (Össur), G: Cheetah Xtreme®, H: Cheetah Xtend®, I:1E90 (Sprinter, Ottobock), J: 1C2 (C-Sprint®), K: Nitro (Freedom Innovation), L: CatapultTM (Freedom Innovation), M: SP1100 (KATANA, IMASEN Engineering Corporation), N: Rabbit (IMASEN Engineering Corporation). (Hobara, 2014) [4]

For the last 15 years, technical advances in prostheses have been a main factor in the increased performance of athletes with lower-limb amputations. The use of materials such as carbon fibres, titanium, and graphite has provided added strength and energy storage capabilities to prostheses while decreasing the weight of prosthetic components. Today, carbon fibres prostheses are most popular in elite running and jumping events.

1.1: Biomechanics of Running with RSPs

Paralympic athletes have achieved remarkable sprint-running performances using RSPs, typically with a J-shape and made of carbon fibre. These prostheses are attached to a socket, which surrounds the residual lower limb of an amputee.
Recent studies have shown that athletes with transtibial amputations using an RSP exert smaller vertical ground reaction forces and have prolonged contact times in their affected leg (AL) compared with their unaffected leg (UL) and to the biological legs of non-amputees [5, 6].
These differences suggest that there is a difference between the stiffness of the non-amputee leg and the RSP during running, moreover there aren't studies that analyse the spring properties of the prosthesis during its use.

Running is a bouncing gait that is well-characterized by a spring-mass model [7-11], and the simplest spring-mass model comprises a massless linear leg spring attached to a mass point that represent the centre of mass (COM) of the entire body. When hopping, the stiffness of the spring leg is an important parameter for determining COM mechanics [12] (Figure 1.1.1).

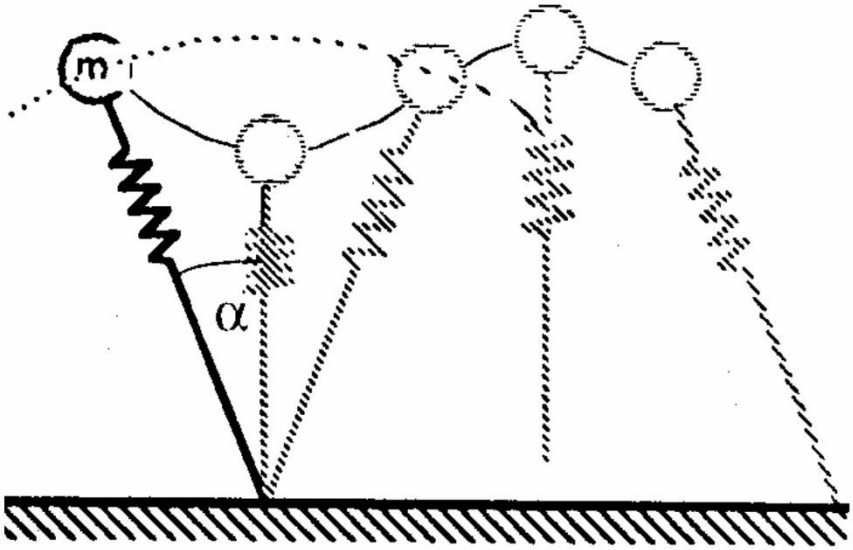

Figure 1.1.1: Schematization of the running with the spring mass-model. (Blickhan, 1989)

In this model the leg stiffness k_{leg} is equals the quotient of the peak vertical force ($vGRF_{peak}$) and the change in leg length (Δl) from touchdown to mid-stance (Figure 7):

$$k_{leg} = \frac{vGRF_{peak}}{\Delta l}$$

Maximum displacement of the virtual leg spring (ΔL) is calculated following Farley et al. [10] using the length of the leg spring at touch-down, which is estimated to be equal to the standing leg length (L_0), and half of the angle swept by the leg spring while the foot was on the ground (θ):

$$\Delta L = \Delta y + L_0\,(1 - \cos\theta)$$

The vertical motion of the system during the ground contact phase can be describe with an effective vertical stiffness k_{vert}. This is calculated from the ratio between the peak vertical force ($vGRF_{peak}$) and the peak of the vertical displacement of the center of mass during the stance phase (Δy) (Figure 1.1.2):

$$k_{vert} = \frac{vGRF_{peak}}{\Delta y}$$

Vertical COM displacement is calculated by twice integrating the COM acceleration with respect to time [13].

In order to account for differences in the athletes' size, k_{vert} and k_{leg} were made dimensionless by multiplying each by the ratio of L_0 and body weight (BW), forming K_{vert} and K_{leg} respectively:

$$K_{vert} = k_{vert} * \left(\frac{L_0}{BW}\right)$$

$$K_{leg} = k_{leg} * \left(\frac{L_0}{BW}\right)$$

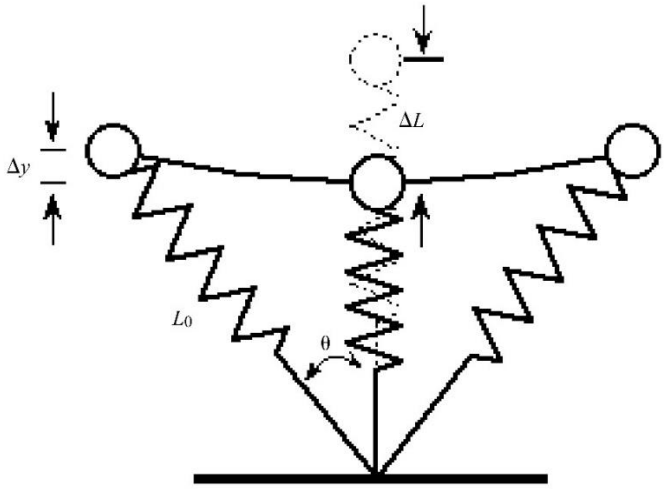

Figure 1.1.2: A schematic of a simple spring–mass model used to characterize the overall biomechanics of bouncing gaits such as running and sprinting.

Upon ground contact, the leg spring compresses and stores elastic energy until mid-stance, and then returns mechanical energy from mid-stance through the end of ground contact [14]. In this model, the leg spring is completely elastic, however the structures of a biological leg are viscoelastic and therefore only a portion of the stored potential elastic energy is returned (due to hysteresis). The spring-like action of the leg conserves a portion of the runner's mechanical energy, theoretically mitigating the additional muscular force and mechanical energy input necessary to maintain running speed [14, 15]. The magnitude of the stored and returned mechanical energy is inversely related to leg stiffness (resistance to compression) and is influenced by the magnitude and orientation of the external force vector acting on the leg.

1.2: Comparison between AL and UL during running

RSPs are made in carbon fibre and are putted in series with the residual limbs, attached to the socket. This material allows to the prosthesis to mimic the mechanical energy storage and return of tendons during ground contact, but, conversely biological ankles, RSP can't generate mechanical power and the energy that is return goes only from 63% to 95%. Also, the prosthesis stiffness can't be varied during running [16, 17, 18].
Instead, biological ankles generate mechanical power through muscles (elastic structures) and this allow to have a 241% of energy return during running at 2.8 [m/s] [16].

Research has shown that the ability to generate vertical force, during the ground contact, limits to speeds in humans with biological limbs.
The performance of the athlete Oscar Pistorius, a bilateral trans-tibial amputee, on the 400 [m] and subsequent scientific studies have stimulated controversy about the use of these passive-elastic RSPs [6]. At the top of the speed, he had 22% lower stance average vertical GRF than performance-matched intact sprinters [6]. In Grabowski studies, with amputee and non-amputee athletes, was found that the F_{avg} was approximately 9% less for the AL compared with the UL across a range of speeds, including top speed and at faster speeds. This data suggests that the RSP or muscle weakness/impairment due to the prosthesis, limit force production rather than some other physiological factor.
Across increment of speeds, subjects increased step frequency in both AL and UL, but the increase was bigger for the non-amputees. This result could seem counterintuitive because the AL had lower F_{avg} than the UL and nearly the same contact time, implying a softer AL vertical spring stiffness. A softer spring would produce a lower take-off velocity, thus one would expect a shorter aerial time and faster step frequency if the landing and take-off height were the same. The studies reveal that the non-amputee's take-off velocity are faster than the amputee's ones, so the take-off height from the UL must have been lower than the landing height of the AL.
Instead, concerning about time of swing phase, there weren't significantly differences between UL and AL at any speeds, but athletes swung both legs more quickly at faster speeds [5].

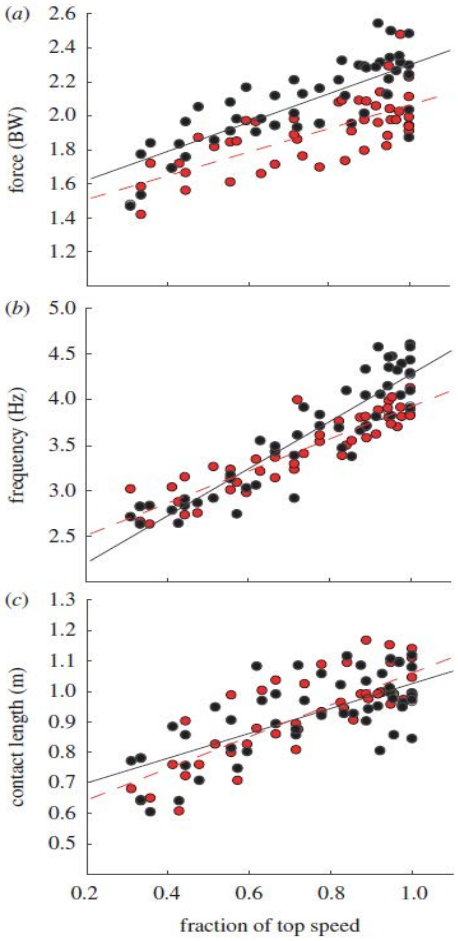

Figure 1.2.1: Biomechanical variables across speed for the UL and AL. Lines are linear regressions for the AL (dashed line) and UL (solid line). R2. 0.55 for each leg's (a) Favg—stance average vertical GRF, (b) step f—step frequency and (c) Lc—contact length (filled black circle, UL; filled red circle, AL). [5]

During running, athletes with transtibial amputation generate a peak of ground reaction force with their affected leg that is 2.1/3.3 times body weight (BW) at speeds of 2.5 to 10.8 [m/s]. Moreover, compared with their UL, this peak is always lower, as mention before in the Grabowski's studies [5] (Figure 1.2.2). The peak typically occurs during the midstance phase and it is oriented vertically. Also, in the same instant, the proximal end of the stance leg's RSP is rotated forward in the sagittal plane compared to GRF's vector.

For the longitudinal forces, the data demonstrated the significantly earlier zero fore-aft shear on prosthetic limbs than intact limbs, indicating that prosthetic limbs had a different ratio of time spent generating braking impulses versus propulsive impulses compared to intact limbs. Therefore, the results shown in Figure 9 indicate that regardless of the amputation levels, amputee runners generate less braking and equivalent propulsive impulses in their prosthetic limbs wearing running-specific prostheses to the intact limbs during running.

The medial and lateral GRFs were not reported in most studies about running and sprinting due to lower magnitude of forces and larger variability compared to the other components

of forces. In the Makimoto's study, there were no significant differences in medial and lateral impulses between the limbs.

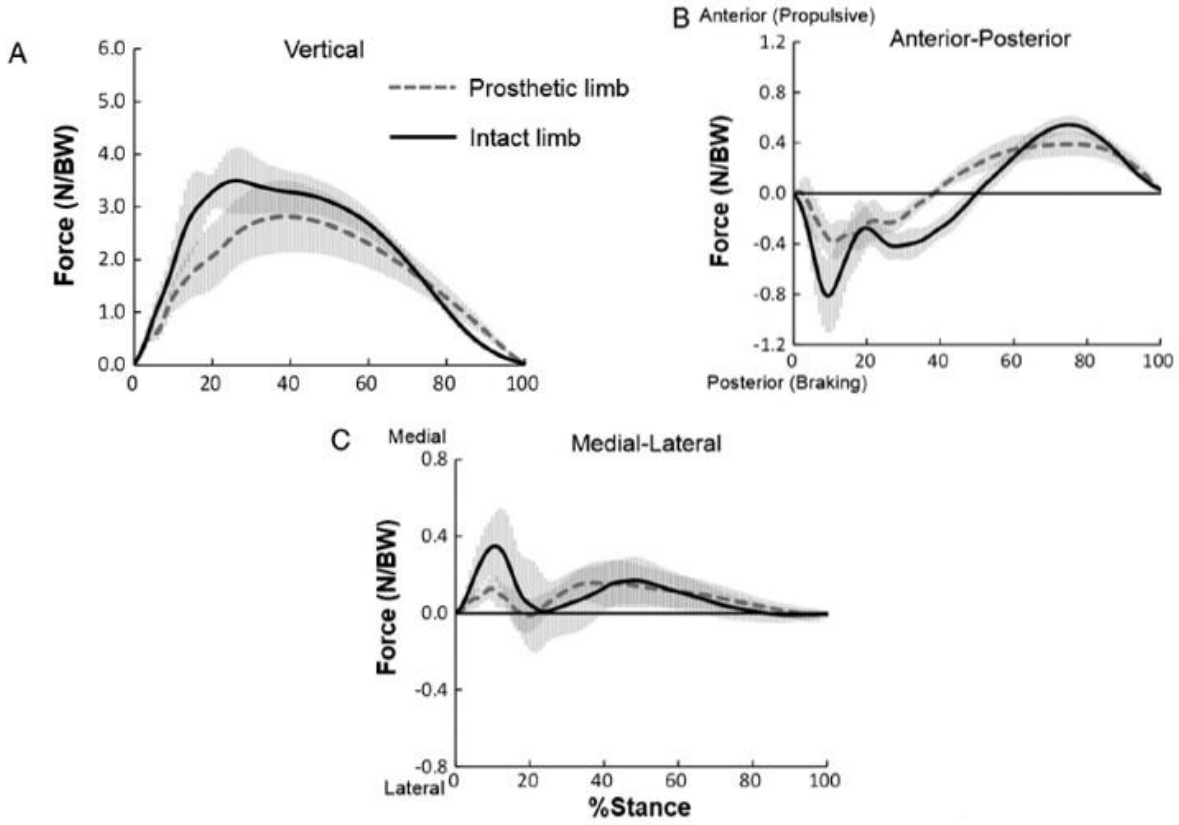

Figure 1.2.2: GRFs. Average time-course profiles of ground reaction forces (GRFs) of prosthetic (red line) and intact (blue line) limbs during maximal sprinting recorded from 9 participants. Shaded area indicates standard deviations. Positive values indicate the vertical (A) and anterior (B)component of the GRFs, respectively. GRFs are normalized with respect to the athlete's weight force, BW. (Makimoto et al., 2017) [19]

1.3: Test bench's state of art

1.3.1: Beck, Taboga and Grabowski, 2016. Characterizing the Mechanical Properties of Running-Specific Prostheses [20]

In the research of Beck, Taboga and Grabowski, 2016 [20] the objective was to determine the mechanical stiffness of the prostheses and the hysteresis in the condition of maximum GRF, varying the travel speed and the height of the prosthesis.
Before starting with the test bench analysis, they measured GRFs form 11 athletes with transtibial amputations, while they ran on a force-measuring treadmill at two different speeds of 3 and 6 [m/s] and with their own prosthesis. Also, the angle β was measured using a motion capture system, it was the angle between the longitudinal axis and the direction of the peak GRF vector in the sagittal plane.
The data's angles that were measured were between 10 and 25°, depending on the speed of running and the type of prosthesis that was used, while the GRF peak is 2.5 to 2.8 times the BW.

To obtain the stiffness curve at different beta angles, a machine testing material was used as test bench for the purpose. The upper limits, concerning the peak of GRFs, for the test were about 3 times the body weight to simulate a 3 [m/s] running and about 3.5 times the BW to simulate 6 [m/s] running [21] (Figure 1.3.1.1).

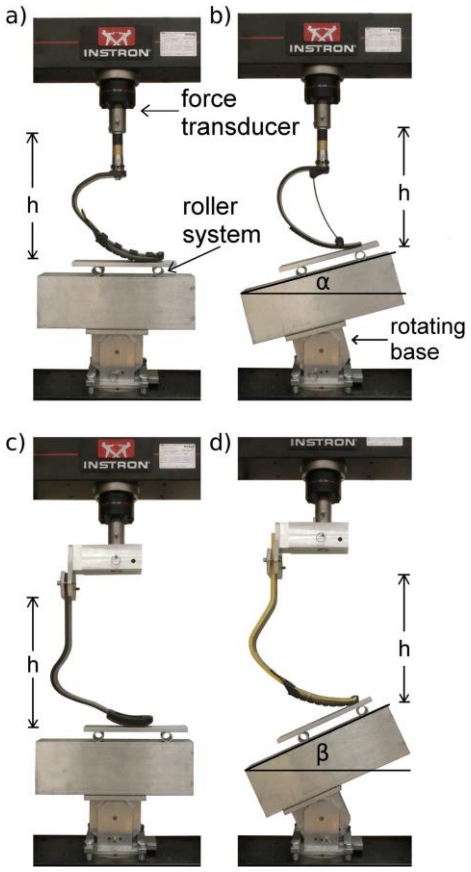

Figure 1.3.1.1: Test bench of Beck, Taboga and Grabowski, 2016 [20]

To minimized shearing forces, a low-friction roller system was used beneath each RSP, in that way the anterior and posterior translation was allowed, while the beta angle was maintained constant during the application of the force, justifying this choice by referring to ISO 10328 2016 [24], which doesn't refer to RSPs.

A very important step, for the evaluation of the energy storage by the RSP during running, is analyze the phase of ground contact that goes from midstance to toe off and it is fundamental for the optimization of the athlete's performance. Also, the whole stance phase evaluation, between heel strike and midstance is essential for see how the prosthesis work under load.

Beck, Taboga and Grabowski suggest that "it is possible that the inverse relationship between affected leg stiffness and running speed found in McGowan et al. [21] can be attributed to decreased prosthetic stiffness via increased angles between the resultant GRF vectors and RSPs at faster speeds" and also "the discrepancies with different research suggest that prosthetic stiffness testing procedures should be standardized".

Putting a plate able to slide on the plane of the test bench was an expedient to generate always a GRF that was orthogonal to the ground, because the shear force was nullify due to the roller system.
But that solution didn't replicate the real condition in which the athletes have ran, because during running, between the sole and the ground there is always friction, so, the cutting force aren't never null, except for the point where the longitudinal force change from breaking to pushing during the midstance phase. In conclusion, this method faithfully reproduces the condition of stress.

1.3.2: Dyer, Sewell and Noroozi, 2014. An Investigation into the Measurement and Prediction of Mechanical Stiffness of Lower Limb Prostheses Used for Running. [22]

In this type of bench test, the prostheses are fixed upside down into a Testometric strength testing machine (Testometric Company Ltd., Lancashire, UK) by means an aluminium fixing block that aligned the prosthesis shank at 60° angle from a horizontal plane. This angle is selected for having a centreline that would run from the distal end of the prosthesis through the midpoint of the fixing bolts that are normally attached to the socket.
For the experiment, two Elite Blade were used, the ESRP's_Chas A Blatchford & Sons Ltd., Basingstoke, UK (that stand for Energy Storage and Return Prostheses).

Both prostheses were loaded from 1500 to 2000 [N] in compression for 10 times at a rate of 50 [mm/min].

Figure 1.3.2.1: Testing machine and ESRP prosthesis (upside down)

Three different configurations for the fixed extremity were though, and they are as follow:

1) *FDE*: Fixed at the prostheses distal end. The distal end of the prosthesis butts against a ledge that prevents it from sliding when compressed.
2) *PSF*: Partial slide then fixed. The prosthesis can slide 28 mm before the distal end butts against a ledge preventing further slide when compressed.
3) *UDE*: Unfixed distal end. The distal end of the prosthesis is unfixed and can slide freely under the load cell platen when compressed.

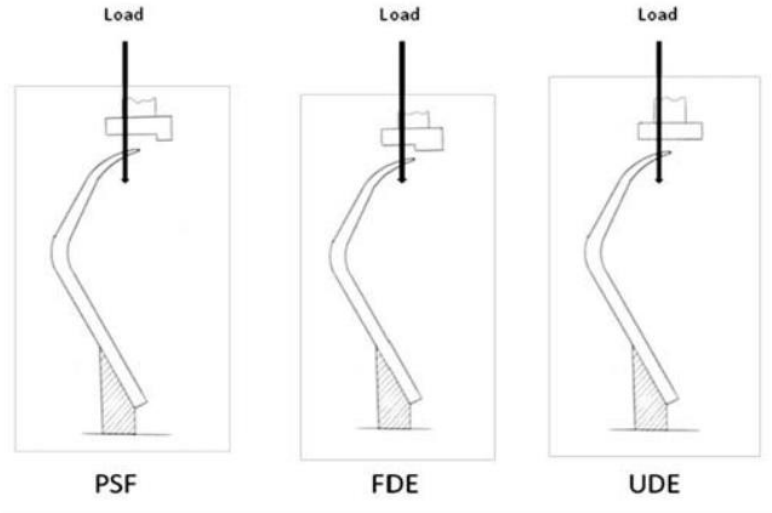

Figure 2: Configurations of the fixed extremity

In this test, it is investigated to see if a limited subset of load and deflection data could be used to accurately predict the stiffness response of higher loads. This would be compared with an additional load and resultant deflection test to the targeted higher load.
A successful method of prediction would allow prosthesis stiffness to be calculated for greater loads than those investigated in this study or for different running events based on a smaller subset of data.

The experiments for the prosthesis 1 are shown in the figure below:

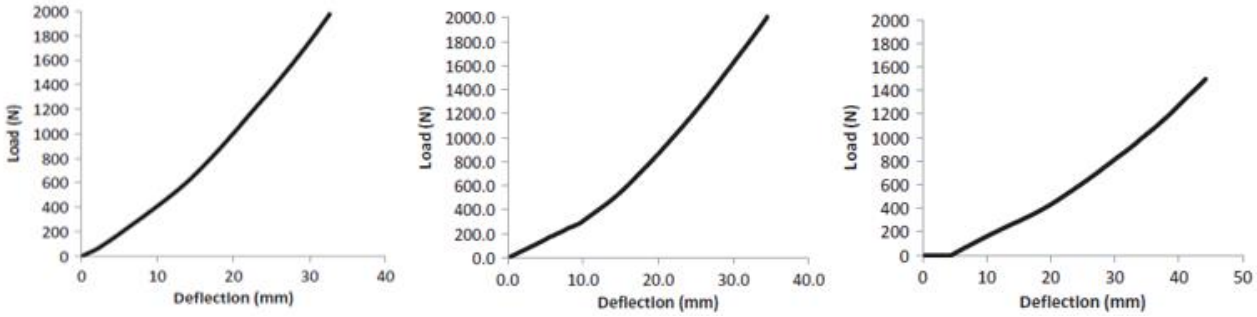

Figure 3: First graph: Prosthesis 1 FDE test; Second graph: Prosthesis 1 PSF test; Third graph: Prosthesis 1 UDE test. Dyer, Sewell and Noroozi, 2014 [22]

The FDE method demonstrated the highest recorded average stiffness, instead the UDE method highlights a more inferior recorded average stiffness. However, in this specific case, the distal end is not fixed meaning the prosthesis is constantly slipping or "arching through" as it is compressed. The recorded deflection is therefore a relative rather than a true deflection. In addition, due to the controlled slippage, the prostheses total length is effectively shortening as it is being compressed. Due to the amount of bend evident, it was decided for safety reasons to cease loading at 1500 N.

With the other prosthesis, number 2, it was used to ascertain if a predictive stiffness can be generated from a smaller load and deflection data set, than stops at a lesser amount a peak load, in this case 2000 [N]. The stiffness value at 3500 [N] were calculated with a prediction from the previous data, by applying both a 2nd order polynomial trend line and a linear trend line to the final 450 [N] "linear like" sample of section 3's data.
The mechanical stiffness was recalculated and then compared to new actual loading cycles of prosthesis 2 performed up to 3500 N of load. This data can be compared in table 1.3.2.1:

Data Set	Sample	Stiffness (N/mm)
st Experiment FDE test	Average stiffness of 0–1,950 N sample	39
	Actual stiffness at 1,950 N loading	48
2nd Experiment FDE test	Average stiffness of 0–1,950 N sample	37
	Actual stiffness at 1,950 N loading	45
	Actual stiffness at 3,500 N loading	53
Predictive stiffness @3500N	2nd order polynomial trend line	55
	1,500–1,950 N loading linear trend line	49

Table 1.3.2.1: Prosthesis 2—FDE test 3,500 N loading and prediction. Dyer, Sewell and Noroozi, 2014 [22]

In conclusion, both prostheses, 1 and 2, produced different levels of stiffness to each other. This only highlight how composite manufacture can be altered by changing parameters such as cloth lay-up, fiber orientation or resin application to change the mechanical properties of a prosthesis, despite looking identical.
The highest recorded stiffness with both prostheses 1 and 2 occurred when using the FDE method. This is likely due to both the UDE and PSF methods having controlled slippage of the distal end causing a relative rather than an actual displacement to be recorded by the loading machine.
The FDE method is recommended for use in the future because its stiffness was both higher than the PSF method coupled with the knowledge that its distal end was fixed and therefore likely a more accurate representation of mechanical performance.
It could be argued however, that measuring stiffness by fixing the prosthesis at the distal end is not representative of it in actual use as the ground reaction strike point will likely not be at the absolute distal end. However, because this strike point would be different between all runners, an alternative approach is to identify a standardized point along the prosthesis length that correlates to the strike point of the human foot.

For the prediction of the stiffness response of higher loads, starting from lower loads, the initial 1950 N maximum load was increased by 45% to 3500 N (or roughly 4.4 times the bodyweight of 80 kg sprinter). The 2nd order polynomial trend line of the whole trace slightly overestimated the 3,500 N load stiffness. It is felt that this is because the latter section of the graph becomes increasingly linear. Instead, when taking the upper, more linear section of the load deflection graph and then extending it to a loading of 3500 N, the obtained stiffness from the mechanical testing and corroborated data was 45 N/mm and 48 N/mm, respectively. The predicted performance was a stiffness of 49 N/mm that is much closer to the actual performance.

The best method would be to take the highest load and deflection data graph trace available and then apply a linear line to that aspect to predict higher load stiffness.

1.3.3: Nishikawa, Hobara, 2018. Mechanical stiffness of running-specific prostheses in consideration of clamped position. [23]

In this experiment the prosthesis was mounted into a two sets of steel jigs, which could change the clamped condition of the prosthesis. In Figure 1.3.3.1 is shown the composition of the testing machine.

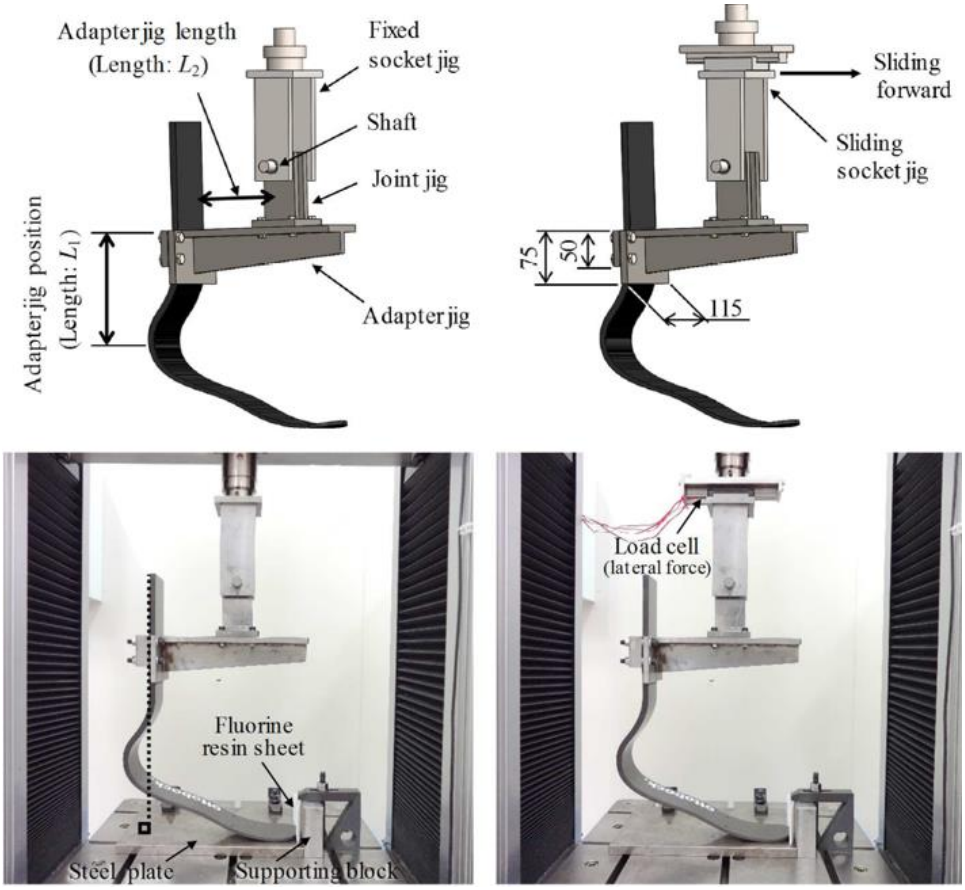

Figure 1.3.3.1: Composition of testing jigs. To the left: fixed socket jig type. To the right: sliding socket jig type. Nishikawa, Hobara, 2018 [23]

There are two different configurations of the testing bench, one is completely fixed, the other one has a sliding socket jigs, that could only slide forward.
The jigs of the machine are extremely rigid as compared with the prosthesis, therefore, the deformation of the jigs themselves was neglected in comparison with the test result.

Fifteen testing conditions were employed in this study. As shown in Figure 1.3.3.1, the length L1 from the top of the calf part to the adapter jig position was set at 205, 255, and 305 mm. These are the same lengths as those from the shank edge to the adapter jig positions of 100, 50, and 0 mm, respectively. The adapter jig length L2 from the prosthesis to the joint jig was set at 75, 100, 125, 150, and 175 mm. Hereafter, the clamped condition is written as L1-L2 (for example, in the case of L1 = 205 mm and L2 = 75 mm, the clamped condition is denoted as 205-75).
L1 and L2 are based on physical characteristic and running performance of the athletes, so

both the parameters do not have a standard length. In this study, L1 was assumed to be longest possible (from 205 to 305 [mm]), instead L2 was set from 75 to 175 [mm] to clarify the influence of L2 on mechanical stiffness during running.

The prosthesis was vertically compressed using a material testing machine (AutoGraph AG-100kNX; Shimadzu co.). The crosshead speed was 100 mm/min. The prosthesis shank was aligned at a 90 ° angle from the horizontal table of the testing machine. The prosthesis toe contacted the supporting block with a fluorine resin sheet. Immediately after loading, the prosthesis toe separated from this block; therefore, the supporting block and the fluorine resin sheet did not influence the test results. The prosthesis bottom surface contacted a steel plate in a line. The surface of the steel plate without surface treatment was smooth.

The prosthesis was loaded in compression for three separate times up to a maximum load of 2500 N; this value was chosen as this was approximately four times the bodyweight of the intended user for the prosthesis's specification. Under the compressive load of 2500 N, the prosthesis bottom surface contacted the steel plate in a line as shown in Figure 1.3.3.2, left image. However, the compression test stopped when the prosthesis slipped backward or slid forward.

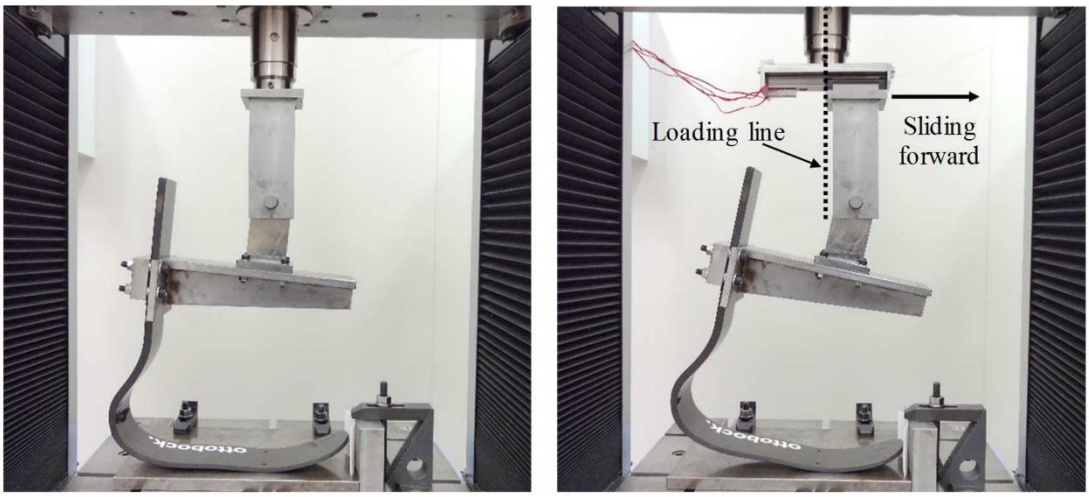

Figure 1.3.3.2: Images of situations after compression tests. To the left: fixed socket jig type. To the right: sliding socket jig type. Nishikawa, Hobara, 2018 [23]

Results and discussions:

For the load-deflection relations, for the case of fixed jigs, the results are plotted in the diagram below (Figure 1.3.3.3):

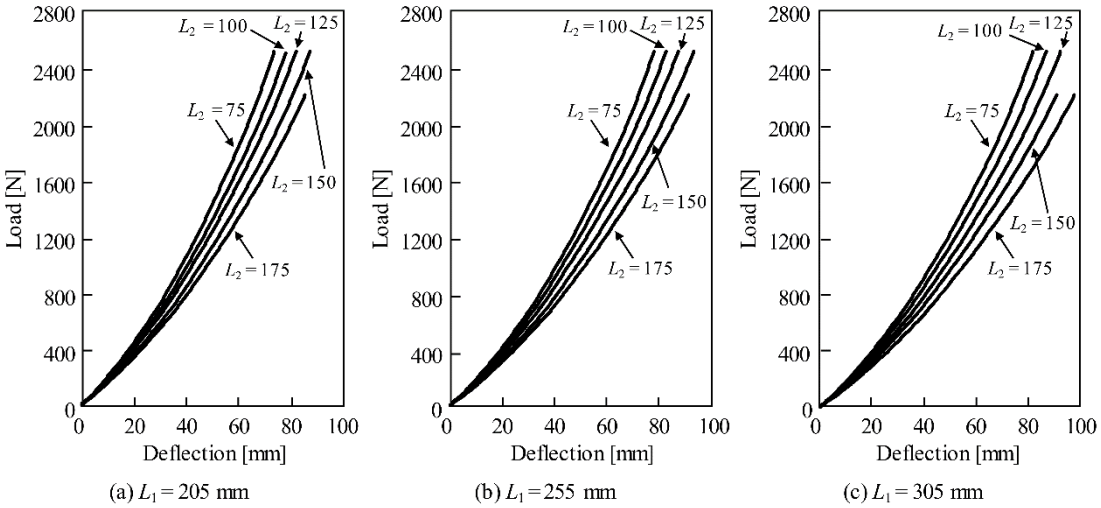

Figure 1.3.3.3: Typical load-deflection diagrams (using fixed socket jig). Nishikawa, Hobara, 2018 [23]

All load and deflection relations were non-linear; this tendency has also been witnessed in other studies [21,23]. This may be due to a combination of the tapered thickness of the toe region and the change in prosthesis length with the movement of the contact line. The mechanical stiffness of the prosthesis is defined as load divided by deflection. In consideration of this definition, as the applied load increased, mechanical stiffness increased independently of the clamped condition. In comparison, at the same load, the stiffness increased with decreasing adapter jig length. Unlike the previous studies [21,23], the testing jigs in the present study applied both vertical load and moment to the prosthesis. Therefore, the moment and deflection decreased with decreasing adapter jig length, leading to higher mechanical stiffness under the same load.

In Figure 1.3.3.4, instead, are shown the typical deflection diagrams in the case of using the sliding socket jig:

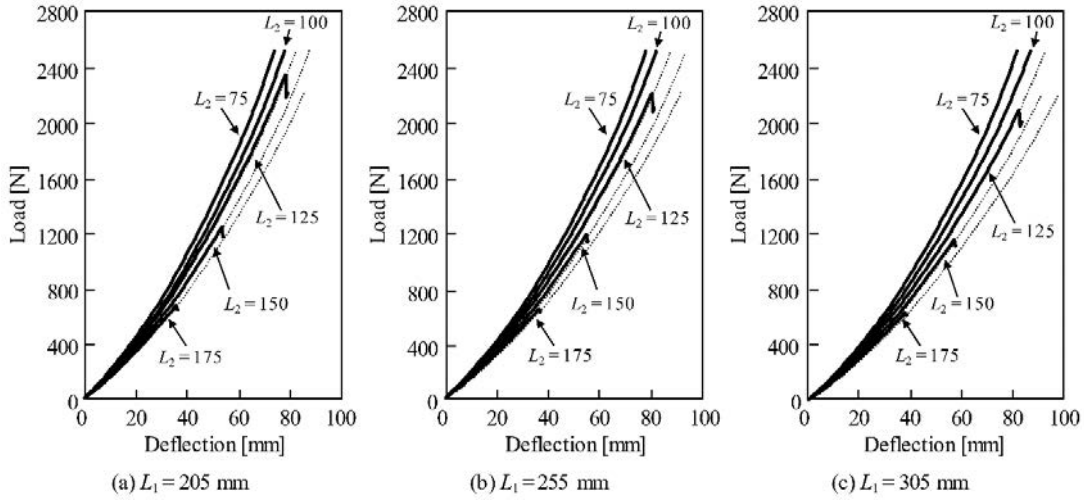

Figure 4: Typical load-deflection diagrams (using sliding socket jig). Nishikawa, Hobara, 2018 [23]

In this case, the prosthesis was slid forward at the maximum load for the shorten lengths of L2, but for the bigger value, it was slid forward at smaller force values.

During the test, was also applied, after loading and to the prosthesis shank, a backward lateral force, acting in the opposite direction to that of RSP. After the backward lateral force reached the peak, the forward lateral force was generated, and it was a propulsive type of force. When the backward lateral force decreased and only the forward lateral force was applied to the shank, the prosthesis was pushed out forward. This means that the minimum necessary vertical load to effectively propel the RSP exists.

For the clamped condition it was studied also the relation between the inclined angle of the shank and the vertical deflection of the prosthesis. It was found that, except for the clamped condition 205-75 (L1-L2), the inclined angle was quite proportional to the deflection in all cases. In the case of 205-75, with an increasing of the vertical load, also the inclined angle increase, but with a small amount in relation with the other conditions (Figure 1.3.3.5).

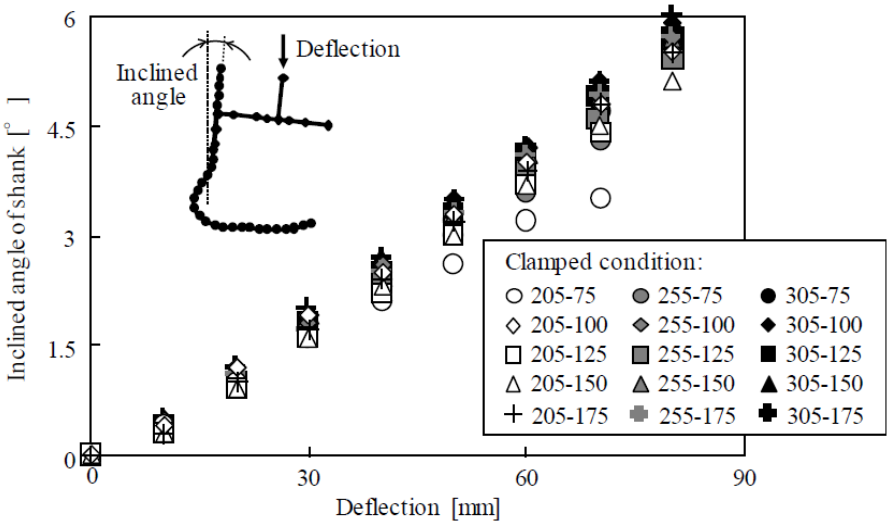

Figure 5: Relations between deflection and inclined angle of shank. Nishikawa, Hobara, 2018 [23]

Figure 1.3.3.6 shows fifteen load-deflection diagrams under all clamped conditions using the fixed socket jig. Each load-deflection behavior corresponded under the certain clamped conditions (for example, 205- 125, 255-100, and 305-75). According to the interaction of the adapter jig position and length, fifteen load-deflection diagrams were classified into seven tendencies.

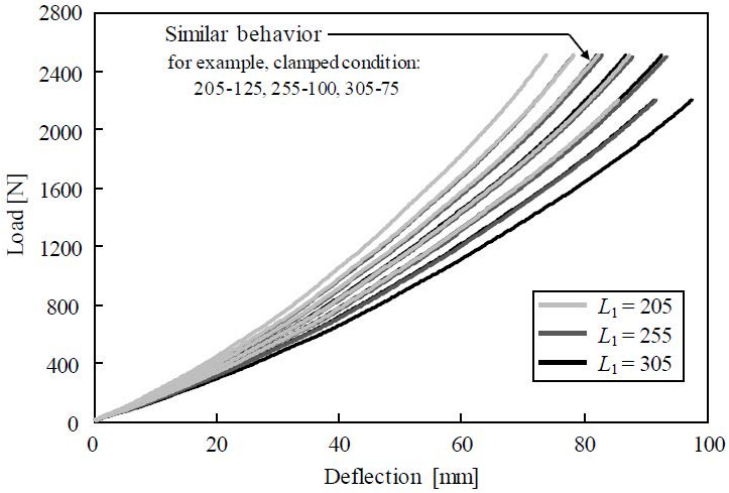

Figure 1.3.3.6: Fifteen load-deflection diagrams classified into seven tendencies (using fixed socket jig). Nishikawa, Hobara, 2018 [23]

Also, for the positional parameter, which is define as the product of L1 and L2, each value corresponded under a certain clamped condition (for example, 205-125, 255-100, and 305-75). The seven classified tendencies of the positional parameter were same as those shown in the load-deflection diagrams (Figure 1.3.3.7).

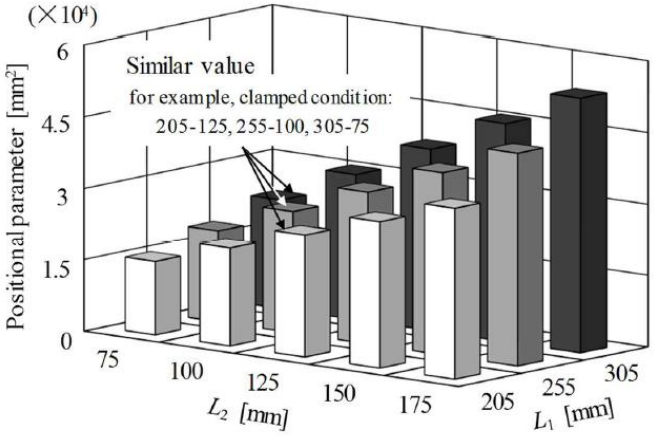

Figure 1.3.3.7: Relations among L1, L2 and position parameter. Nishikawa, Hobara, 2018 [23]

Figure 1.3.3.8 shows the relations among mechanical stiffness, applied load, and the positional parameter. The mechanical stiffness was calculated as the average load divided by average deflection in the load range of ± 25 N. As for these relations, it can guide the athletes with lower extremity amputations in selecting the RSPs with the most suitable mechanical stiffness in consideration of their clamped condition.

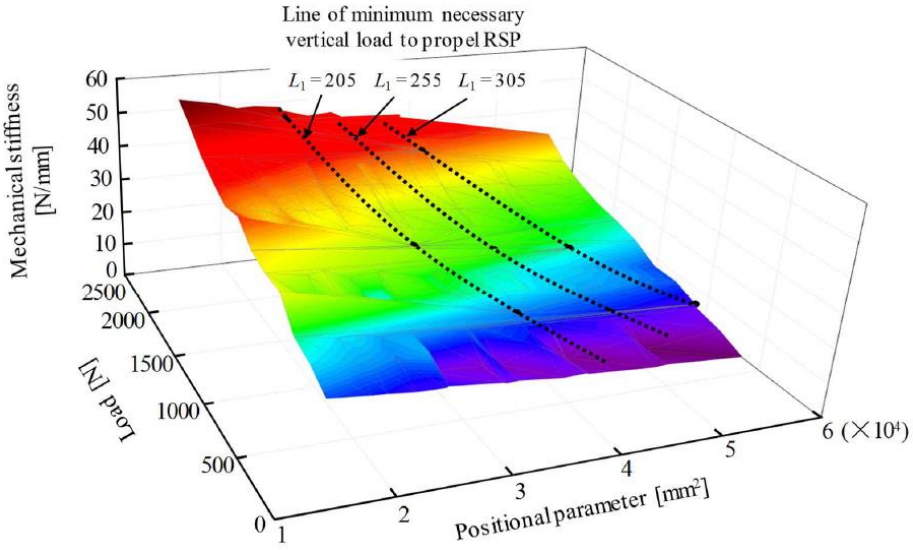

Figure 1.3.3.8: Relations among mechanical stiffness, applied load, and positional parameter. Nishikawa, Hobara, 2018 [23]

In this study, mechanical stiffness of RSP was evaluated under fifteen clamped conditions by changing the adapter jig position and length, the results are summarized as follows:

1. Immediately after loading, the backward lateral force was applied to the prosthesis shank, and then, the forward lateral force was generated in continuing loading. It is also possible to say that there was a minimum necessary vertical load to effectively propel the RSP.
2. All load-deflection relations were non-linear. The mechanical stiffness increased with increasing applied load and decreasing adapter jig length.
3. According to the interaction of the adapter jig position and length, fifteen load-deflection diagrams were classified into seven tendencies. From the observation results of the deformation behavior, the product of the adapter jig position and length was defined as positional parameter, which quantitatively indicated clamped condition. Consequently, the evaluation method of mechanical stiffness correlated with the applied load and positional parameter was proposed. [23]

1.3.4: Gianfabio Costa, Design and construction of a multichannel bench test for running specific prostheses, 2018 [25]

The aim of the test bench was to determine the mechanical stiffness of RSPs, applying a known vertical force and measuring the corresponding reaction forces. It was needed that the test bench had a rigidity of, at least, one order of magnitude higher than the prosthesis, otherwise the measurements will be invalidated. So, the first requirement was the stiffness of the bench, correlated with simplicity of construction and light weight.
The test bench is made of two slides, one on which the prosthesis is fixed and the other one carries the ground, where prosthesis hits. Considering that the speeds involved can be high, the two slides must be light, in order to minimize the inertial forces.
This bench is the same used for this thesis.

Video analysis of running with RSP and concept of test bench

Before design the test bench, it was first necessary to understand how the RSP works during running. For this reason, it was made a video analysis of an athlete with transfemoral amputation, from a recent article (Makimoto et al., 2017) [39].
From the video was analyze different phase of the run, as 0, 20%, 40%, 60, 80 and 100% of the stance. On each frame were plotted in red:

- The foot axis of the prosthetic foot (Y_F)
- The axis of the socket (Y_S)
- The axis of the ground (X_G)

Also, the absolute angle of the leg, θ_{SH}, define as the angle between the axis of the socket and the normal to the ground, and the angle γ, define as the fixed angle of alignment in the sagittal plane between the foot and the socket, were estimated in each phase of the run (the angle of alignment still remain the same). In Figure 1.3.4.1 are shown the trend of the shank's angle during different phases.

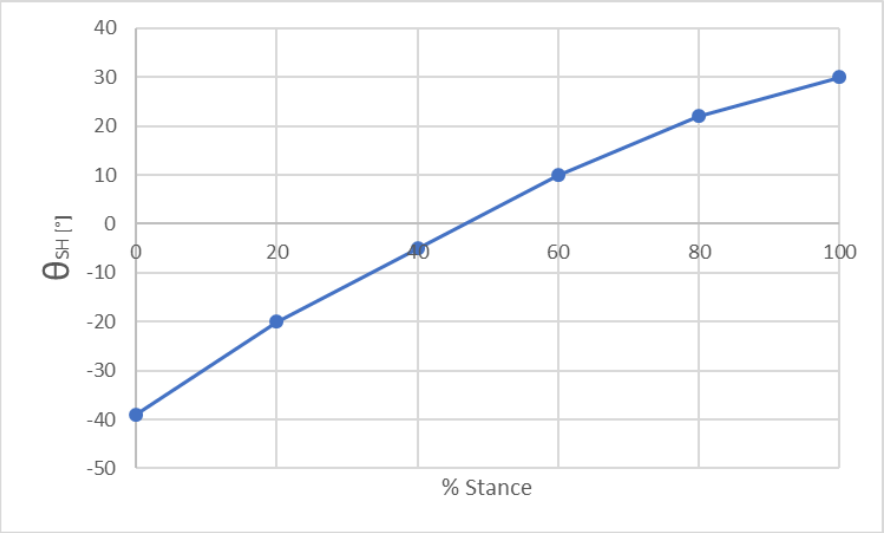

Figure 1.3.4.1: θ_{SH} trend during the stance phase.

The athlete ran over a force platform, so the forces applied during running are known in every stance phase. These forces are the GRFs, and with the absolute angle of the leg is then possible to evaluate the forces acting on the socket, where the vertical one is Y_S and the longitudinal is X_S and they are plotted in Figure 1.3.4.2:

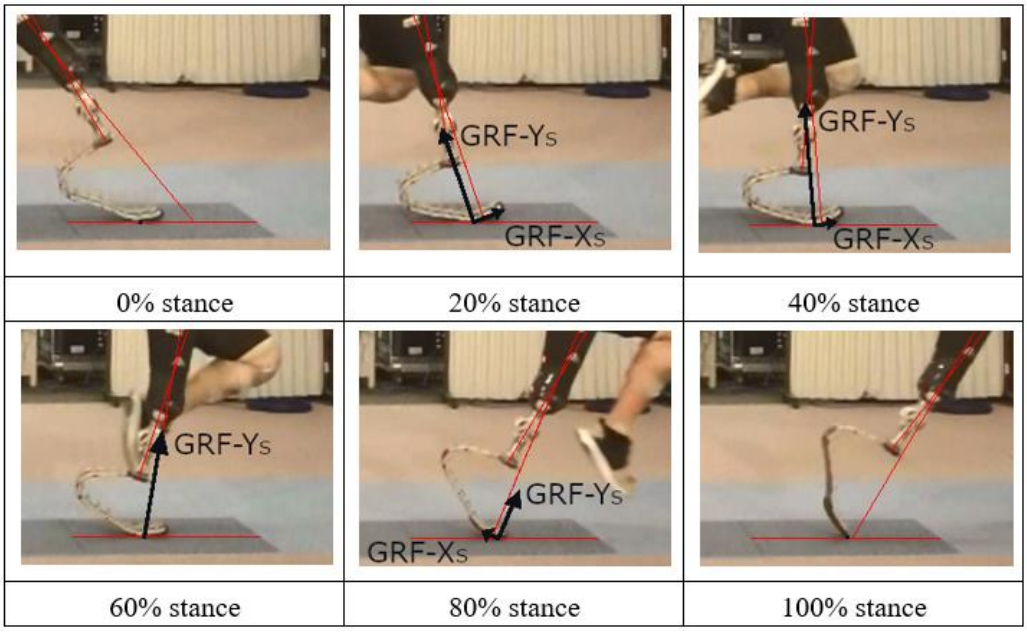

Figure 1.3.4.2: Video frames with GRFs GRF projected into the socket reference system. (Makimoto et al., 2017) [39]

In the first and last images, the forces are null cause it is the moment where the RSP starts to touch the ground and the other where it leaves.
In Figure 1.3.4.3, it is possible to see that the prosthesis is mainly stressed in the vertical direction, compared to the axis of the socket, and this agrees with the spring model. However, the shear force isn't negligible, but there is an instant where it is zero and change its sign, cause move from breaking phase to a pushing phase. This finds demonstration also in the graph of the GRFs read by the force platform (Figure 1.3.4.3).

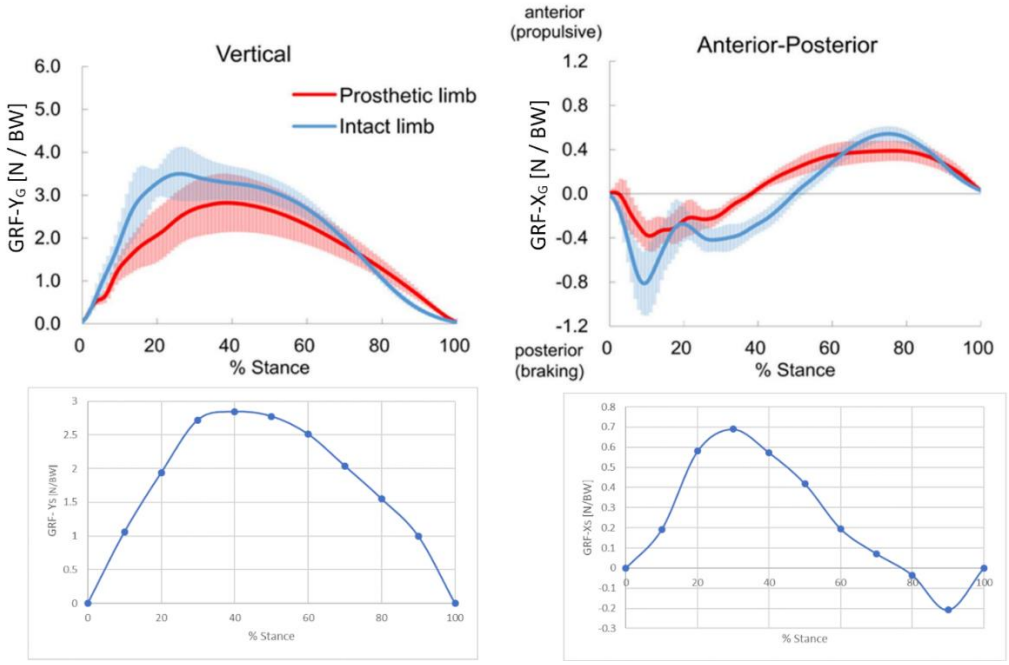

Figure 1.3.4.3: Comparison between the GRF components expressed in the soil reference system and the components with respect to the socket reference system.

For design correctly the test bench with all the movement that it should allow, concerning about the ground, the kinematics of the socket was studied. It was observed that the socket didn't have a simple rotation, but it has a roto-translation in the sagittal plane.
To simplify the movement of the ground, that the test bench should have, it has been thought hinged in a point that translate along an axis orthogonal to the axis of the socket. So, the kinematics of the prosthesis is schematized in Figure 1.3.4.4:

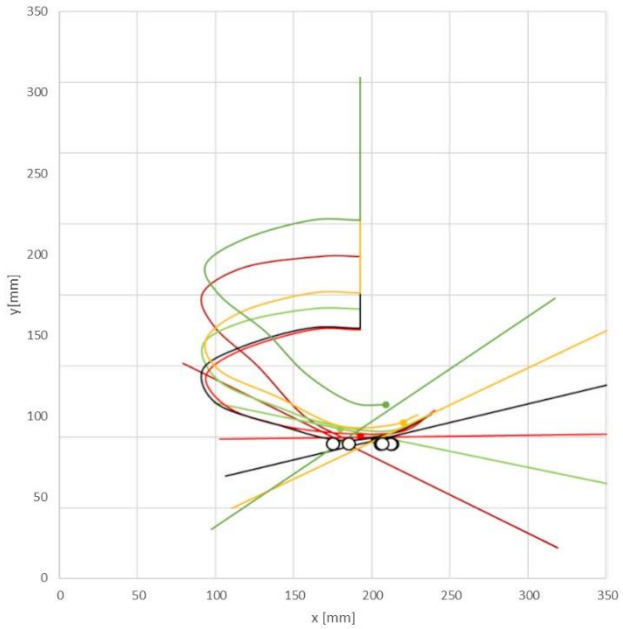

Figure 1.3.4.4: Schematic representation of the movement of the ground for the test bench

In this way, the movements or degrees of freedom of the test bench are 3:

1) Translation of the prosthesis along Y_S axis, defined as displacement C1
2) Rotation of the ground about point G, corresponding to the already defined rotation θ_{SH}
3) Translation of the G point along X_S axis, defined as the displacement C2

Also, a new reference frame is defined, called "Global" reference system (O; X_G; Y_G; Z_G), corresponding to a general system thanks to which is possible to refer for all the measurements.

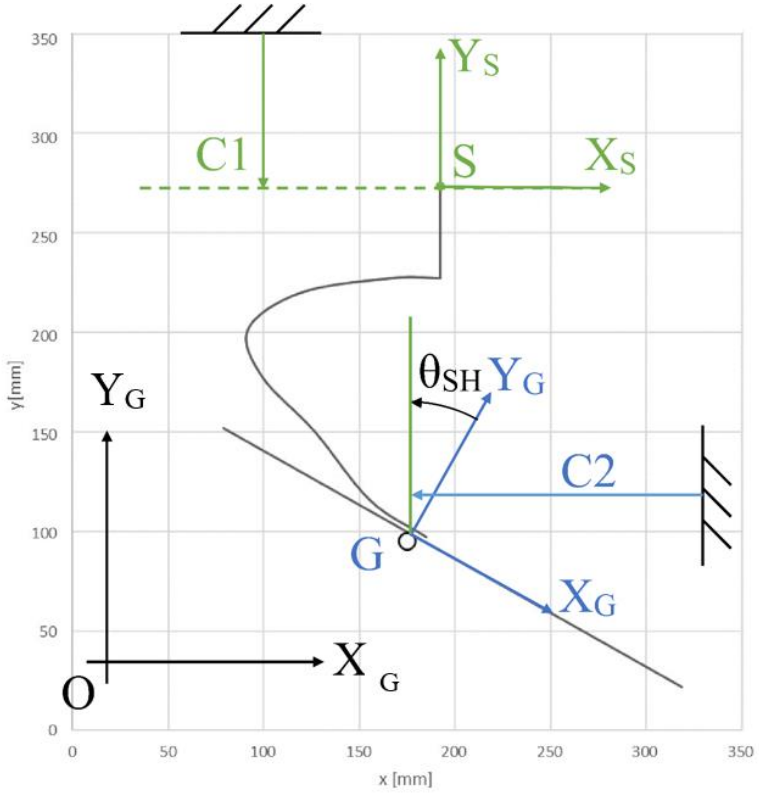

Figure 1.3.4.5: Test bench reference system

The hinge point of the ground was decided to be placed as close as possible to the center of pressure (COP) of the prosthesis, in order to minimize the Ground Moment (GM) that is transmitted to the ground to balance the stress acting on the prosthesis.

Test bench design

For applying the forces F1 and F2, and the displacement C1 and C2, two hydraulic actuators were used, produced by MTS Systems Corporation. Both can produce a force up to 14700 [N] and the oil control system is made by MOOG servo-valves.
The control software and control station are always produced by MTS Systems Corporation, which operates feedback control on the servo-valves. The movement of the pistons can take place under force or displacement controls, by means a uniaxial force transducer, positioned on the head of the steam, for the force control, and by means of a potentiometer put inside the cylinder for the displacement control.

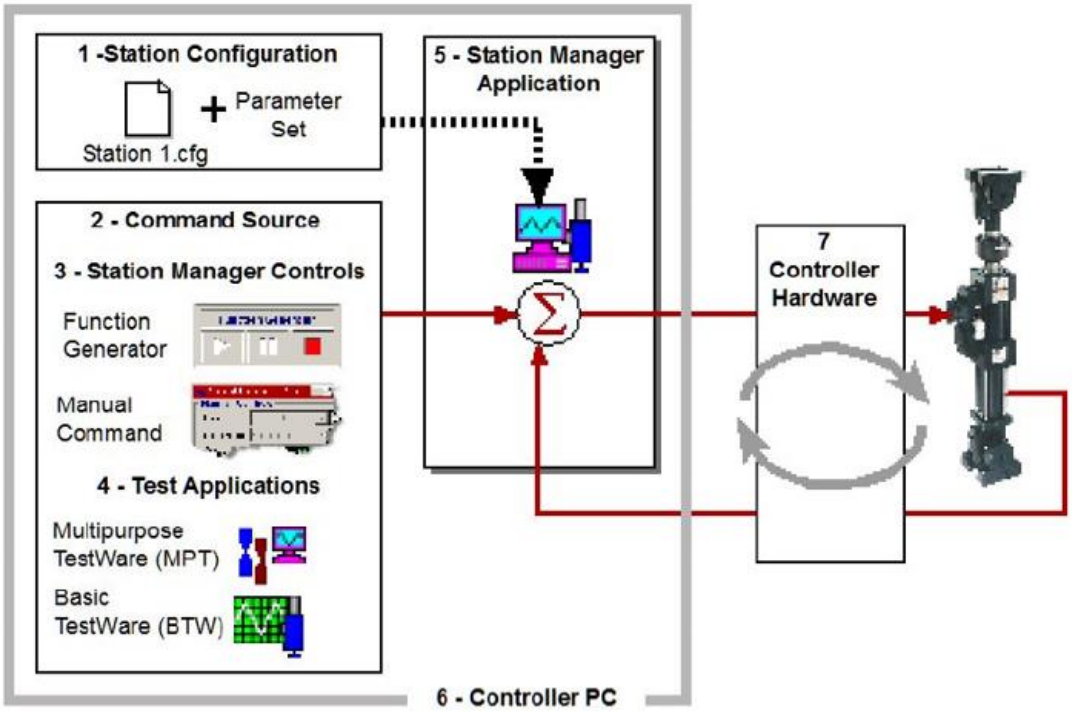

Figure 1.3.4.6: MTS control system [MTS manual]

To support the hydraulic actuators, a double portal has been designed with structural aluminum profiles. The design also allows to have a flexible solution for assembly and disassembly, moreover permit the possibility of changing the configuration of the project at any time.
The aluminum profiles have a square section with unified T-slot on each side, to allow the insertion of the fixing nuts. The internal slots are design to minimize weight while maintaining a high moment of inertia of the section.
It was selected a double portal to avoid the overturning of itself. Its height is about 3 [m] in order to create space for the vertical actuator, the vertical slide, the prosthesis and the horizontal slide. Instead, the width was set to 500 [mm], so that the horizontal slide could comfortably accommodate.

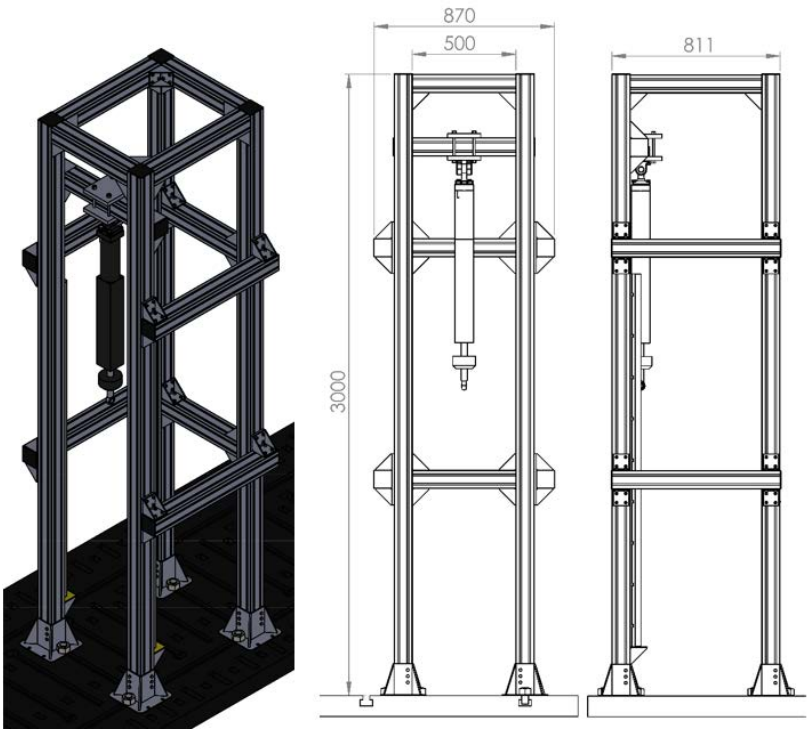

Figure 1.3.4.7: Double portal design and its general dimensions

Vertical slide:

The vertical slide was designed looking for a rigid and light structure, so it was made with the same type of aluminum profile of the portal, but with a lower section.
The vertical slide flows up and down on two cylindrical bars, attached on the column of the portal, that are made by tempered steel with a superficial carburizing treatment. On each bar, it was placed two linear recirculating ball bushes.

To avoid an excessive consume of the buses, the actuator's axis must be aligned with the sliding axis.
Moreover, it was necessary to place an horizontal beam on the slide, so that the prosthesis can be moved upward and backward for align the COP with the plane identify by the two axes of the rails (Figure 1.3.4.8).

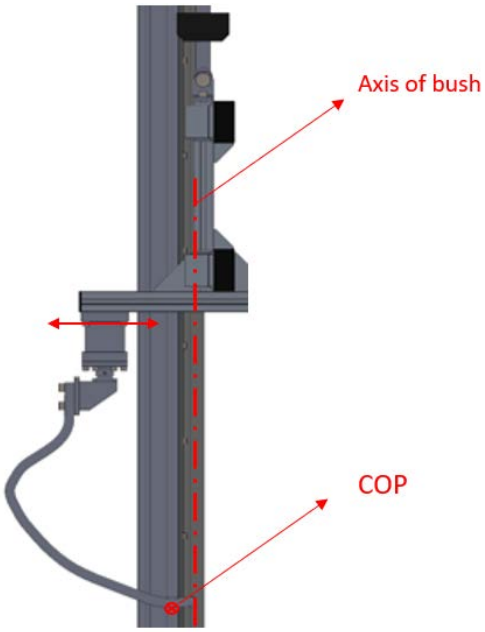

Figure 1.3.4.8: Alignment between COP and bush's axis

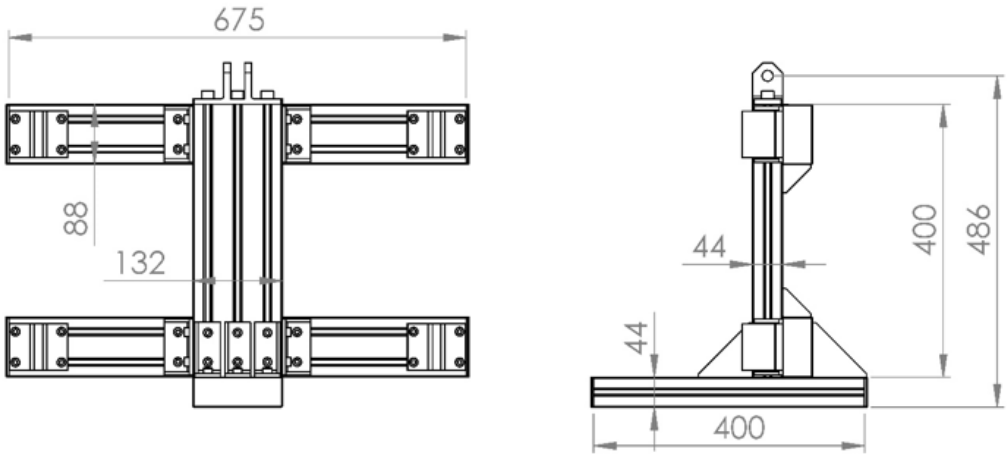

Figure 1.3.4.9: Dimensions of the vertical slide

Horizontal slide:

The horizontal slide is made with the same profile of the vertical one, and it was placed on two cylindrical bars where it could flow forward and backward.
On the top of the slide was put the ground where the prosthesis hit. As mentioned before, it was necessary to have a tilted plane for simulate the different phases of running, so, on the base, made of aluminum profile, it was created this plane that can be manually tilted to fixed θ_{SH} angles.
To keep the fixed inclination, two aluminum plates were made, fixed on the upper part of the flange, with a slotted hole. The friction between the aluminum plates and the lower part of the flange allows to keep the inclination of the flange fixed (Figure 1.3.4.10).

For simulate in real manner the running boundary conditions, a layer of specific material for running track was put as ground, and it is called "Tartan".

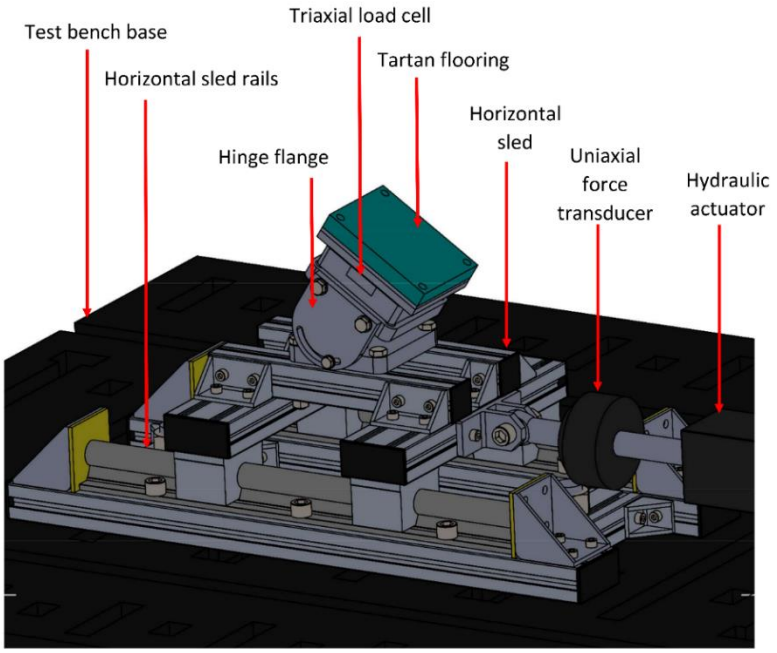

Figure 1.3.4.10: Horizontal slide with tilted ground plane

Figure 1.3.4.11: Test bench used for the in-vitro tests.

CHAPTER 2:

INSTRUMENTATION AND REFERENCE SYSTEM

For each prosthesis it is needed to have a reference frame for the forces that act on the blade, because in the entire system, different types of sensors are used, each with its proper coordinate system, so it's necessary to clarify all the forces directions and signs.
There are two different environment conditions where the prosthesis was used:

- In-vivo, where the athlete uses the prosthesis with the sensors (SG bridges) and hits a force platform fixed into the ground. For the running tests with the athlete Simone Manigrasso, it is thought to perform different adjustment to the set-up of the prosthesis. In this way the athlete can found his better configuration for run.
- In-vitro, where the prosthesis, always with all its sensors applied, is tested on a test bench, that have also 2 load cells (6 and a 3 axis). The machine is composed by two hydraulic actuators, one vertical and one horizontal, that apply the force in a specific direction.

First of all, it is necessary to define the coordinate frame for the socket and for the RSPs. They have different orientation compared to each other.

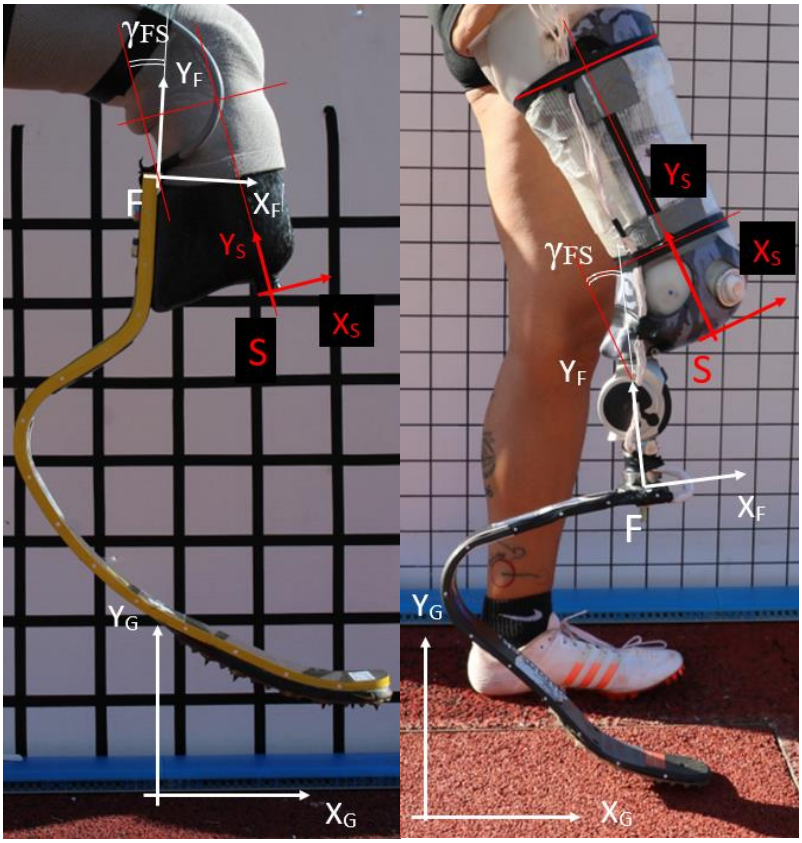

Figure 2.1: Reference frames for RSP and Socket
To the Left: Cheetah Xtreme cat.5
To the right: Runner 1E91 cat.3

Figure 2.1 shows the reference frames for the configuration of Cheetah Xtreme (to the left) and Runner (to the right) RSPs:

- Prosthesis (X_F; Y_F): For the Cheetah, the origin is centered on the upper and internal edge of the blade. Instead for the Runner, it is on the external surface of the prosthesis, at the middle point of the pyramidal attachment. It is draw in white arrows.
- Socket (X_S; Y_S): For Cheetah, its origin is on the lower point of the vacuum valve. Instead, for Runner, it is one the bottom of the socket. The frame is draw in red.

For the origin of each frames, it is selected a point that could be easily found with the video analysis.

In the picture, the Global Reference System, applied on the ground, is also reported.

The angle γ_{FS} is the angle between the axis of foot and the axis of the socket.

2.1: Adjustment terminology

For the in-vivo tests with Manigrasso, the RSP adjustment will be prepared following a consolidated approach, based on the shape, the orientation and the placement of the Foot with respect to the Socket.

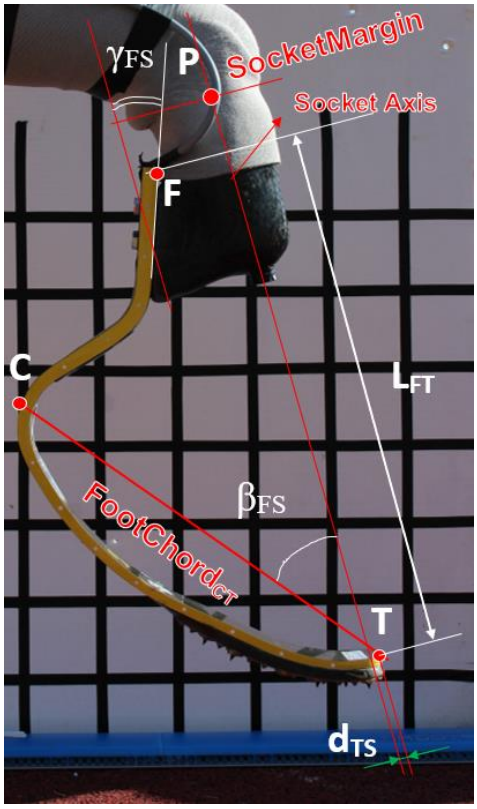

Figure 2.1.1: Cheetah Prosthesis parameters

Prosthesis adjustment parameters:

Points:

- Foot tip: point **T**
- Foot posterior curve: point **C** (most posterior point of the prosthesis, from the tip, point T)
- Socket Patellar Tendon level: **P**

Axes:

- Foot Chord **CT**: line between **C** and **T**
- Socket axis: midline axis of the socket

Angles:

- Angle γ_{FS}: angle between the axis of the foot and the axis of the socket; the angle is positive when the rotation of the prosthesis leads the tip backward.
- Angle β_{FS}: angle between the orthogonal to the ground, that is equal to the socket axis, and the Foot Chord CT.

Segments:

- **L_{FT}**: length of the prosthesis, from the tip to the origin of the prosthesis reference system **F**
- **d_{TS}**: foot forward displacement, defined as the distance between the T point and the socket axis Y_S measured perpendicular to socket axis, when the prosthetic foot is undeformed.

2.2: In-vivo instrumentation and reference systems:

In Figure 2.2.1 it is shown the coordinate system of the force platform used for the evaluation of the loads for the affected or unaffected leg, during running.

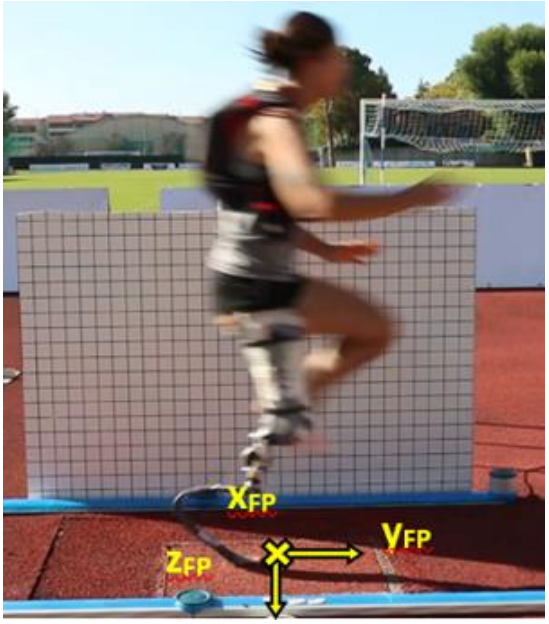

Figure 2.2.1: Coordinate system of Force Platform

In the force platform, the reference system is express by (x_{FP}; y_{FP}; z_{FP}) and it is distinguished by the FP (Force Platform) subscript. The $\mathbf{y_{FP}}$ axis is positive in the gait direction, $\mathbf{z_{FP}}$ is positive into the ground and $\mathbf{x_{FP}}$ complete by the Right-Hand Rule.
Ground reaction forces are writing like "GRF", with their directions, "GRF_V" vertical (+ upwards), "GRF_L" longitudinal (+ forward), "GRF_T" transvers (+ from Lateral to Medial).

For align the notation of the forces read by the force plate with the global reference system, for indicate the forces on the ground, it is used the GRFs notation:

- GRF-L: positive in running direction (Longitudinal)
- GRF-V: positive upwards (Vertical)
- GRF-T: complete by the Right-Hand Rule (Transverse)

To complete the system with a global view, it is also reported in Figure 2.2.2 the global reference frame, that is used also for the laboratory environment. This frame is characterized by the G (Global) subscript: (X_G, Y_G, Z_G).

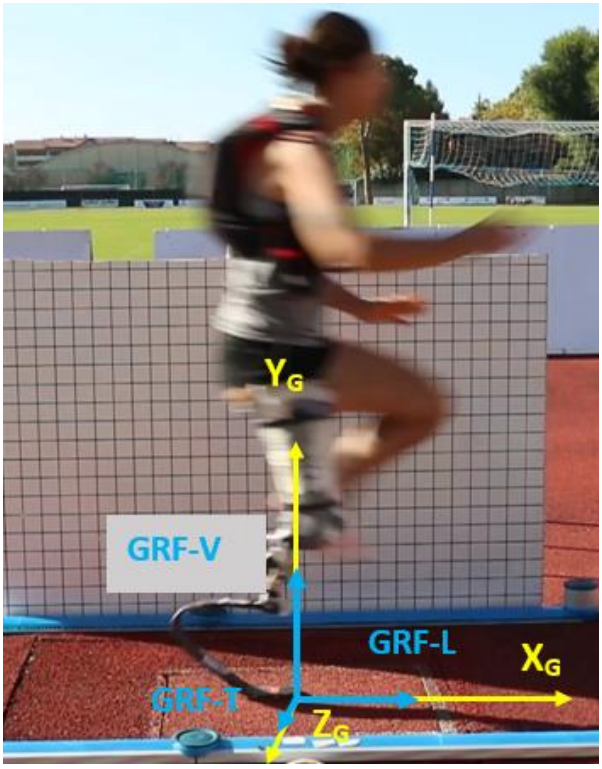

Figure 2.2.2: Reference system of GRFs and Global Reference System

2.3: In-vitro acquisition system and reference frame

In the in-vitro test, a more complex system of data acquisition is used. It is composed by:

- 3-axis load cell
- 5-axis load cell
- 2 force and 2 displacement transducers of the actuators
- 3 half bending moment bridges and 1 half torque bridge on the RSP

It is needed to report the reference frame of each instrumentation.

Concerning the two load cells, they have their proper reference system, reported also on the surface. But it is better to have the same reference frame for each measuring instrumentation, so in that way, it is easier to compare the results.

2.3.1: 3-axis load cell:

To measure the GRFs, a triaxial load cell is placed on the ground, able to measure the three components of force. Exactly, it is used the K3D120 ± 5kN / VA produced by ME (Germany). The 3-axis force sensor K3D120 is suitable for measuring force in three mutually perpendicular axes. It is ready for 50N to 5kN in all three axes.

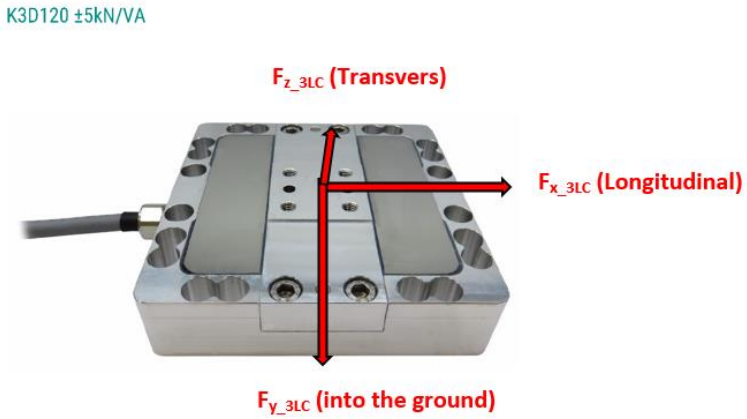

Figure 2.3.1.1: Three axial load cell

Figure 2.3.1.1 is about the own coordinate system of the load cell, but, concerning the GRFs and global system, the coordinate frame is different.
About the GRFs, the GRF-L (Longitudinal) is positive in the running direction, the GRF-V (Vertical) positive when is vertical and the GRF-T (Transvers) when complete the Right-Hand Rule (Figure 2.3.1.2).

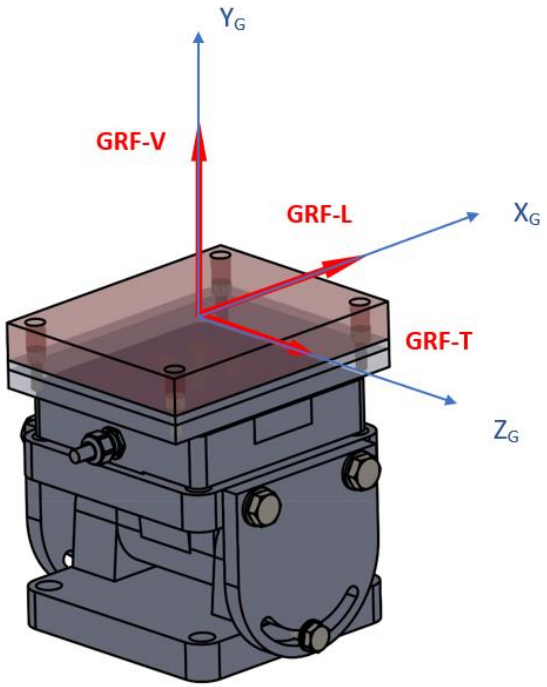

Figure 2.3.1.2: Reference system of the GRFs

The data read by the force platform are acquired by the SoMat system, but, before connecting and measuring it is necessary to make the set-up file of the 3-axes FP with the TceMs software.

Once open the software TceMs, first step is to create a new channel, on the window "*Transducer and Message Channel Setup*" pushing on "*Add*" and a new window appear, on which is necessary to select the type of channel. So, on *Bridge* click OK; in the next phase, it is asking the default type for the channel added, click on *Blank [No defaults]* > OK.

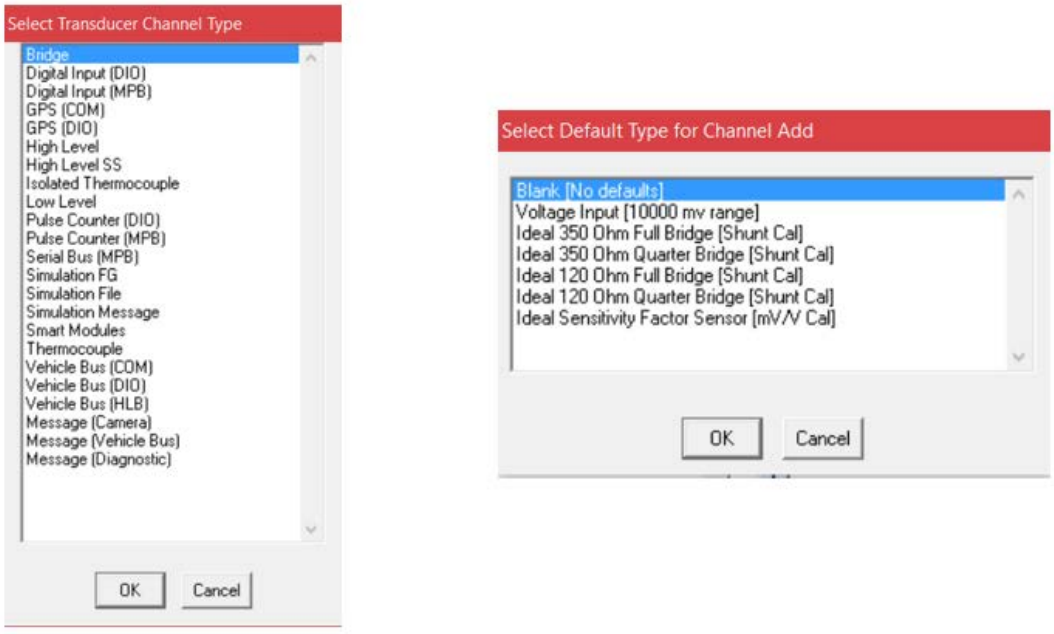

Figure 2.3.1.3: Steps for channels selection

In the next window, on the *ID* slot goes the name for the channel, for example *Fx_3axes* (because it refers to the used load cell).
On the *Connector* box is shown the dedicated position for this channel into the SoMat, so that the wire of the specific load cell axis must go inside the right hole and right bridge of the acquisition system. In the figure below, Figure 2.3.1.4, it is possible to see how the system write the position, for example, *Brg_3c01,* means that the connection goes into the third bridge and channel 1 of the SoMat.
The "*Output Data type*" is a parameter that has to be modify, from the scroll menu, the option "*32 Bit Float"* has to be select.
As output value from the force platform it is want directly the value of force in [N], so in the "*Desired Measurement*" box, it is selected the option *Force*, instead in "*Units*", it is put *N* (*Newton*).

In the section "*A/D Conversion and Digital Filtering*", a value of *100 [Hz]* has to be insert for the *Output Sample Rate*; this low value is acceptable for the quasi-static tests, instead for the dynamic tests this value has to be increase.
On each procedure, no data filters will be used, so, on *Digital Filter Type* has to be select: *None.*

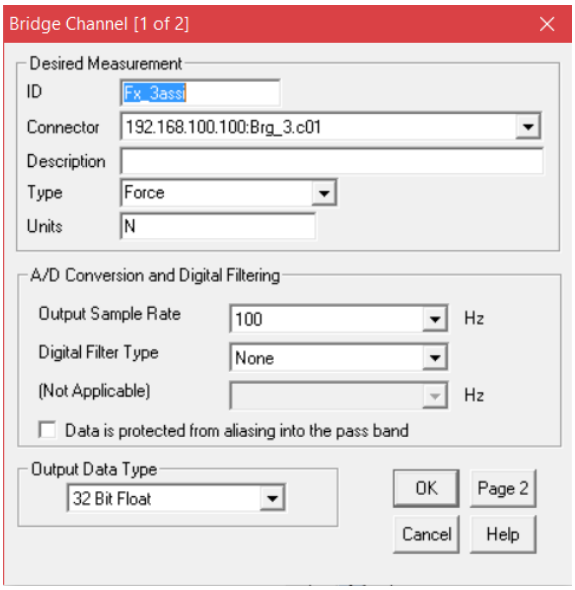

Figure 2.3.1.4: Page 1 of Bridge Channel Configuration

On page 2 it is necessary to define, to the software, the typology of the bridge that will be attached by means the following parameters:

- *Excitation Range*: it is the alimentation value of the bridge, in [V]; in this case is equal to 5[V], as specified on the technical table of the 3-axes load cell;
- *Bridge Type*: it is the type of bridge, in this case, inside the load cell there is a full bridge, as it is written on the technical table;
- *Bridge Resistance*: it is the resistance value of which the bridge is composed, in this case equal to 700 [Ω];
- *Gauge Factor*: this value is written on the technical data of the extensometer or of the instrumentation, in this case is 2;

- *Bridge Factor*: it is the amplification value of the signal measured by the bridge, in this case there is a *Full Bridge*, so it is equal to 4.

On the option *Leadwire Resistance*, the box with write *Do Leadwire Correction* has to be deselected.

Next step is to define the full-scale values, in this case, only compression tests will be made, that are characterized by + sign, so the *Maximum* value is equal to the full scale of the load cell, and it is *5[kN]*, while the *minimum* value is set to *-100 [N]*, for the traction force.

For obtain directly the force values in [N] form the SoMat data, the "*Calibration Table*" has to be built correctly, with the calibration coefficient associated with the full-scale values of the 3-axes force platform.
On the data sheet, provided by the manufacturer, there are written the characteristic values in [mV/V] compared to a force of 5 [kN], from this it was possible to calculate the calibration coefficient for each channel:

Characteristic values:

- X-axis: 1.1105 [mV/V] for 5 [kN] load
- Y-axis: 1.0901 [mV/V] for 5 [kN] load
- Z-axis: 1.3084 [mV/V] for 5 [kN] load

For obtain the value of the calibration costant the following formula is applied:

$$F = C * ch$$

Where the measurement units are:

$$[N] = \left[\frac{N\ V}{mV}\right] * \left[\frac{mV}{V}\right]$$

The software needs to know that a define force values match with a specific values of the *Input signal,* in this way the calibration linear curve can be plotted by two points.
For do that, on the box "*Mode*", it is need to select, from the scroll menu, the option *Define Value*, and after the specific values have to be insert:

- For a zero force, the channel has an input signal equal to zero;
- For a force of F=5[kN], for the X-axis, the input signal expressed in [V], can be calculated from the signal in [mV/V], as:

$$ch = 1.1105 \left[\frac{mV}{V}\right] * 5[V] * \frac{1}{1000} = 0.0055525\ [V]$$

And in the same way for the other channel:

- Y-axis: $ch = 0.0054505\ [V]$
- Z-axis: $ch = 0.006542\ [V]$

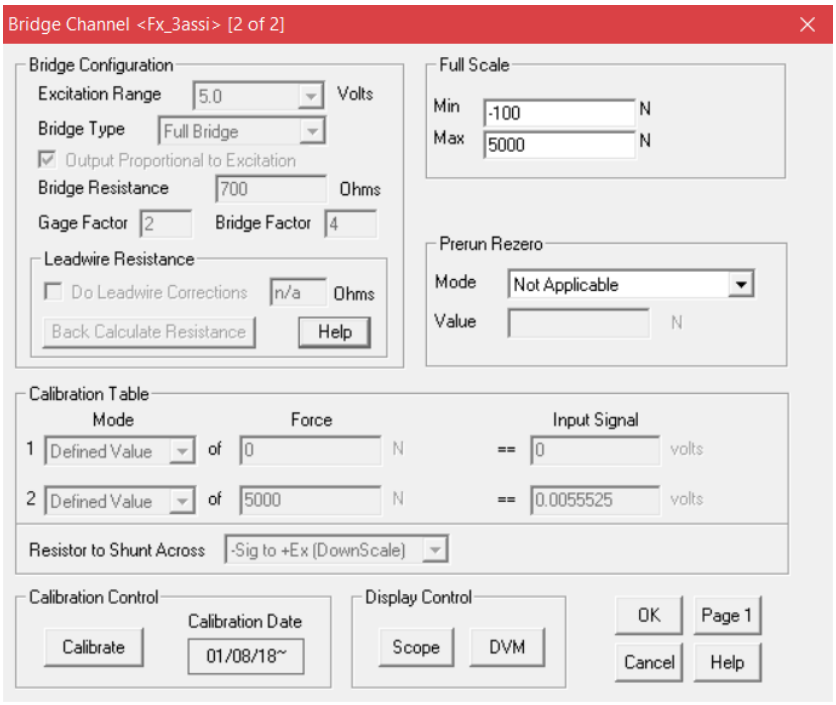

Figure 2.3.1.5: Page 2 of Bridge Channel Configuration

Once all the configurations for each channel are complete, a check test will be performed, for verify that the output signals are expressed in [N] and are the right ones, for example for a known weight put on it.

2.3.2: 6-axis load cell:

For measuring the forces acting on the socket into the test bench, it was thought to apply a 6-axes load cell upwards the attachment of the prosthesis to the vertical slide. The cell that is used is the K6D68 10kN/500Nm/CG produced by ME (Germany-Figure 2.3.2.1) and it can measure the three forces component and the three moments.

Figure 2.3.2.1: The 6-axes load cell that was used

The cell is installed to the vertical slide by means a custom-made aluminum plate and for fixing the RSPs to the cell it was designed an angular aluminum bracket with a special attachment.
Below the 6-axes load cell, an ottobock pyramid receiver is connected on the inferior surface, so that the RSPs, equipped with a pyramid attachment can be fixed. This configuration is typical for the C-shaped prosthesis, like the 'Runner' (ottobock). Instead, for the J-shaped prosthesis, generally the athletes attach it with two screw on the backward surface of the socket, so it is thought to adopt the same configuration, but it is also possible to use a clamped arrangement, between two aluminum plates (Figure 2.3.2.2).

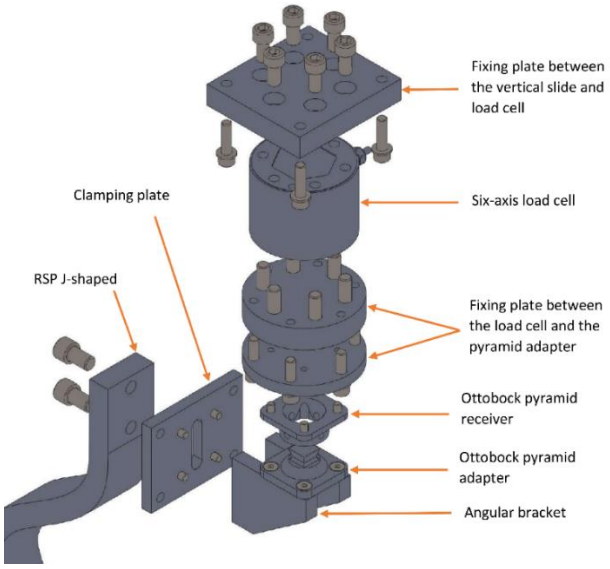

Figure 2.3.2.2: Exploded view of the attachment of the RSP to the load cell

Figure 2.3.2.3 shows the six stress components that can be measured by the 6-axes load cell, which is aligned with the reference system of the prosthetic foot (X_F; Y_F; Z_F).

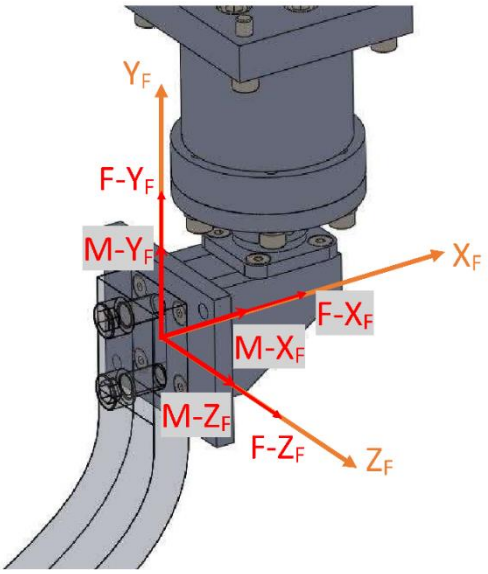

Figure 2.3.2.3: Components measured by the 6-axes load cell

During the test bench setup, it was seen that one channel didn't working, it was out of order. Before sending to assistance, the opportunity to make a calibration of the cell was took, transforming it into a 5-axis load cell. The problem of this cell is that the manufacturer didn't provide the diagram of strain gauges bridges and the geometry of the deforming elements, so it was impossible to understand what could be inside. Moreover, the calibration matrix is not diagonal, and this suggest that all channels can feel all the components of an applying force.
It was decided to delete a channel, and the channel selected was the moment M_Z.

Proceeding with the calibration, the sensitivity matrix has to be constructed. Sensitivity parameter is defined as the ratio between the bridge imbalance (expressed in [mV/V]) and the load [N or Nm].

$$\{ch\} = [S]\{L\}$$

$$\begin{Bmatrix} ch1 \\ ch2 \\ ch3 \\ ch4 \\ ch5 \end{Bmatrix} = \begin{bmatrix} S11 & S12 & S13 & S14 & S15 \\ S21 & S22 & S23 & S24 & S25 \\ S31 & S32 & S33 & S34 & S35 \\ S41 & S42 & S43 & S44 & S45 \\ S51 & S52 & S53 & S54 & S55 \end{bmatrix} \begin{Bmatrix} F_{XF} \\ F_{YF} \\ F_{ZF} \\ M_{XF} \\ M_{YF} \end{Bmatrix}$$

Where:

- {ch}: is the channel vector
- [S]: is the sensitivity matrix
- {L}: is the external load vector

The components of the sensitivity matrix are defined as:

$$Sij = \frac{ch_i}{F_j}$$

And so, for obtain all the elements of the matrix [S] in every single component *ij*, it is needed to:

- Apply only the F_j force
- Measure, with only F_j applied, the value of ch_i

For checking the linearity of the relation between Force and channel value, it is plotted the curve by multiple points. The slope of the curve is the sensitivity.

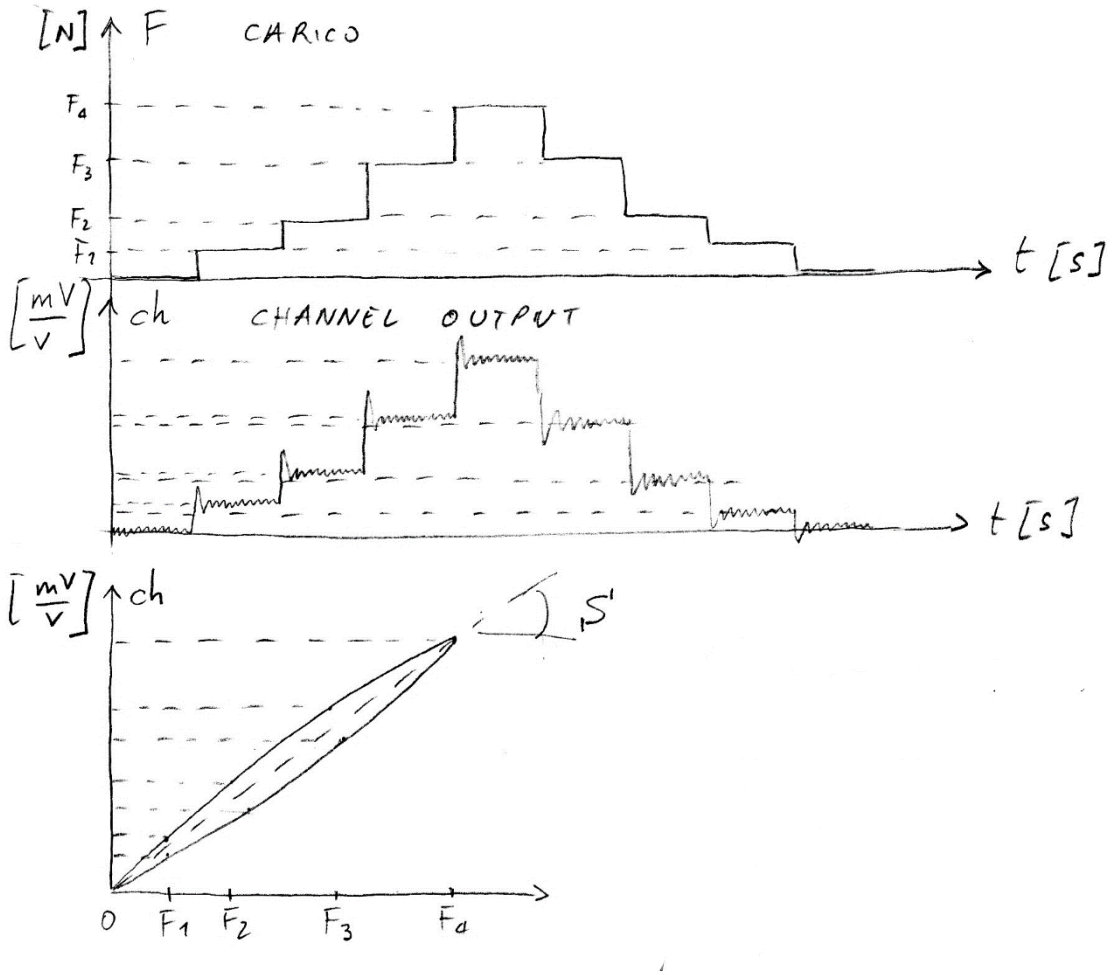

Figure 2.3.2.4: Step load curve

To obtain the sensitivity values of the matrix, the specific forces in their directions are applied one at time, with a step loading and unloading curve.
For the fourth and fifth columns it is necessary to apply the specific moment, but for doing that they are applied by a force with a lever arm. Due to this, for calculating the sensitivity coefficients it is needed also to consider the presence of the cutting forces.

For example, for the M_{XF} moment, it is applied a FY_F with a long lever arm b, consequently:

$$ch_i = S_{i2} * FY_F + S_{i4} * MX_F$$

So the sensitivity coefficient is given by:

$$S_{i4} = \frac{ch_i - S_{i2} * FY_F}{MX_F}$$

In conclusion, the calibration matrix is:

$$\begin{pmatrix} F1 \\ F2 \\ F3 \\ F4 \\ F5 \end{pmatrix} = \begin{bmatrix} 114.79 & 72.66 & 13.50 & 36.98 & 91.75 \\ 2.41 & 50.43 & 51.41 & -51.76 & -51.46 \\ -167.27 & 26.75 & -148.25 & -184.09 & -11.09 \\ -0.40 & 8.43 & 8.88 & -2.47 & -2.67 \\ -12.75 & -6.69 & -2.97 & -2.01 & -12.45 \end{bmatrix} \begin{pmatrix} ch1 \\ ch2 \\ ch3 \\ ch4 \\ ch5 \end{pmatrix}$$

2.3.3: Hydraulic actuator reference system

In Figure 2.3.3.1 are represented the sign directions for the displacement and force of the hydraulic actuators:

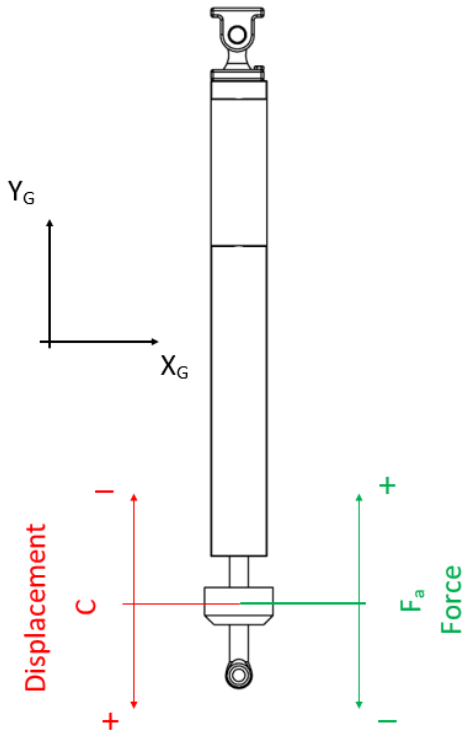

Figure 2.3.3.1: Force and displacement reference system for the actuators

The displacement sign is positive when the cylinder moves out, and negative when moves in. The force applied by the actuator (Fa), is positive when it is traction, negative when it is compression.

CHAPTER 3:

SENSORS POSITIONING ON RSPs

To evaluate the performance of an athlete during the in-vivo tests, the forces acting on the socket of the athlete during the run have to be know. To enable force measurements of a run without any external constraints, like the location of a force platform, an directly measurement system is designed. This internal system consists of various strain gauge bridges applied to the RSP.

The first attempt that was made on Cheetah Xtreme prothesis (Össur) was to place two full bridge, one for bending moment and one for shear force. The bending bridge was positioned where the moment reaches its maximum value, so on the biggest curvature, instead the shear bridge was placed on the quasi-flat surface on the inferior part of the prosthesis (Figure 3.1).
The problem was that the inferior part is the most deformable, so it was impossible to perform a good calibration cause the lever arm of the force was always changing during loading.

Figure 6: First bridge configuration

Another system was design for avoid keeping measure in the inferior part, where a huge deformation occurs.

Observing the two types of prosthesis, J and C shaped, it is possible to see that exist a pseudo-linear segment, that could be seen like a beam section, where it is possible to evaluate the shear and axial forces.
Therefore, three bending half bridges are attached to the upper, rigid segment of the RSP. The bridges are positioned in such a way, that it is possible to calculate the shear and axial forces acting on the BM1 section of the prosthesis with the independent strain obtained from the bridges. From these shear and axial force, the forces acting at the foot clamp can be resolved.

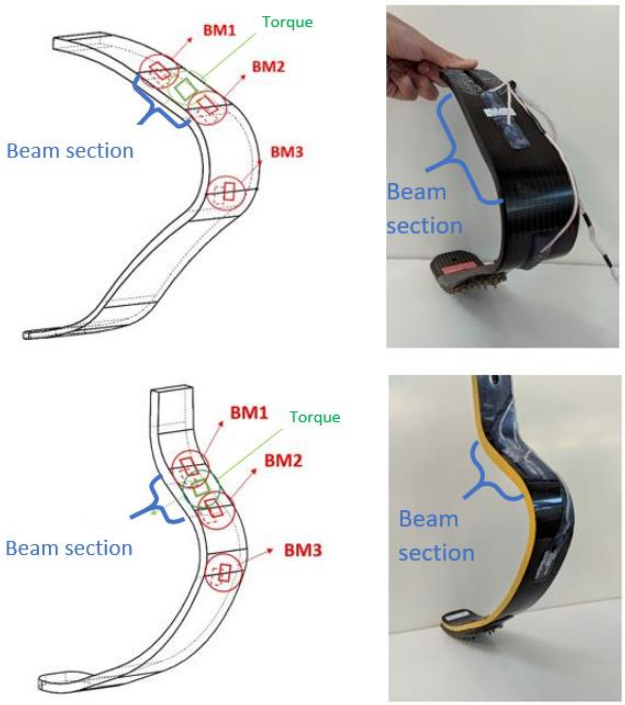

Figure 7: Positioning of strain gauge Bridges
Above: Runner (Ottobock®) C-shaped
Under: Cheetah (Ossur®) J-shaped

The first two bending bridges (BM1 and BM2, Figure 3.2) are attached on the straight segment near the socket clamp. In order to have a considerable difference between the two measured moments, the distance between the bridges (L) is maximized. The third bridge (BM3) is positioned orthogonally with respect to the flat tract, along the arch of curvature. In addition, in order to know the torque applied by the athlete during contact with the ground, a torsion bridge is added between BM1 and BM2.
This method has been adopted for each type of RSP, both for Cheetah (Ossur®) and Runner (Ottobock®).

3.1: Calculation of forces

From the disposition of the strain gauges on the beam section, it is possible to evaluate the shear force thanks to the voltage outputs from BM1 and BM2 by the formula of the "two component load cell" (Figure 3.1.1):

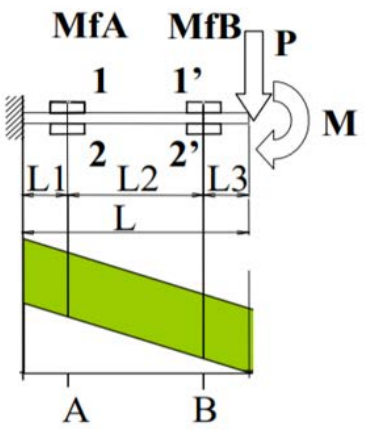

$$P = \frac{MfA - MfB}{L2}$$

$$M = MfB - \frac{MfA - MfB}{L2} * L3$$

Figure 8: Equations of two component load cell

The bending bridges allow to calculate the forces acting on the prosthesis when a load is applied. The reference scheme in figure 3.1.2 is used for the evaluation of the forces, and it regard the dimensions and loads direction acting on the RSPs. The reference scheme is similar for both types of RSP. (Figure 3.1.2):

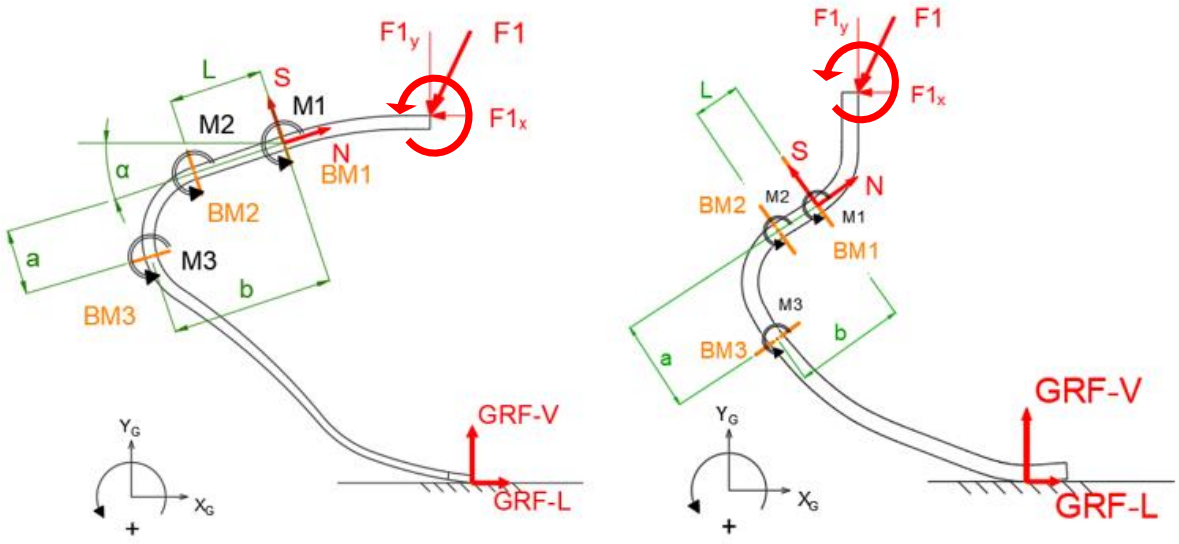

Figure 9: Scheme of dimensions and forces
On Left: Runner (ottobock)
On Right: Cheetah Xtreme (Ossur)

The action of the athlete on the prosthesis is represented by F1. Although F1 generates a state of tension along the whole blade, it is only possible to evaluate the bending moment

at the location of the strain gauge bridges.
In addition, the ground reaction forces measured through a force platform positioned on the ground are represented with GRF-V (Vertical) and GRF-L (Longitudinal).

The moments acting on the three strain gauge sections are calculated with the output values of the half bridges, by means the calibration coefficients, with the formula:

$$M_i = C_i * Ch_i$$

$$[Nmm] = \left[\frac{Nmm * V}{mV}\right] * \left[\frac{mV}{V}\right]$$

The calibrations coefficients C_i are obtained by the in-vitro calibration executed for each type of prosthesis, about this is discussed on the "Chapter 4".

The value of the shear force, that acts on the superior flat segment in the BM1 section, is obtained by the moments values on the section BM1 and BM2:

$$S = -\frac{M2 - M1}{L} \quad [N]$$

$$\frac{[Nmm] - [Nmm]}{[mm]} = [N]$$

Where 'L' is the distance between the two strain gauges, expressed in [mm], 'M1'[Nmm] is the moment on the section of the first half bridge due to the force F_{a1} [N] applied on the top, and 'M2' [Nmm] is the moment on the second half bridge, also caused by F_{a1}.

It is also possible to evaluate the axial force [N] acting on section BM1. For its evaluation only the segment between BM1 and BM3 sections is considered (Figure 3.1.3):

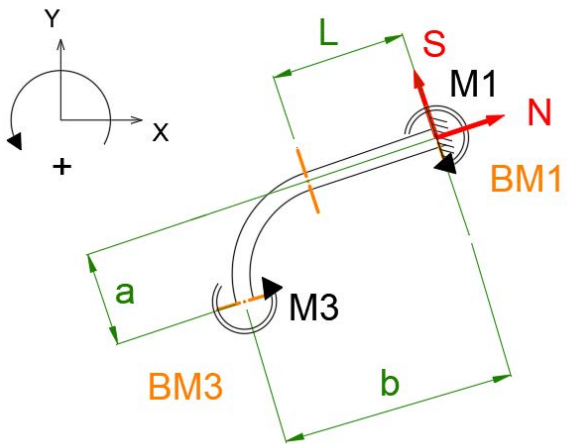

Figure 10: Forces acting between BM1 and BM3

In the scheme in figure 3.1.3, the extremity of BM1 is considered fixed. Therefore, the bending moment M1 is its constrain reaction. From this, it is possible to calculate the axial force 'N' by means the structural solution of the loads solving the equation:

$$\sum M_{BM3} = 0$$

$$M3 + T * b - M1 - N * a = 0$$

Rewriting the formula with respect to 'N' gives:

$$N = \frac{M3 - M1 + T * b}{a} \; [N]$$

$$\frac{[Nmm] - [Nmm] + [N] * [mm]}{[mm]} = [N]$$

Knowing the loads S and N at the location of BM1, makes it possible to evaluate the forces acting at the foot clamp (subscript F). Assuming angle alpha is a constant, the forces at the foot clamp can be calculated by means of trigonometry. For the decomposition of the forces, the following reference scheme is made (Figure 3.1.4):

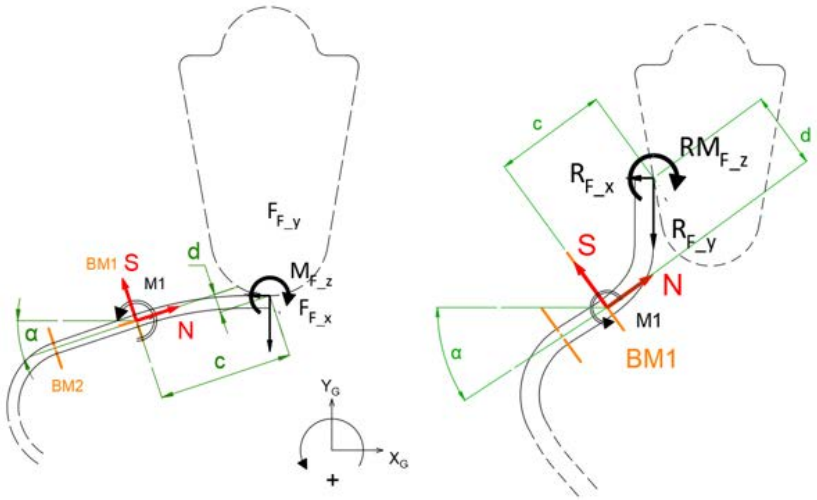

Figure 11: Forces at the foot clamp, on left for the Runner (ottobock), on the right for the Cheetah Xtreme (Össur)

The final forces at the foot clamp, acting on the prosthesis, of the Runner prosthesis are:

- $F_{F\_y} = -S * \cos\alpha - N * \sin\alpha$
- $F_{F\_x} = +S * \sin\alpha - N * \cos\alpha$
- $M_{F\_z} = S * c + N * d$

Instead, the forces at the foot clamp, acting on the prosthesis, for the Cheetah prosthesis are:

- $F_{F\_y} = -S * \cos\alpha - N * \sin\alpha$
- $F_{F\_x} = +S * \sin\alpha - N * \cos\alpha$
- $M_{F\_z} = S * c - N * d$

The forces at the foot clamp, acting on the socket, are the same in values of the forces acting on the prosthesis, but in opposite direction:

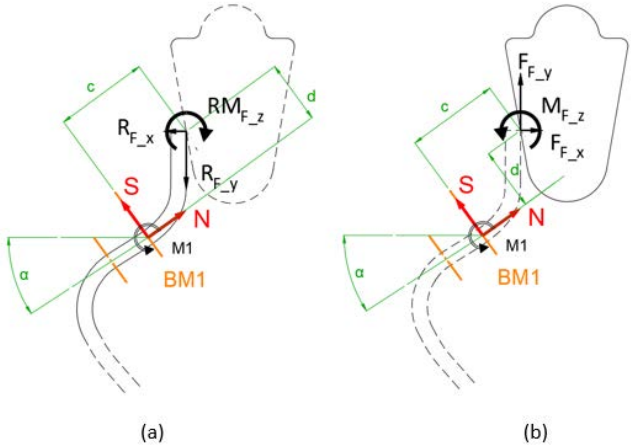

Figure 3.1.5: (a) Forces at the foot clamp acting on the prosthesis; (b) Forces at the foot clamp acting on the socket.

To be sure that all the strain gauges bridges measure an appropriate value along the prosthesis, a FEM evaluation of the force diagram has been made (Figure 3.1.6), where a vertical force of 1500 [N] is applied to the socket. For the other boundary conditions, reference is made to the case where the RSP is fixed on the bench test at the same conditions of the calibration procedure. Therefore, where the prosthesis is attached to the actuator, the vertical displacement (Uy) is free, instead all the other displacements are fixed (Ux, Uz, Rot(x,y,z)). Conversely, in the tip of the foot, where the prosthesis hit the horizontal sledge, the vertical displacement (Uy) is fixed.

Refer to these boundary conditions, the axial force, shear and bending moment diagram are plotted, and it is possible to see that the force value in BM1, BM2 and BM3 sections could be measured (Figure 3.1.7, 3.1.8, 3.1.9):

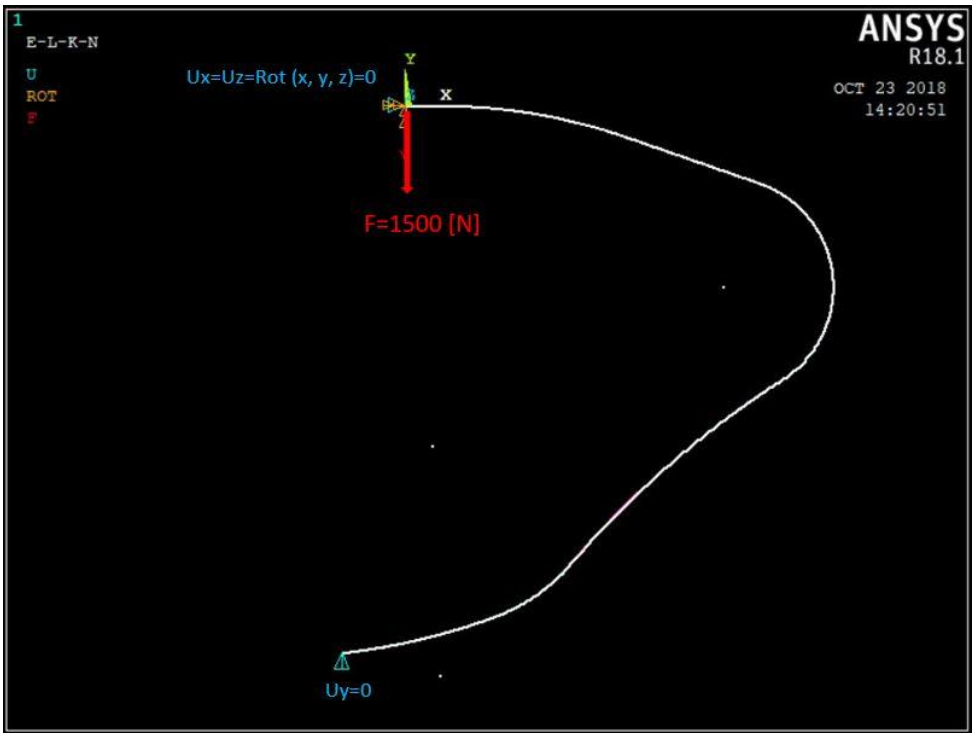

Figure 3.1.6: All boundary conditions

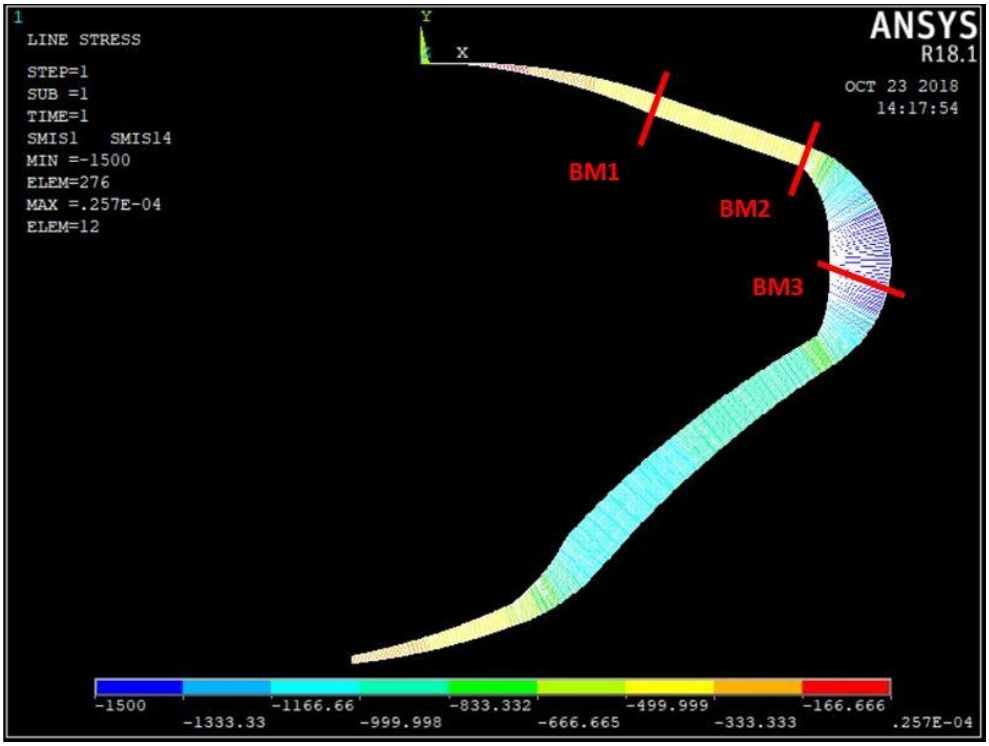

Figure 3.1.7: Axial force diagram

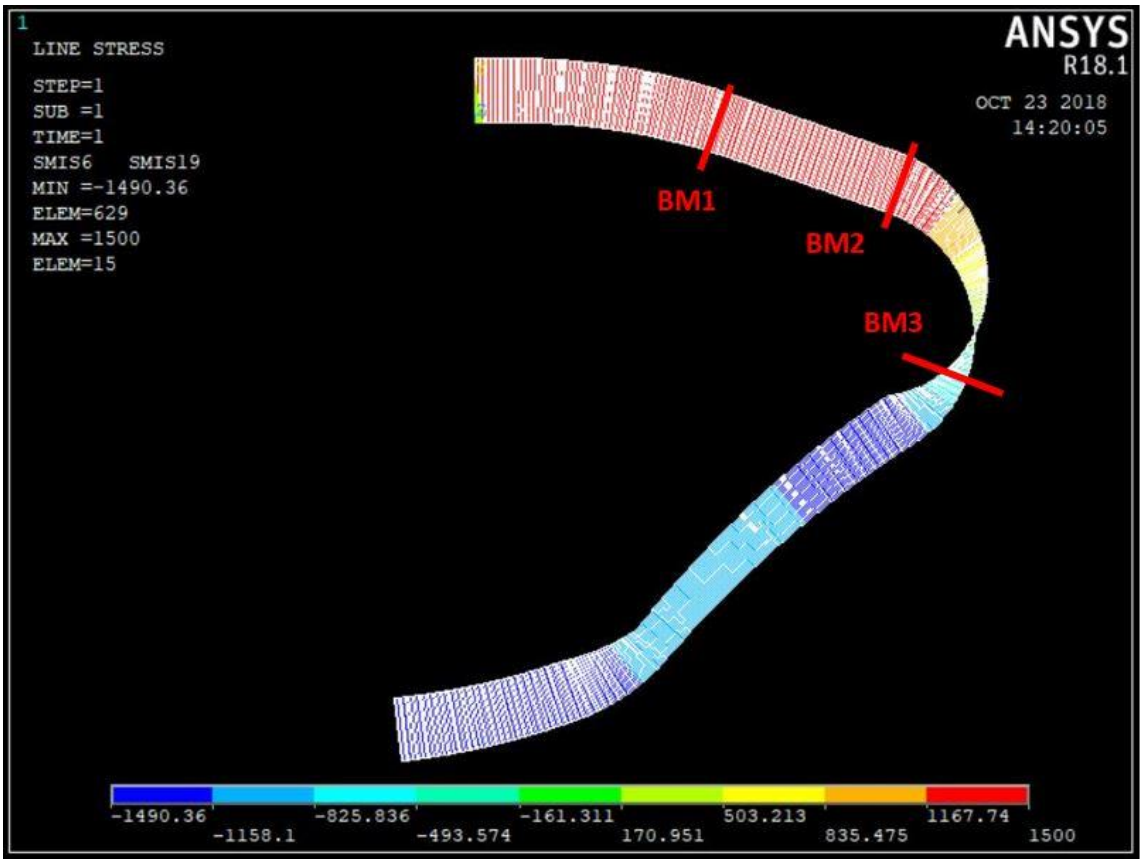

Figure 3.1.8: Shear diagram

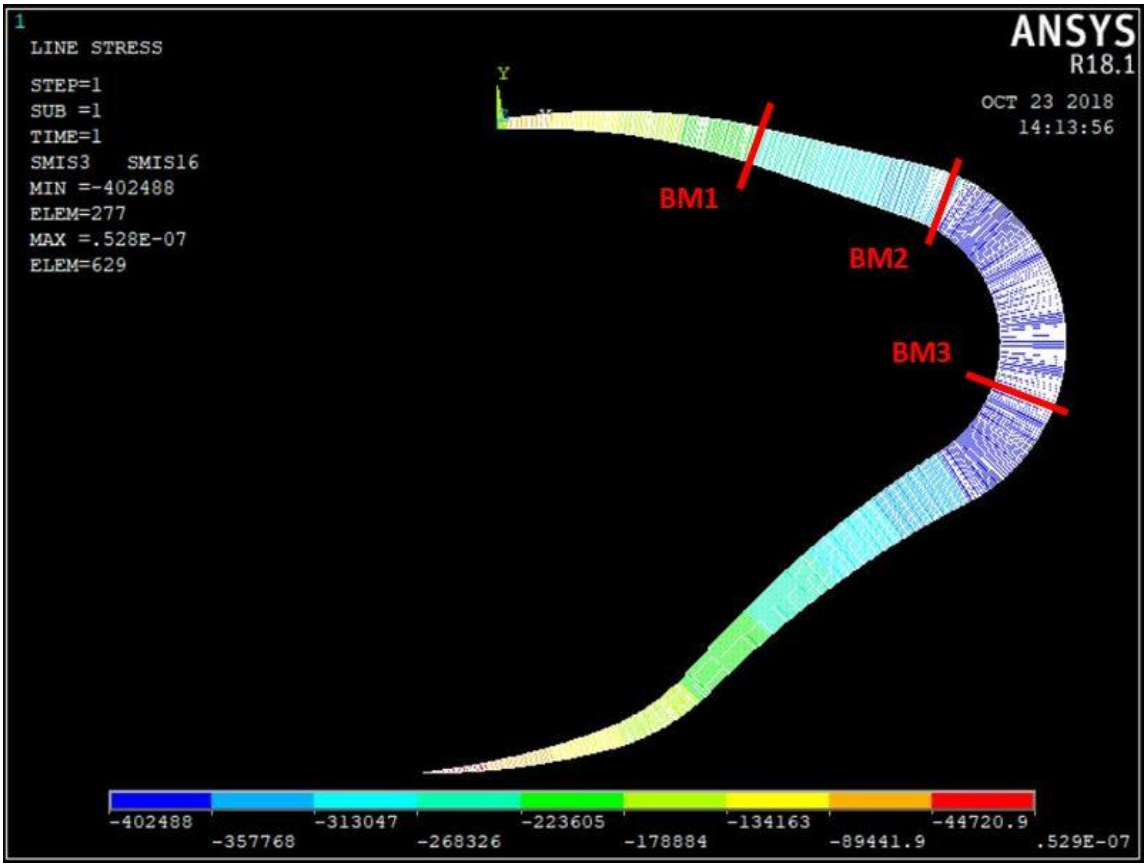

Figure 3.1.9: Bending moment diagram

3.2: Sensors application on RSPs

On the RSP are applied three half strain gauge bridges for measure bending moment and one half bridge for torque moment. The half bending bridges are composed by two strain gauges each, that are positioned symmetrically one on the external surface and one on the internal surface.
The strain gauges are composed by a resistive grid that is highly sensitive to the variation of the resistance values. It could be damage by the presence of external inclusion on the surface where it will be glued, so, the process has to be made carefully. The strain gauges, that compose an half bridge, have to be symmetric on the thickness of the blade, because they have to read the same value of bending moment.

Therefore, a specific procedure is adopted for each type of RSP:

1. Step one, the sections where the strain gauges will be put are identified by means a metal set square. Once find the flat segment, also the orthogonal section is known, thanks to the 90° of the set square (Figure 3.2.1):

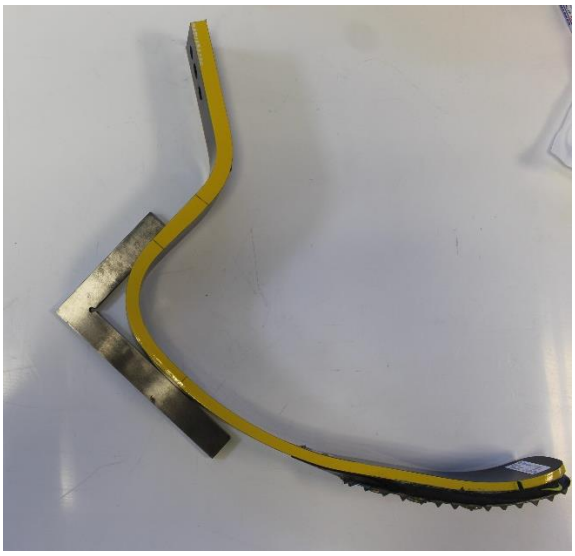

Figure 3.2.1: Marking of the sections

2. The sections are marked using a cutter, with a low-tack tape straps used like a guide.(Figure 3.2.2):

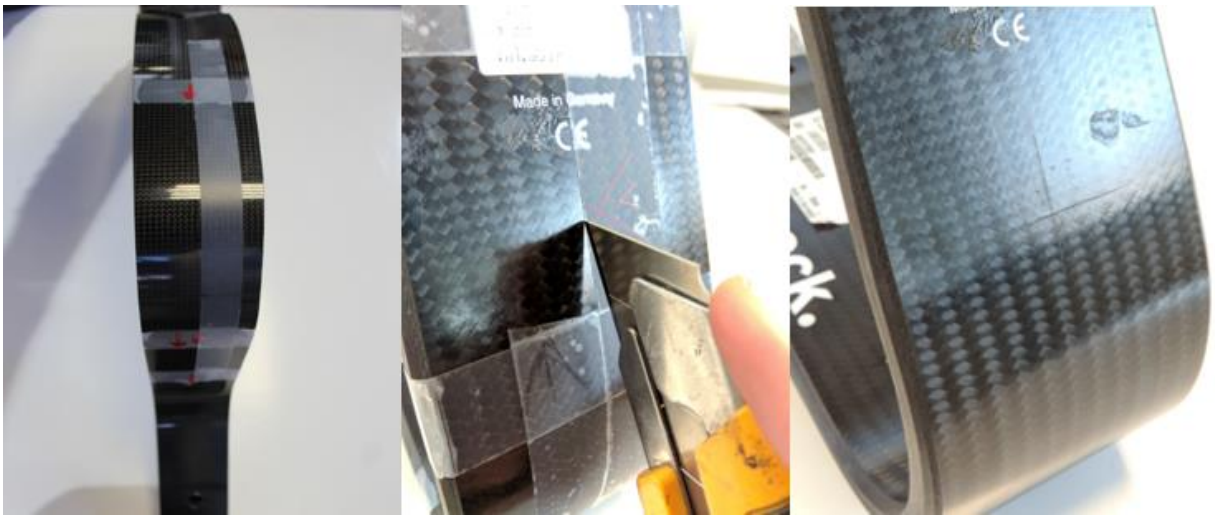

Figure 3.2.2: Marking of the prosthesis

3. Step 3: It is required to pay attention when the strain gauge is taken from the box, because it must not be soiled and contaminated from the external environment. For this reason, a pair of tweezers and low-tack tape are used (Figure 3.2.3).

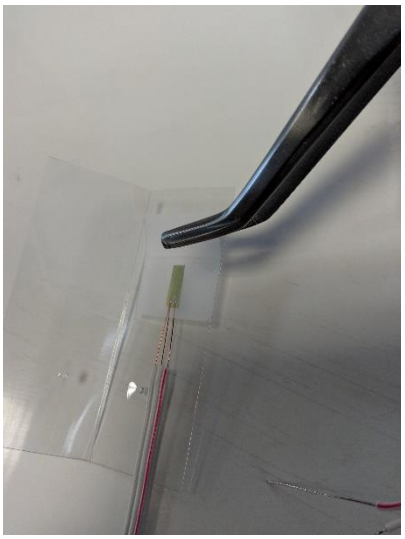

Figure 3.2.3: Taking the strain gauge

4. Step 4: The strain gauge is lightly positioned on the prosthesis's surface and the resistive grid is aligned with the marks. Once it is arranged, the extremity of the strain gauge, with its tape, where the wires are tinplated, is lifted and some drops of glue are placed. With a layer of plastic, the glue is spread uniformly and hold down with the finger for few minutes to be sure that the strain gauge is glued (Figure 3.2.4).

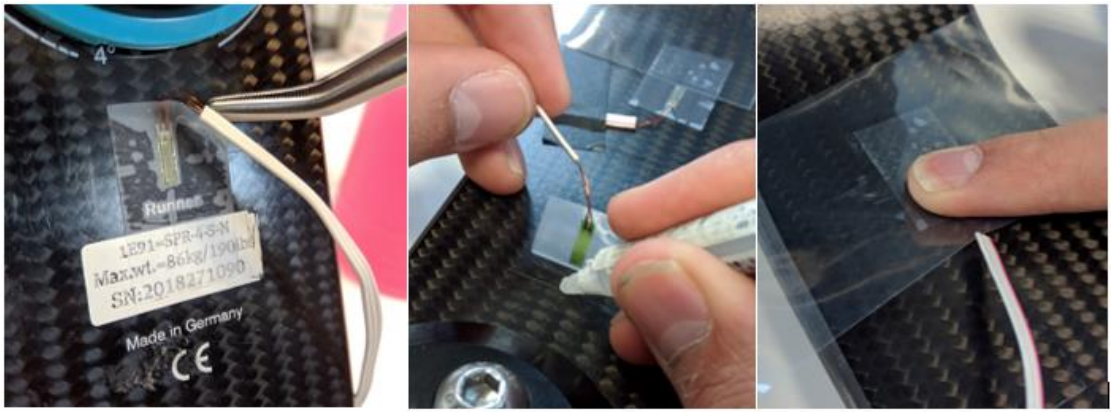

Figure 3.2.4: Bonding of the strain gauge

All that points must be executed for each strain gauge, and once all of them are fixed, a layer of silicon is spread for cover all the system.

3.3: Connecting of strain gauges half-bridge

Figure 3.3.1 shows the common half bridge configuration:

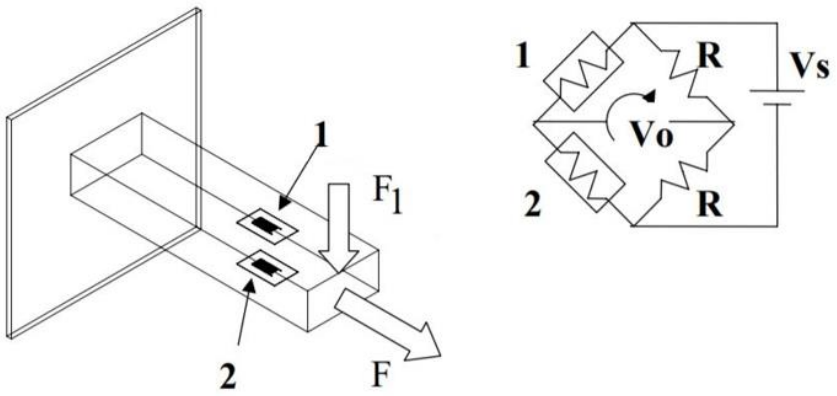

Figure 3.3.1: Half bridge configuration

In the example of the beam under tension + bending, the strain acting on the surfaces (top and down) are:

- For the SG1 (Strain Gauge 1): $\varepsilon_1 = \frac{M_f}{E\,W_f} + \frac{F}{E\,A}$
- For the SG2: $\varepsilon_2 = -\frac{M_f}{E\,W_f} + \frac{F}{E\,A}$

The general equation of a full bridge that convert the value of strain into a voltage measure is the following:

$$V_0 = V_s * \frac{K}{4} * (\varepsilon_1 - \varepsilon_2 + \varepsilon_3 - \varepsilon_4)$$

For the half bridge configuration and with the values of strain mentioned before, the formula become:

$$V_0 = V_s * \frac{K}{4} * \left(\frac{M_f}{E\,W_f} + \frac{F}{E\,A} + \frac{M_f}{E\,W_f} - \frac{F}{E\,A}\right) = V_s * \frac{K}{4} * \frac{2M_f}{E\,W_f}$$

Some notes can be writing about that:

- Half Bridge on two opposite faces of the beam is proportional only to bending;
- Half Bridge Output is therefore decoupled from Tensile loads;
- The total strain measured by the bridge is twice the bending strain on the material surface (Bridge Factor 2).

The missing strain gauges are replaced by two resistances and once the bridge is attached to the acquisition system (SOMAT), it is balancing itself.

For the wiring of the strain gauge it is necessary to follow the SoMat cable's connections on the tube socket, because the position of the alimentation and signal are already defined.

The sequence which the SoMat's wires are joint into the pin of the tube socket is $V, +, -, G$; where:

- V is the alimentation (Red wire , PIN 1)
- G is the Ground (Black, PIN 4)
- $+$ *and* $-$ are the signals (+ is White, PIN 2, - is Green, PIN 3);

Each strain gauge has three wires that going out, which the white&red one is the "+" signal, instead the white wires together are the "-" (Figure 3.3.2).

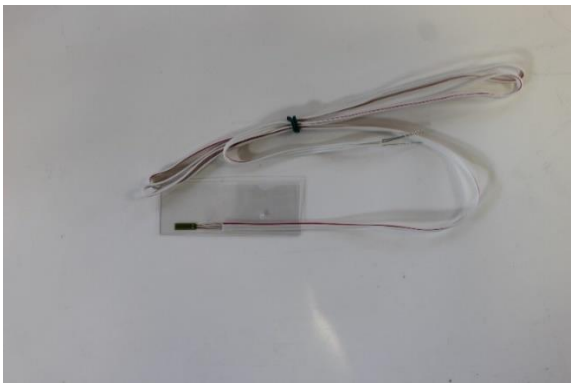

Figure 3.3.2: Strain gauge

For the wiring, it is necessary to build the scheme of an half bridge into the tube socket, following the pin sequence before mentioned (Figure 3.3.3).

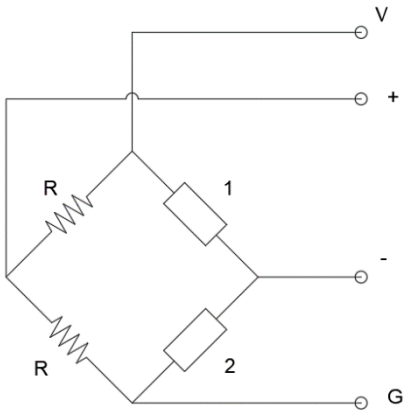

Figure 3.3.3: Half bridge scheme

The connection between the two strain gauges take place on the "-" signal of the SoMat. A wire of SG1 is placed into PIN 1, that it could be the white or white&red, and the other one goes into PIN 3 with a wire of the SG2. The other wire, of the second strain gauge, goes into PIN 4 (Ground). The full system is composed by 3 half bending bridges and one torque bridge, so it is necessary to use a fifthteen Pin tube socket, where, the first four pins are for bridge 1, second fourth pins for bridge 2, third fourth for bridge 3 and the last 3 pins are dedicated to torque bridge. The wiring of this one is little bit different from the previous, here each wire goes into a proper pin independently, and, refer to the SoMat configuration, it is used only the signals *"V", "-" and "G".*

Figure 3.3.4: Wiring of the entire system

For completing the configuration of the acquisition system, the tube sockets of the bridges and of SoMat wires are plugged together. For avoid any cutting risk for the wires of the strain gauges, they are tinplated into a thicker 15-pins cable.

CHAPTER 4:

IN-VITRO CALIBRATION OF RSPs

Before a calculation of the forces acting on the prosthesis during the in-vivo tests can be made, a calibration of the entire SGs system needs to be performed using the test-bench in laboratory. The goal of this calibration is to obtain calibration coefficients that can be used to translate the voltage data acquired from the half bridges into bending moments.

The calibration method consists of a cycle of tests. During the procedure the Y-force acting on the socket is gradually increased, reaching a maximum value of 1500 [N]. The horizontal sledge is able to move freely to maintain the X-forces to zero. During the test, all the data of the machine's system are acquired with the SoMat. With this data and the force measured by the 3-axis load cell it is possible to calculate the moment acting on the BM1, BM2 and BM3 's sections. These values are compared with the voltage signal from the SG bridges and plotted into a graph, the slopes of the three linear curves are the sensitivity of each bridge.
With the obtained sensitivities it is possible to translate the voltages measured by the half bridges to bending moments.

4.1: Set up of the calibration procedure

The two typologies of prosthesis, that were used by the athletes, are the Cheetah® Xtreme (Össur) and Runner (ottobock), and they differ by the shape and also for the type of attachment to the socket. The J-shaped (Cheetah®) is fixed by two screw to the posterior lateral side, instead the C-shaped (Runner) is fixed with a special device called "pyramidal attachment", produced by ottobock (Figure 4.1.1).
The test bench was designed for replicating these two different modes of joint, so it is possible to reproduce as much as possible all the real-conditions.

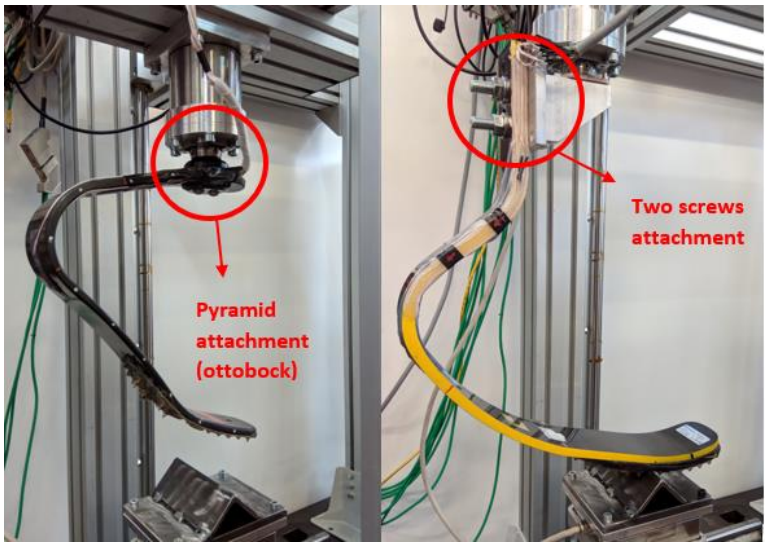

Figure 4.1.1: Types of attachment to the "socket"

Previous small tests in the test bench were always performed with a flat layer of 'tartan' on the 3-axis load cell acting as the ground. Because the estimation of the center of pressure (COP) of the RSP was too difficult with a flat ground surface, the 'tartan' layer was removed and instead a plate of steel with a spike welded on it was placed (Figure 4.1.2). In this way the COP is defined as a fixed point, so it is possible to measure the lever arms in a simple way.

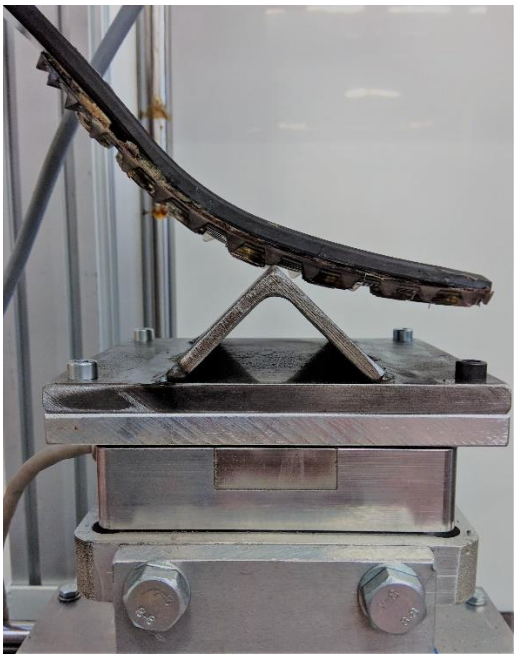

Figure 4.1.2: COP for the prosthesis

For the measurements of the moment arms, a steel set square with a measuring tape, glued on it, was used. The measurements were made by putting the ruler sideways to the 3-axis load cell (Figure 4.1.3).

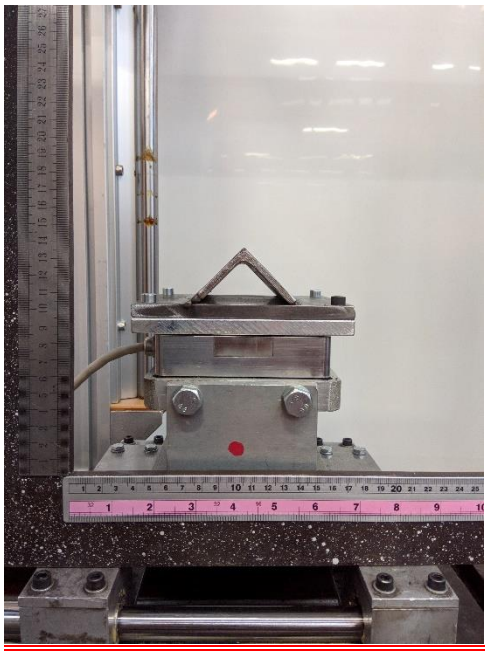

Figure 4.1.3: Measuring configuration

The lever arms that were needed to take are the vertical (“a”) and horizontal (“b”) distance between COP and section where the SG’s bridges were placed, and in relation to BM1, BM2 and BM3 they are called a1; b1, a2; b2 and a3; b3 (Figure 4.1.4). Definitely, measures are affected by parallax errors during the reading of the value or errors in the positioning of the set square sideways to the load cell, so this could be influencing the calibration by generating a margin of error.

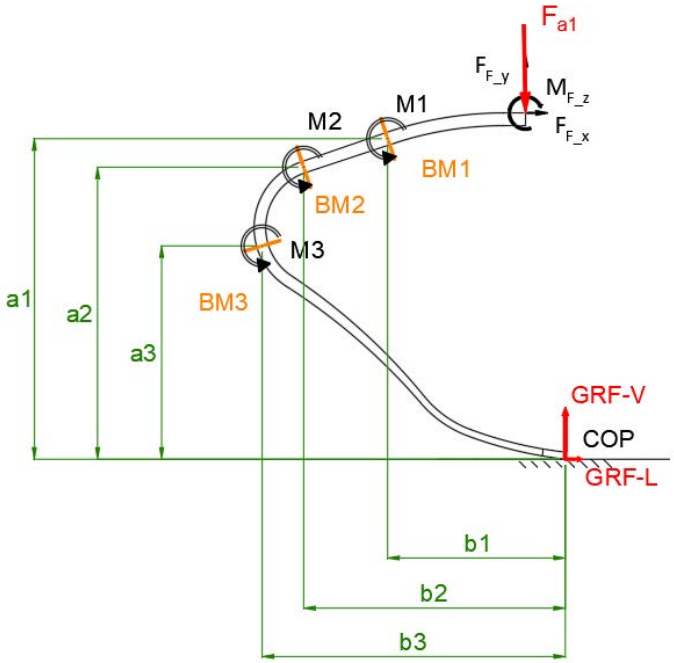

Figure 4.1.4: Lever arms that must be measured

The loads were applied according to a schedule of increasing value, from zero to a maximum, that was selected from the highest peak that the athlete reached during a run

with another type of prosthesis. The measure of that was acquired with a force platform placed on the ground.

The hydraulic actuator number 1 gave the vertical force F_{a1} according to the schedule of value:

$$0,300,500,700,900,1100,1300,1500\ [N]$$

This slow increase of values was applied for reaching the maximum gradually, moreover it is possible to have a major number of points in the graph to be plotted and thus, permitted a better linear interpolation.

For the Runner category 3 (ottobock®) prosthesis, it was necessary to decrease the peak of 1500 [N] to 1460 [N]during the calibration procedure, otherwise the vertical sledge hit the set square that was needed for the measuring. The highest value for the Cheetah Xtreme (Össur®) was set to 1300 [N], because the deformation that occurred on the rubber sole of the RSP was very high, and there could be permanent damage on it (Figure 4.1.5).

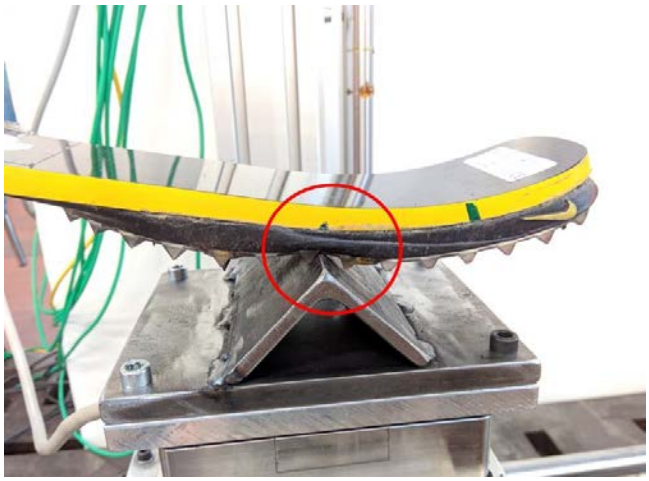

Figure 4.1.5: Deformation on the rubber sole for Cheetah Xtreme

This deformation didn't occur on the other types of prostheses because they did not have the layer of rubber between the external profile of the RSP and spikes, or if there was, was very thin.

Concerning the horizontal hydraulic actuator during the calibration, it is controlled by the system with the condition of maintain the force F2 equal to zero, in that way the horizontal sledge is free to move, according to the longitudinal force that is generated by the prosthesis, due to vertical load. However, presence of friction along the rail produce a low longitudinal force that is read by the 3-axis load cell.

The last set-up that was done, was the SoMat acquisition system, for the acquisition of all the forces and signals of the entire system.
The instrumentation that is connected to the SoMat is:

- Three half moment bridges (BM1, BM2, BM3)
- One Torque bridge
- 5-axis load cell

- 3-axis load cell
- Two force and two displacement from two hydraulic actuators

Force and displacement of actuator are also read from the program that controls the hydraulic system, but for having all the data together it was thought to joint their signal with the SoMat.

4.2: Procedure of calibration

Once all the system is prepared, the oil pump was activated and high pressure to pistons was given. The prosthesis is placed very slow and carefully on the welded spike, in order to avoid that the sole could be damage during loading.
This procedure is performed by moving the vertical actuator on displacement mode, so, when the force F_{a1} reads into the control program differs from zero, it means that the sole hits the ground. In this condition, the manual command of the actuators is switched to the horizontal actuator and the force F_{a2} is set to zero.
After that, the schedule of vertical loads is gradually applied, and after each increment the measure of the lever arms is taken, from the COP to the sections of the SG bridges. Before starting the load procedure, the SoMat acquisition has to be starting.

The loading procedures for the different types of prostheses are:

- Cheetah Xtreme (Össur), J-shape: $0, 300, 500, 700, 900, 1100, 1300\ [N]$
- Runner category 3 (ottobock), C-shape: $0, 300, 500, 700, 900, 1100, 1300, 1460\ [N]$
- Runner category 4 (ottobock), C-shape: $0, 300, 500, 700, 900, 1100, 1300, 1500\ [N]$

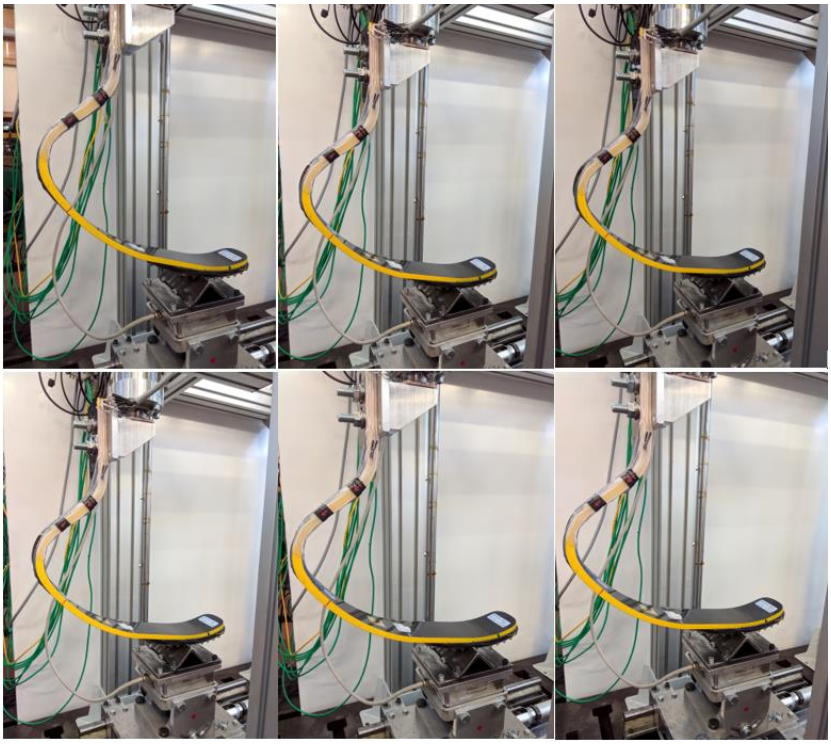

Figure 4.2.1: Loads applying sequence, from 300 [N] to 1300 [N], for Cheetah Xtreme

4.3: Data analysis

After all the measurements are done, the acquired data are analyzed with Excel and InField software.
In Excel, all the lever arms measured and the forces read from the 3-axis LC are imported, in relation to the specific load applied. With this data is possible to calculate the moment, due to the GRFs, acting on the three section where the half bending moment bridges were located (Table 4.3.1). The reference system for the measures is shown in Figure 4.3.1:

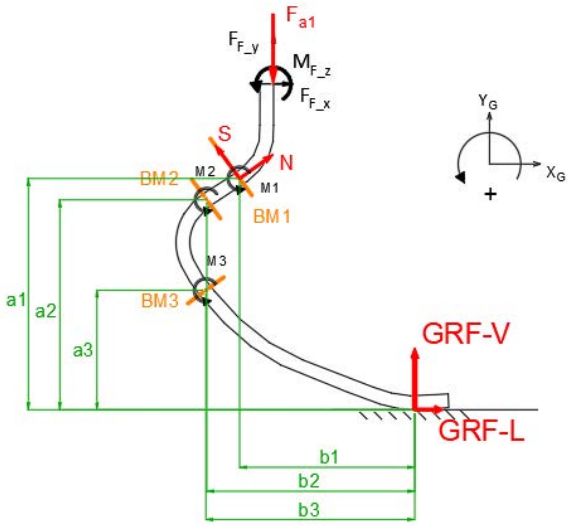

Figure 4.3.1: Lever arms for the GRFs compared to the strain gauge sections

free to move_horizontal_sledge						
F_{a1}	a1	b1	a2	b2	a3	b3
(N)	(mm)	(mm)	(mm)	(mm)	(mm)	(mm)
-300	324	172	292	218	175	221
-500	318	178	285	225	168	225
-700	311	184	276	229	160	229
-900	301	190	263	234	152	233
-1100	292	196	254	240	142	237
-1300	282	200	250	245	135	240

Load_Cell_3ax		
GRF-T	GRF-L	GRF-V
(N)	(N)	(N)
0	0	0
-1.2	-9.5	313.8
0.8	-8.0	512.4
-6.3	-15.2	714.7
-7.9	-21.7	921.7
-9.0	-17.5	1117.3
-10.7	-21.1	1321.4

Moment acting on the RSP		
M1	M2	M3
(Nmm)	(Nmm)	(Nmm)
0	0	0
57056.57	71185.69	71012.55
88666.5	113014.1	113950
126792.8	159486.9	161246.7
168586	209965.7	211454.3
213870.9	263695.6	262304.6
258334.9	318472.5	314289.9

Table 4.3.1: Calculation of the moments at the SG bridges sections, for Cheetah RSP

The presence of GRF-T is due to a non-perfect horizontal alignment of the prosthesis with the pyramid attachment. The horizontal alignment could be called Roll, it is the rotation about the X_F axis of the RSP and it was less than 0.5°, but it was enough for the birth of a transverse force.
The moments acting on the prosthesis are calculated with the force measured by the 3-axes load cell. In Figure 4.3.1 are shown the lever arms between the COP and the sections where the half bending bridges are applied.
Refer to that condition, the moments M1, M2 and M3 are calculated as:

$$M_i = GRF_V * b_i + GRF_L * a_i \qquad \text{where } i = 1, 2, 3$$

In the Excel files is also imported the output signal, in [mV/V], of the bending bridges. They are taken from the InField software, where there is plotted the signal in connection with time. The data in InField looks like as shown in Figure 4.3.2 and after, for each step of force, the average values are imported into an Excel table (Table 4.3.2).

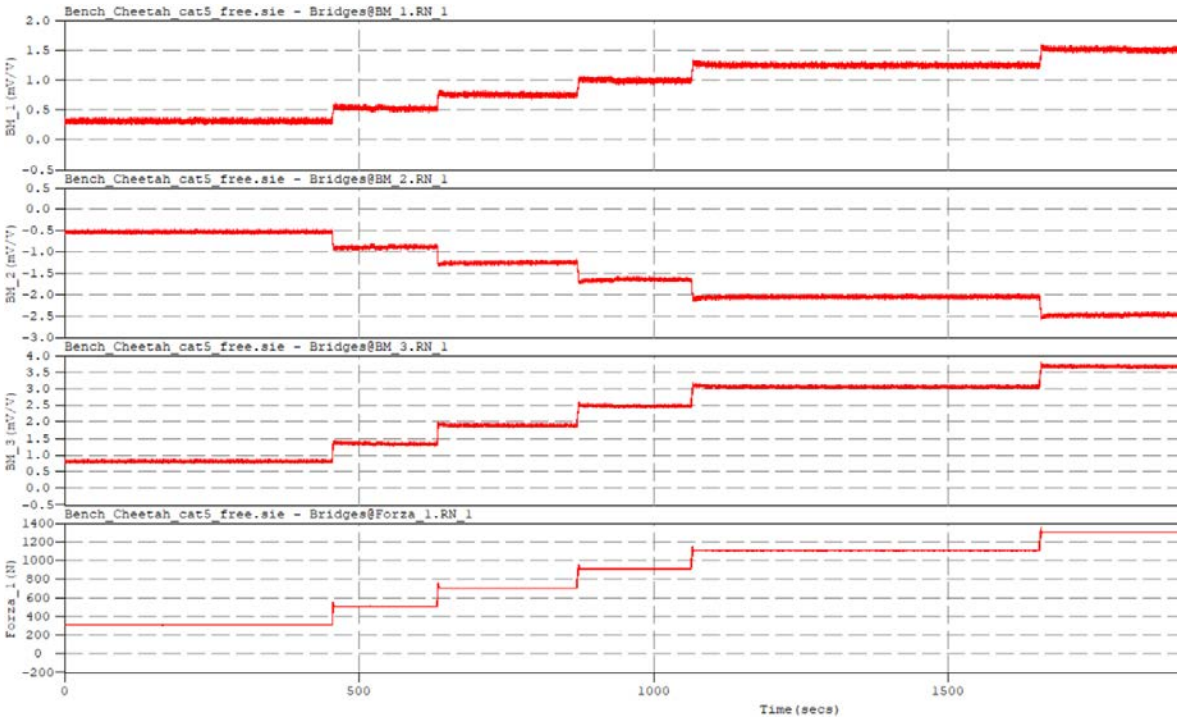

Figure 4.3.2: Output signals of strain gauge bridges for Cheetah cat.5

Channels of strain bridges		
BM_1	BM_2	BM_3
(mV/V)	(mV/V)	(mV/V)
0	0	0
0.311192	0.532758	0.806866
0.527475	0.887633	1.33933
0.749981	1.257	1.89535
0.991309	1.65	2.47389
1.24505	2.05621	3.06086
1.5138	2.48153	3.67214

Table 4.3.2: Values in [mV/V] of the strain gauge bridges

With data about Moments and output signals, the relation can be plotted (Figure 4.3.3):

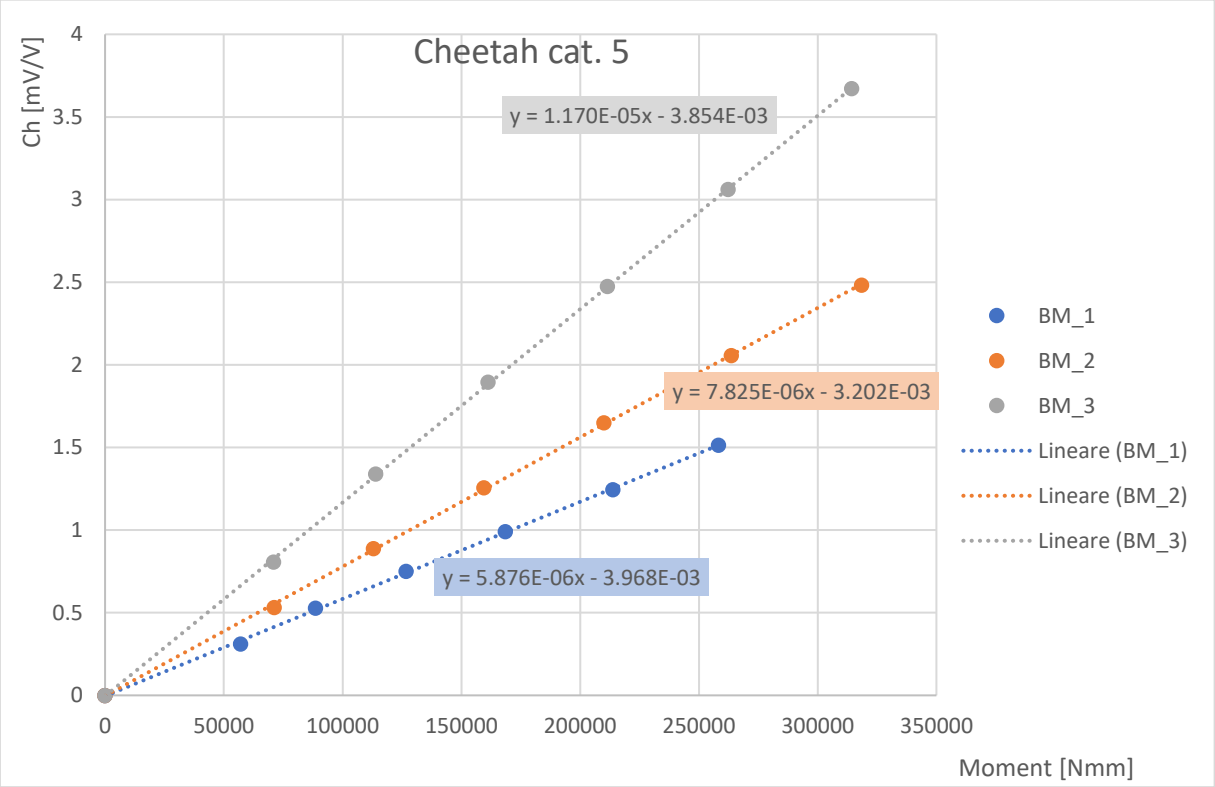

Figure 4.3.3: Relation between Force and Channels output for Cheetah RSP

The relation between Moments and Signals is linear, and the slope of each curve is the sensitivity coefficient of the half bridge.

The sensitivity coefficients for the Cheetah Xtreme (Össur) are:

- BM1: $Sensitivity\ coefficient = 5.876 * 10^{-6}$
- BM2: $Sensitivity\ coefficient = 7.825 * 10^{-6}$
- BM3: $Sensitivity\ coefficient = 1.170 * 10^{-5}$

The calibration coefficient can be calculated as the invers of the sensitivity:

$$C_i = S_i^{-1}$$

The values of the calibration coefficient for each bridge are:

- BM1: $C_1 = 1.702 * 10^5$
- BM2: $C_2 = 1.278 * 10^5$
- BM3: $C_3 = 8.547 * 10^4$

With these values is possible to calculate the moments M1, M2, M3, acting on BM1, BM2 and BM3 section, applying the formula:

$$M_i = C_i * Ch_i$$

For the Runner prostheses, category 3 and 4, the results are presented in the “APPENDIX A”, but, below, it is presented the Force-Channel graph for the Runner cat.3:

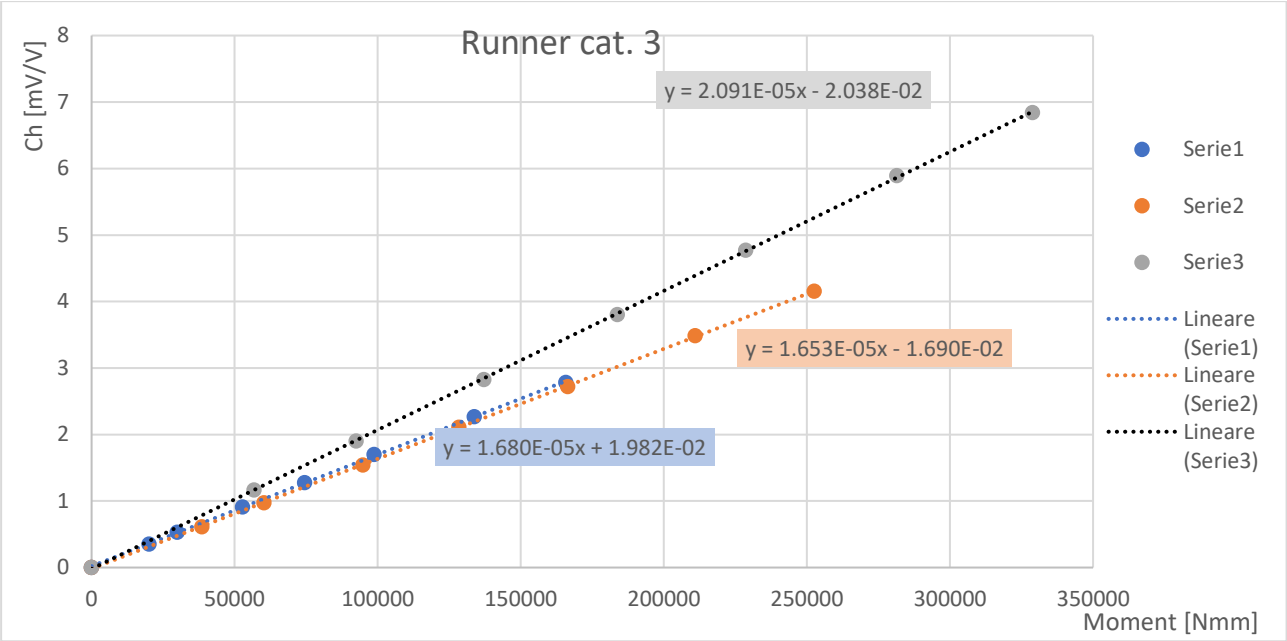

Figure 4.3.4: Relation between Force and Channels output for Runner cat.3 RSP

In this graph, Figure 4.3.4, it is possible to see the close correlation between the curves of BM1 (Blue) and BM2 (orange) calibration. The two trends are almost overlapping, that means that BM1 and BM2 feel the same stress, in fact both are placed in the flat beam section and feel the moment in the same way.

With these data is possible to calculate the forces acting on the prosthesis. The shear force acting on the BM1 section, is calculated like:

$$S = -\frac{M2 - M1}{L} \quad [N]$$

Instead the axial force is calculated as follow:

$$N = \frac{M3 - M1 + S * b}{a} [N]$$

Where the dimensions reported on the formulas are shown in Figure 4.3.5:

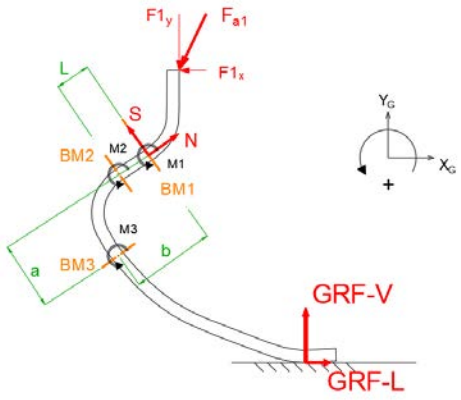

Figure 4.3.5: Data measured on the prosthesis

Data										
F_{a1}	M1	M2	M3	l	a	b	c	d	alpha	alpha
(N)	(Nmm)	(Nmm)	(Nmm)	(mm)	(mm)	(mm)	(mm)	(mm)	(°)	(rad)
0	0	0	0	56	93	128	182	70	36.5	0.637
-300	52771.24	67962.5	68845.22	56	93	128	182	70	36.5	0.637
-500	89448.02	113232.9	114277.3	56	93	128	182	70	36.5	0.637
-700	127180.1	160352.1	161719.3	56	93	128	182	70	36.7	0.641
-900	168104	210486	211082.8	56	93	128	182	70	37.2	0.649
-1100	211132.8	262305.1	261165.5	56	93	128	182	70	37.5	0.654
-1300	256706.8	316562.1	313322.5	56	93	128	182	70	38.1	0.665

Table 4.3.3: Data measured for the evaluation of shear and axial forces on Cheetah Xtreme cat.5

The angle α has been considered uniform in the superior flat segment of the prosthesis as an assumption, because the deformation isn't so big than the inferior part, but for more accuracy, in the data analysis, it was measured during the loading, and it is possible to see a variation of 2 degrees.
The forces acting at the foot clamp are measured as follow:

- $F_{F\_y} = S * \cos\alpha\, N * \sin\alpha$
- $F_{F\_x} = -S * \sin\alpha + N * \cos\alpha$
- $M_{F\_z} = -T * c - N * d$

loadcell	shear	axial force	Forces at the foot clamp, on socket			
GRF-V	S	N	F_{F_y} (V)	F_{F_x} (L)	M_{F_z}	e%_V
(N)	(N)	(N)	(N)	(N)	(Nmm)	%
0	0	0	0	0	0	0
313.8	-271.27	-200.53	337.34	-0.17	-35334.78	7.51
512.4	-424.73	-317.59	530.33	2.66	-55069.39	3.50
714.7	-592.36	-443.90	740.22	1.90	-76736.12	3.57
921.7	-756.82	-579.51	953.20	4.02	-97176.00	3.42
1117.3	-913.79	-719.71	1163.09	14.70	-115930.76	4.10
1321.4	-1068.84	-862.33	1373.20	19.08	-134166.79	3.92

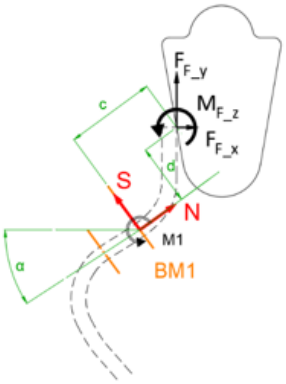

Table 1.3.4: Forces at the foot clamp for Cheetah Xtreme cat.5 (Össur)

The error between the F_{F_y} and the force GRF-V, that is the vertical force read from the 3-axis load cell, is calculated in the column of "e%_V";
It is possible to see that the difference is acceptable for the high values of force, instead the error that occurs for the small value (300 [N]) is over 5%, but for running evaluation it isn't a problem, because the athletes reach forces that are around, or more, the maximum values used for the calibration.

Table 4.3.5 shows the calibration results for the Runner cat.3 and the point where the forces at the foot clamp are calculated. For this type of prosthesis, the calibration errors are higher than the previous, but still remain valid.

loadcell	shear	axial force	Forces on the foot clamp, on socket			
GRF-V	S	N	F_{F_y} (V)	F_{F_x} (L)	M_{F_z}	e%_V
(N)	(N)	(N)	(N)	(N)	(Nmm)	%
0	0	0	0	0	0	0
306.37	-307.13	-119.71	325.12	54.37	-22149.45	6.12
506.91	-505.12	-167.59	528.93	58.91	-36193.98	4.34
706.57	-701.25	-266.18	741.06	115.86	-50515.46	4.88
919.63	-899.63	-326.50	948.75	125.70	-64686.33	3.17
1110.86	-1126.50	-505.27	1209.59	247.36	-81770.68	8.89
1313.72	-1286.42	-585.13	1385.56	278.33	-93443.80	5.47
1475.67	-1445.85	-697.06	1569.22	337.54	-105339.93	6.34

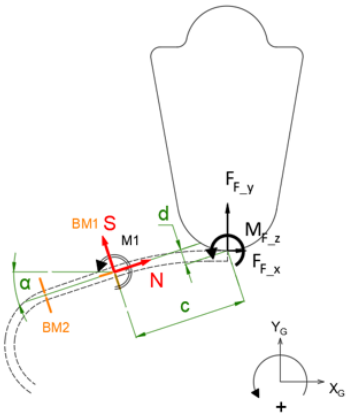

Table 4.3.5: Forces at the foot clamp, on socket, for Runner cat.3

4.4: Static validation of the calibration

After calibrating the half bridges, it is necessary to check the accuracy of the calibration. This validation is performed in two ways: A static validation using the test bench and a dynamic validation using the data obtained during the in-field test. Below it is discussing about the static validation, instead for the dynamic validation is discuss in the "paragraph 5.3".

The procedure for the static validation is similar to the procedure of the calibration. The prostheses are exposed to a gradual increased load, only now the horizontal sledge is fixed. For fixing the sledge, the control mode of the actuator number 2 is set into displacement, and equal to a predefine measure that allows the prosthesis to hit the spike of the ground without damaging the sole.
The forces are applied according to the same schedule of calibration test:

- Cheetah Xtreme (Össur): $0, 300, 500, 700, 900, 1100, 1300\ [N]$
- Runner category 3 (ottobock): $0, 300, 500, 700, 900, 1100, 1300, 1460\ [N]$
- Runner category 4 (ottobock): $0, 300, 500, 700, 900, 1100, 1300, 1500\ [N]$

And while loading, between the different steps, the measures of the lever arm are taken.

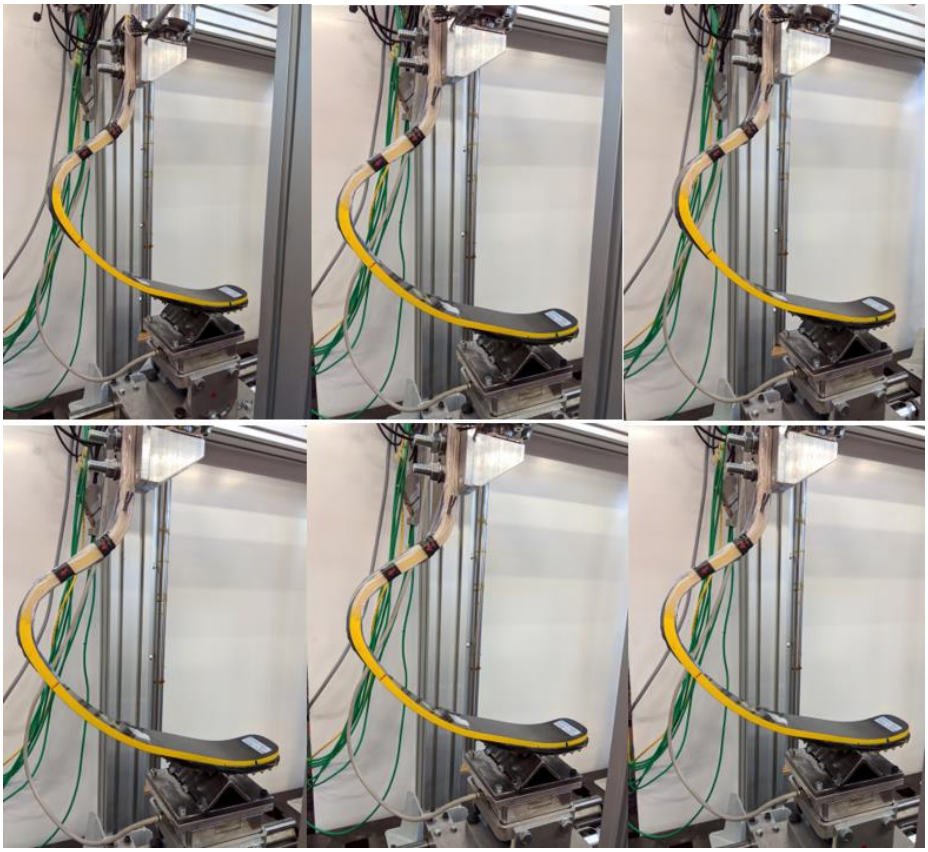

Figure 4.4.1: Loading sequence, from 300 to 1300 [N] for Cheetah® Xtreme

All the data acquisition is done by the SoMat. By multiplying the values of the strain gauge bridges with the calibration coefficients, the moment values are obtained. With the moments obtained by the half bridges, the lever arms in relation to the foot clamp, the lever arms in relation to BM1's section and the angle of the flat inclined surface, it is possible to calculate the forces acting on the foot clamp with the same formulas used for the calibration procedure, for shear (T), axial force (N), and the forces at the clamp (F_{F_y}; F_{F_x}; M_{F_z}).

The vertical force at the foot clamp (F_{F_y}) is compared with the vertical force read by the 3-axes load cell (GRF-V) and the error that occurs between them is calculated (e%_V). Also the error on the longitudinal forces is calculated (e%_L), between the longitudinal force acting at the foot clamp (F_{F_x}) and the longitudinal force on the force-plate (GRF-L) (Table 4.4.2).

Data										
F_{a1}	M1	M2	M3	l	a	b	c	d	alpha	alpha
(N)	(Nmm)	(Nmm)	(Nmm)	(mm)	(mm)	(mm)	(mm)	(mm)	(°)	(rad)
0	0	0	0	56	93	128	182	70	36.1	0.630
300	20154.19	43583.26	51919.23	56	93	128	182	70	36.1	0.630
500	25037.78	60368.43	82702.48	56	93	128	182	70	35.4	0.618
700	29090.54	75819.94	111327.35	56	93	128	182	70	35.3	0.616
900	33492.85	93710.29	144567.52	56	93	128	182	70	35	0.611
1100	38669.50	111361.28	177310.26	56	93	128	182	70	34.8	0.607
1300	44148.57	128794.89	209708.55	56	93	128	182	70	34.4	0.600

Table 4.4.1: Data for the validation of Cheetah Xtreme cat.5

Loadcell		shear	axial force	Forces at the foot clamp, on the socket				
GRF-V	GRF-L	S	N	F_{F_y}	F_{F_x}	M_{F_z}	e%_V	e%_L
(N)	(N)	(N)	(N)	(N)	(N)	(Nmm)	%	%
0	0	0	0	0	0	0	0	0
317.2	-102.7	-418.38	-234.27	476.07	-57.22	-92543.39	50.08	44.31
527.0	-207.7	-630.90	-248.29	658.10	-163.08	-132205.01	24.88	21.48
719.2	-309.8	-834.45	-264.23	833.72	-266.55	-170366.53	15.92	13.96
939.4	-431.1	-1075.31	-285.65	1044.68	-382.78	-215701.96	11.21	11.21
1149.5	-547.5	-1298.07	-295.83	1234.74	-497.91	-256956.13	7.42	9.06
1352.1	-661.5	-1511.54	-300.19	1416.79	-606.28	-296113.57	4.78	8.35

Table 4.4.2: Validation of Cheetah Xtreme cat.5

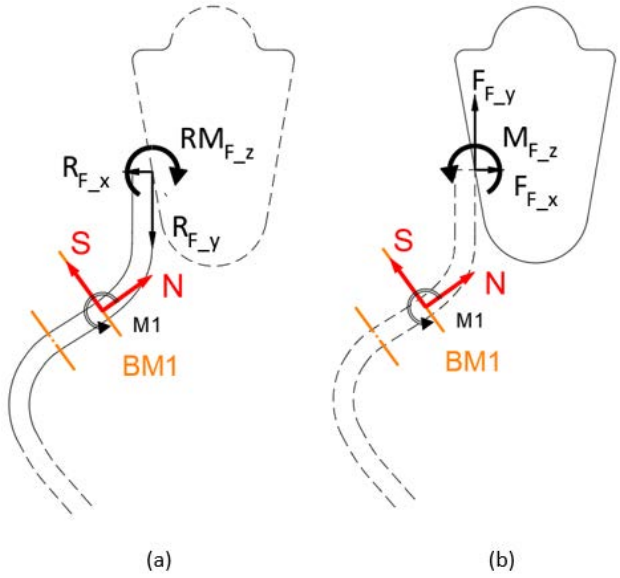

Figure 4.4.2: Reference system for Cheetah Xtreme cat.5
(a) Forces acting on the prosthetic foot
(b) Forces acting on the socket

For the forces at the foot clamp, acting on the socket on positive direction, reference is made like is shown in Figure 4.4.2 (b). For the forces acting on the prosthesis, the values are the same, but the direction is opposite Figure 4.4.2 (a).

In Table 4.4.2 it is shown the errors value for Cheetah Xtreme. On vertical force, it is less than 5% for the peak value that was applied (1300 [N]), and the error for the longitudinal force is less than 10% for the higher values. The results obtained are good, so the calibration coefficient could be used for the in-vivo tests.

In Table 4.4.3 and 4.4.4, it is reported the results for both Runner prosthesis, cat.3 and cat.4.

Loadcell		shear	axial force	Forces at the foot clamp, on socket				
GRF-V	GRF-L	S	N	F_{F_y} (V)	F_{F_x} (L)	M_{F_z}	e%_V	e%_L
(N)	(N)	(N)	(N)	(N)	(N)	(Nmm)	%	%
0	0	0	0	0	0	0	0	0
300.2	-42.5	-268.72	3.43	262.34	-58.31	-18514.24	12.61	27.16
505.6	-126.0	-462.68	62.45	439.58	-157.28	-31425.05	13.05	19.89
709.6	-208.8	-658.92	119.57	620.11	-252.87	-44509.23	12.61	17.42
910.1	-294.6	-855.22	179.95	796.62	-359.40	-57570.32	12.47	18.03
1116.5	-385.8	-1057.42	249.26	977.58	-473.92	-70967.67	12.44	18.60
1317.6	-477.5	-1251.89	326.76	1145.25	-602.00	-83766.17	13.08	20.68
1488.9	-559.0	-1414.97	399.00	1281.48	-720.53	-94441.26	13.93	22.41

Table 4.4.3: Validation table of Runner cat.3 prosthesis

Loadcell		shear	axial force	Forces at the foot clamp, on the socket				
GRF-V	GRF-L	T	N	F_{F_y} (V)	F_{F_x} (L)	M_{F_z}	e%_V	e%_L
(N)	(N)	(N)	(N)	(N)	(N)	(Nmm)	%	%
302.17	47.70	-289.75	-19.72	287.93	-37.94	-18971.96	4.71	20.46
506.31	118.11	-487.66	27.92	473.59	-119.63	-31502.67	6.46	1.28
714.21	179.34	-686.04	70.72	662.34	-192.25	-44097.87	7.26	7.20
917.04	236.81	-882.98	112.00	851.03	-260.65	-56609.74	7.20	10.07
1115.08	312.94	-1072.73	178.49	1029.17	-351.30	-68477.75	7.70	12.26
1326.19	396.54	-1274.57	251.11	1221.15	-443.15	-81089.23	7.92	11.75
1529.20	475.56	-1472.74	315.11	1410.91	-526.87	-93522.51	7.74	10.79

Table 4.4.4: Validation table of Runner cat.4 prosthesis

Analyzing the blade 3, the error which occurs between the vertical force on the foot F_{F_y} and the vertical ground reaction force GRF-V, is around 12% (e%_V). Instead, the error on the longitudinal forces, between GRF-L and F_{F_x}, is higher, around 20%.
For the blade 4, the error between the vertical forces (e%_V) is less than 8% for the biggest values, and the error between the longitudinal forces (e%_L) is around 11% in the peak values.

The whole procedure of data and plots, for the Runners RSPs, is reported in the "APPENDIX A".

The calibration of the Cheetah RSP is better than for the Runner prostheses, but the procedure was the same. Differences may lie in the different shape of the prosthesis and in the technology or arrangement of the carbon fiber, that could be cause a different reaction between the two types of prosthesis.

However the sensitivity coefficients of the calibration procedure are still good, and they should be used for the evaluation of the in-vivo running parameters.

CHAPTER 5:

IN-VIVO TESTS

The purpose of the in-vivo tests was to obtain all force parameters of a run for athletes with transtibial or transfemoral amputation. For measuring the ground reaction forces, a force platform (Kistler) was used. Moreover, athletes ran with RSPs on which were applied strain gauges bridges, with the purpose to measure the forces that act on the foot clamp, and also, by means video analysis of the run, it was possible to evaluate the forces on the ground (GRFs) and compare them with the ones of the force platform. If the comparison was good, that means having an error lesser than 10% between the two measurements, it could be possible to perform tests without the force plate, that will be better because the athletes can run without the limitation of hitting the FP with the affected leg (AF).
For the video analysis, two high speed acquisition cameras were used for the slow-motion videos in the sagittal plane, instead a common reflex camera was used for the frontal plane. With the slow-motion videos it was wanting to see the deformation of the prosthesis during loading and the movement of the whole-body while is running.

5.1: Set-up for the in-vivo tests

Tests were performed into a race track, where on one side near the boundary, there is a specific hole that has the purpose to hold the force platform. The problem of this hole is that it is too close to the boundary, so it was necessary to change the direction of running for the athletes depending on which was the AL, in this way athletes with right amputations ran from left to right, vice versa if the AL was the left one.

On the ground it was put the Optogait running data acquisition system, which is composed by two rails, with infrared sensors and receivers, that were placed parallel to each other to form a corridor within the athletes will run. This system can measure all the parameters of the running, like the speed, time of contact, time of swing and frequency of steps.

Three cameras were used for the tests, two of them placed orthogonal to the running direction, for filming the slow-motion on the sagittal plane, and one almost in the same direction.
The videos on the sagittal plane were focused to catch the movement of the body (**Camera 1**) and of the prostheses (**Camera 2**) during loading. As background was put a whiteboard with a grid of 5x5 [cm] as reference for the video analysis.
The last camera was put on the frontal plane for having a panoramic view of the athlete, in this way it was possible to see with which step he/she entered on the Optogait system and for correlate the step number of the of the SoMat acquisition with the step on the force platform.

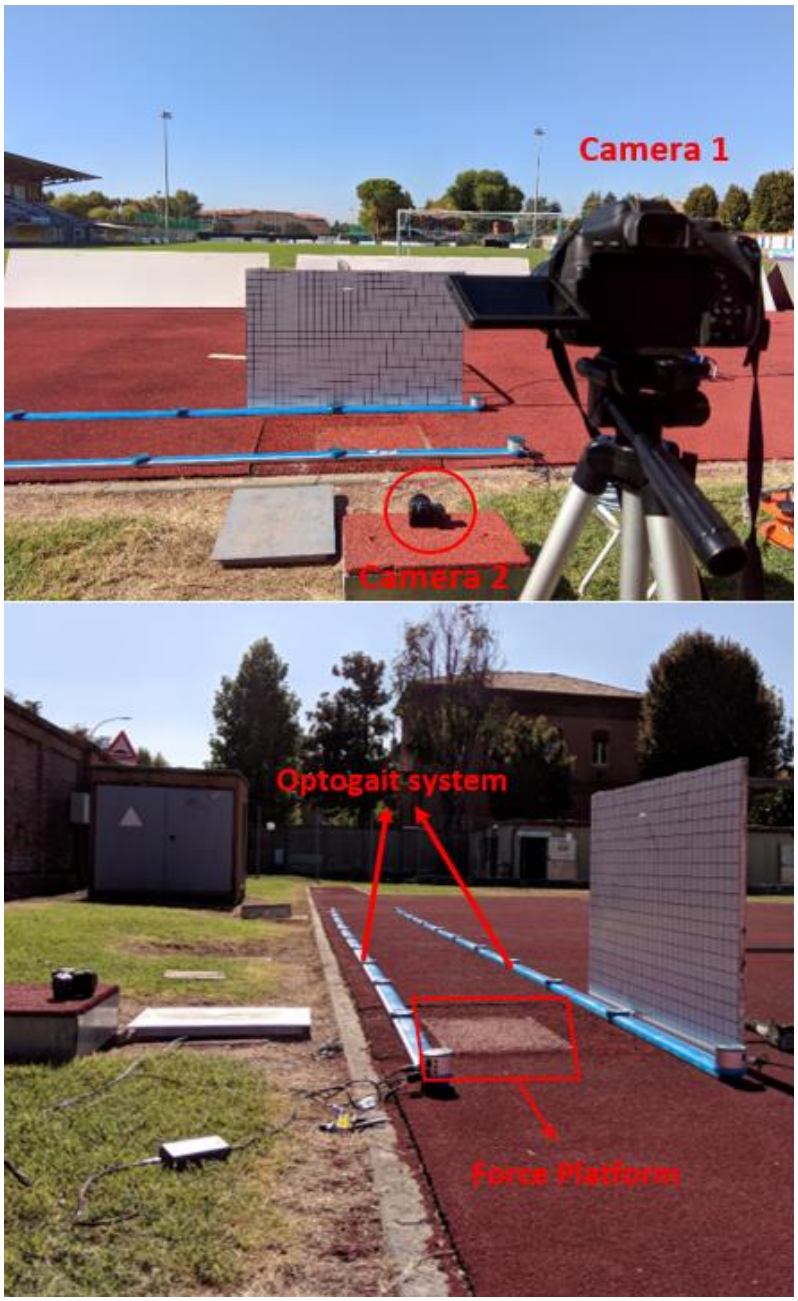

Figure 5.1.1: In-vivo test environment and disposition of the instrumentation

5.2: Methodology

For the in-vivo tests, it was planned to perform sprint discipline of athletic with 2 different amputee-athletes:

- Contraffatto Monica: Transfemoral amputee and bronze medalist at the 2016 Paralympic Games on the 100 meters category T42
- Manigrasso Simone: Transtibial amputee and silver medalist in the 400 meters at the 2017 World's Championships

The athletes used their own RSP in the few first attempts for warming up and after they wore the instrumented prosthesis design with the SG bridges.

During the run, athletes have to hit the force-plate placed on the ground, so, in this way, the GRFs were measured. Moreover the SoMat acquisition system has acquired the signals from the bridges during all the performance.

Contraffatto performed 3 runs with the instrumented Runner cat.3 prosthesis, on which two of them are valid and in the other one she hit the force-plate with the unaffected leg (UL).
With these two valid datasets it is possible to calculate the average forces trend, both for SoMat acquisition and for the Force Platform. Once the SoMat data are transformed into the GRFs on the foot clamp, they are compared with the GRFs on the tip of the foot for the evaluation of the dynamic validation of the strain gauge system. It is also possible to compare the step of the AL with the one of the UL.

For the tests with Manigrasso, which ran with the Cheetah Xtreme cat.5 prothesis, it was planned different adjustment for the attachment of the prosthetic foot to the socket, because this is a future purpose for the analysis of the performance, but, for now, it is required to make an evaluation of the dynamic validation of the strain gauge system.
For him was made 5 different tests, which means 5 different set-up adjustments for the attachment of the prosthesis to the socket:

Configuration	Set-up	Image
0	Base adjustment	
1	Foreward displacement of the foot of 2.5 [cm]	
2	Backward displacement of the foot of 4.5 [cm]	
7	Foreward diplacement of the foot of 2.5 [cm] and Backward rotation of the tip about +4°	
8	Backward displacement of the foot of 4.5 [cm], with forward rotation of the tip about -6°	
9	Backward displacement of the foot of 6.5 [cm], with forward rotation of the tip about -6°	

Table 5.2.1: Set-up adjustments of the prosthesis

All these set-up adjustments were made on the instrumented prosthesis and he ran with them and gave feed-back for each one.

In the third test with configuration 2, while Manigrasso was breaking after the run, he cut with the sole of the UL a wire of the strain gauge system and so the SoMat didn't acquired the right data for the following runs. However is always possible to evaluate the first two datasets.

5.3: Dynamic validation

For the dynamic validation, data obtained during a sprinting performance is analysed. For a few runs both force plate and SoMat data of a corresponding step are collected. This data is separately processed and afterwards compared. The dynamic validation is done using MATLAB 2018b (APPENDIX).

5.3.1: Force plate data

The raw measurements acquired with the force platform have a total duration of three seconds. In this time the ground reaction forces of one step, with a duration of roughly 0.14 seconds, are measured. Because the only interest is in the actual contact phase of the step and therefore the raw signal is cut.

Assuming that there is no force on the force plate when there is no contact, a zero adjustment of the force plate data is made before cutting it down. The selection of the starting and ending point of the contact phase is based on the fact that the ground reaction force in the y-direction is always positive during the contact phase. Only y-forces greater than zero are relevant and therefore all the other data is removed with the help of a threshold. The selected datapoints are also used for the shortening of the forces in the other direction. Figure 5.3.1.1 and 5.3.1.2 show the ground reaction forces of one step after reducing the signal for orientation 1 of Manigrasso's in vivo test and orientation 3 of Contraffatto's in vivo test.

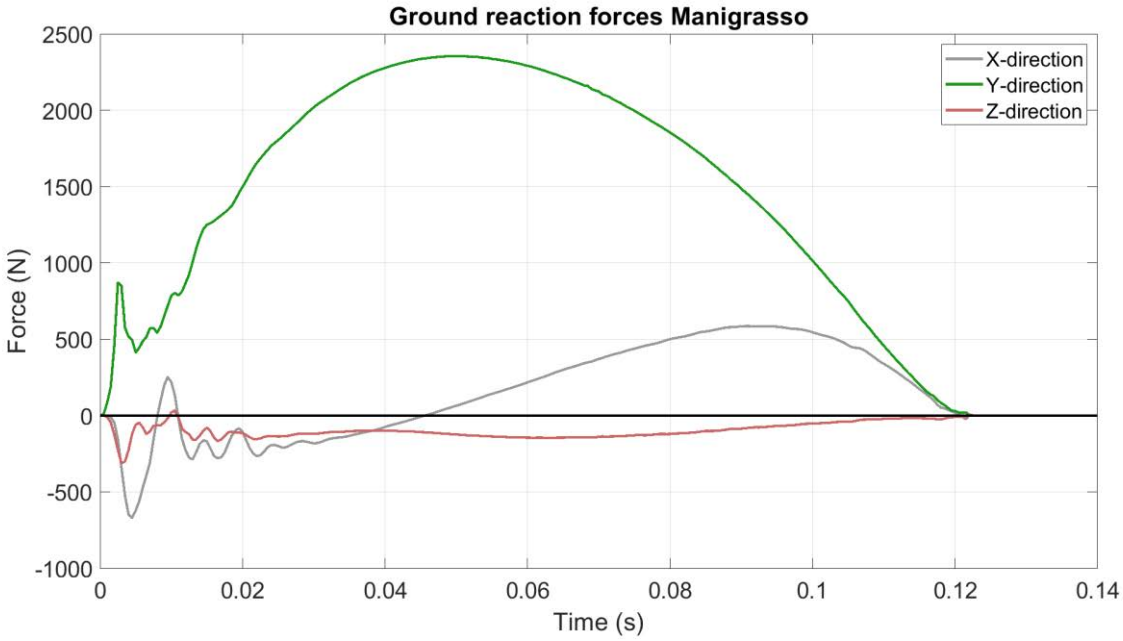

Figure 5.3.1.1: Ground reaction forces measured by the force platform during Manigrasso's in vivo test, configuration 0

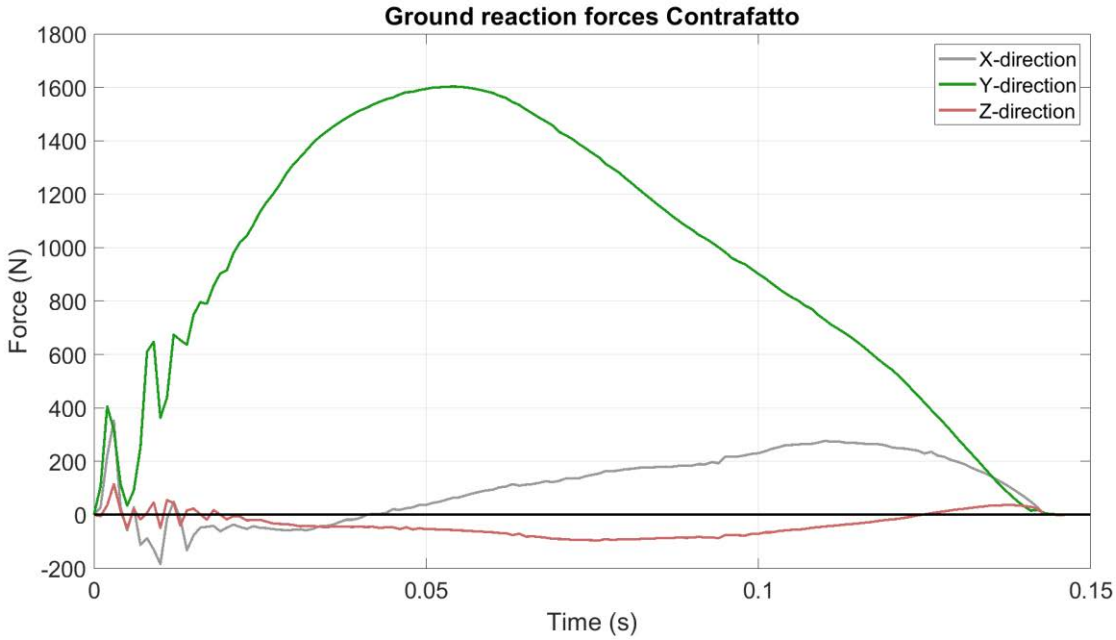

Figure 5.3.1.2: Ground reaction forces measured by the force platform during Contraffatto's in vivo test, orientation 3

In these two plots, it is possible to see, in the first 0.02 [s], the initial vibration of the prosthesis due to the landing on the ground. It is present in all the directions, but, with a different width and frequency and this is probably due to the behaviour of the carbon fibre layup.

5.3.2: SoMat data

In contrast to the force plate, the SoMat data contains a measurement of every step of the prosthetic leg during a run. It has information about the bending of the prosthesis at the location of BM1, BM2 and BM3 given in voltages. Before analysing the SoMat data, a zero adjustment is made. Only a small part of the SoMat data contains information about the actual sprint. Using a threshold of $\frac{1}{2} * maximum\ value$ of the SoMat data, only the steps during the sprint are selected (Figure 5.3.2.1). The rest of the data, during the start and recovery, is not of interest.

Like in the static calibration, the voltages of the data are translated to bending moments by multiplying them with the calibration coefficients (Table 5.3.2.1). Thereafter, the forces acting on the clamp of the socket can be calculated using equations formulated in the paragraph "Calculation of forces".

Table 5.3.2.1: Calibration coefficients

Calibration Coefficients [Nm*V/mV]			
Location/prosthesis	Runner cat. 3	Runner cat. 4	Cheetah cat. 5
Bridge 1	$5.86*10^4$	$7.03*10^4$	$1.74*10^5$
Bridge 2	$6.01*10^4$	$7.86*10^4$	$1.30*10^5$
Bridge 3	$4.82*10^4$	$7.05*10^4$	$8.64*10^4$

For the validation of the strain gauge bridge system, only the forces of the step that corresponds with the step on the force plate should be determined. Considering all steps of a run have a similar gait pattern, a pattern detection algorithm is used to distinguish individual steps. To remove the noise (high frequencies) that makes gait detection difficult, the data is first filtered with a 2nd order Butterworth filter with a cut off frequency of 30 Hz.

The step recognition is based on the fact that every step has its own maximum peak. After counting which particular step is of interest within the video footage, this same step can be determined in the SoMat data using the maximum peaks. In Figure 5.3.2.2 a selection of the 8th step is visualised.

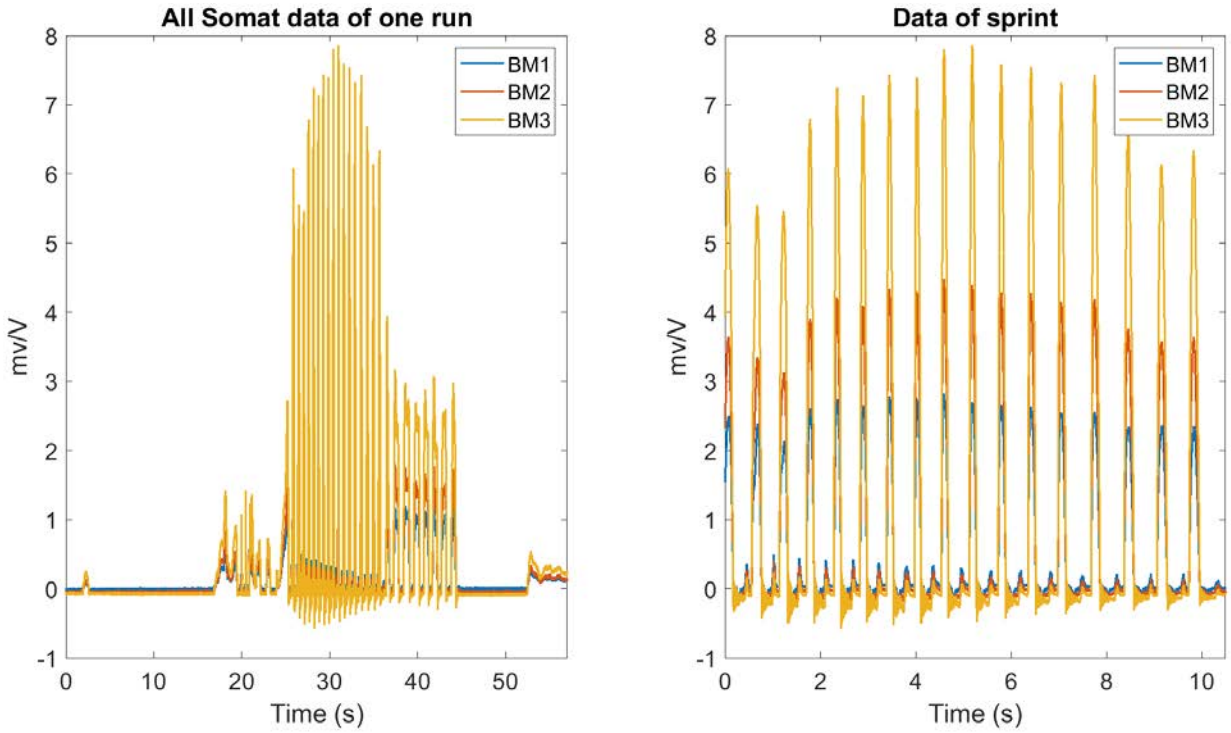

Figure 5.3.2.1: The right image shows the full SoMat data and the left image shows only data of the sprint that is acquired after applying a threshold.

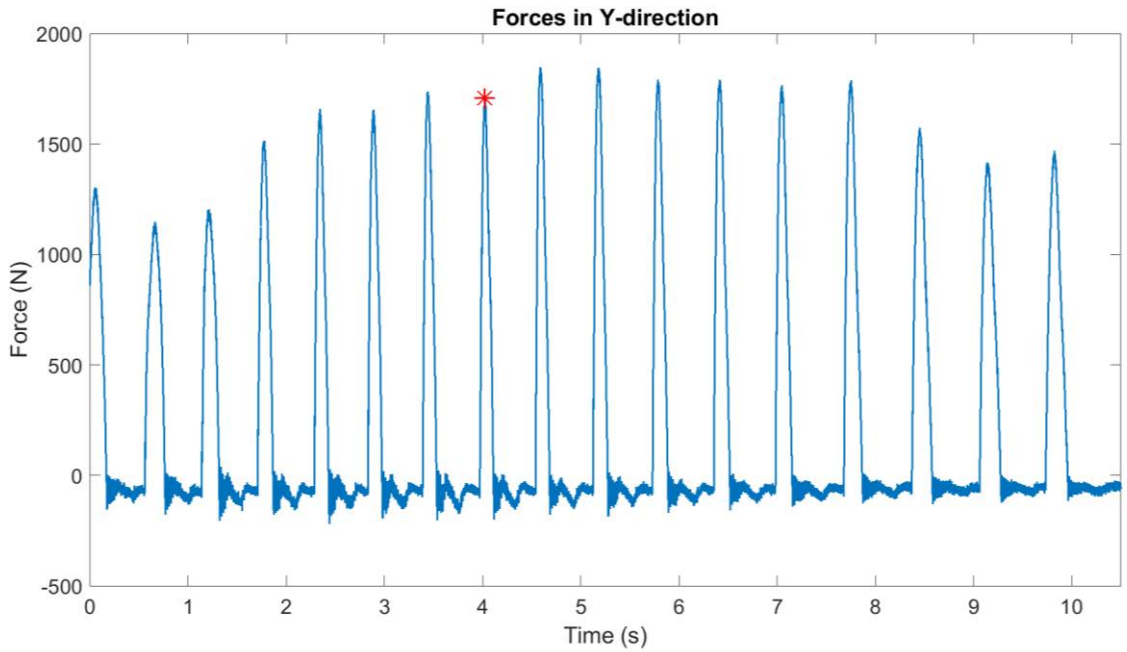

Figure 12.3.2.2: Selection of the 8th step of a run

After selecting the peak of interest, the first minimum peak before and after this maximum peak are selected. Assumed is that the locations of these minimum peaks are respectively the starting point and the ending point of the force plate contact. The values of the starting and ending point are used to cut the raw signal. However, using a filtered signal for the selection of the starting and ending point of a step creates a small offset and slightly overestimates the contact time. To correct for this offset, all values underneath a threshold are removed. The threshold is obtained by taking the maximum of the constant part of the overestimated graph. Now only the points of interest are selected and the forces of one particular step can be seen like in Figure 5.3.2.3 and 5.3.2.4.

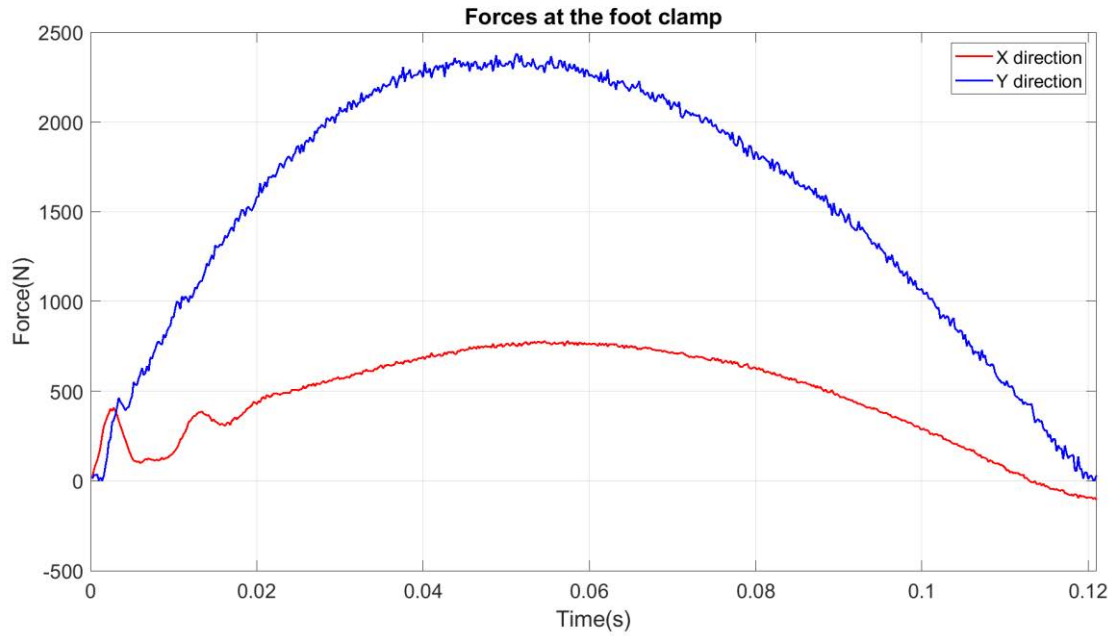

Figure 5.3.2.3: Forces acting on the socket calculated with the SoMat data, trial 3, step 8, Manigrasso

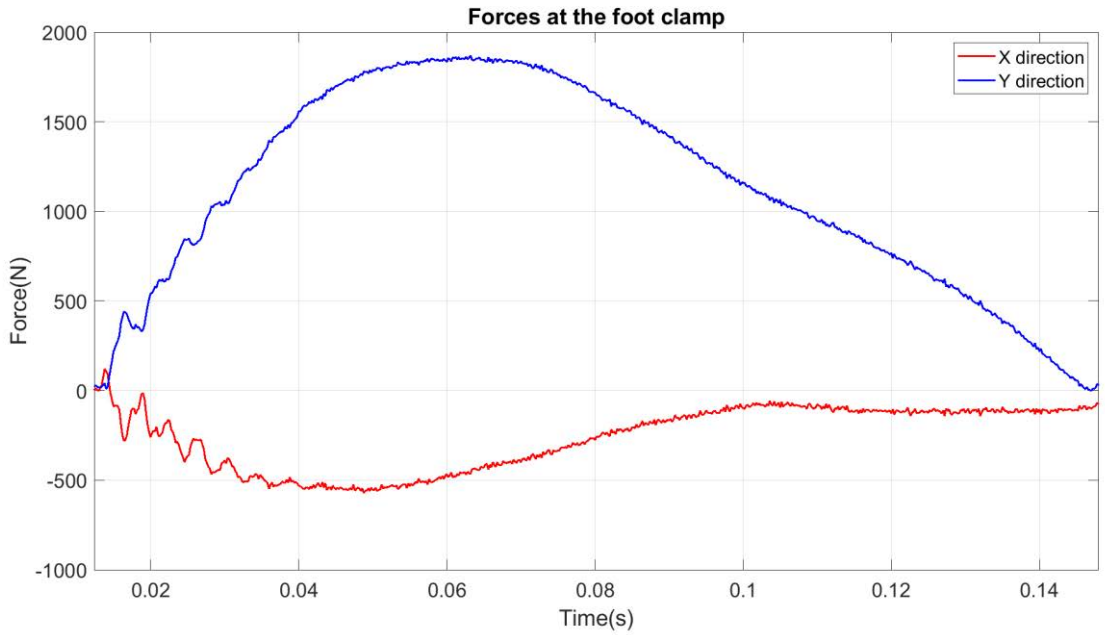

Figure 5.3.2.4: Forces acting on the socket calculated with the SoMat data, trial 3, step 8, Contraffatto

5.3.3: Comparison

To validate the forces calculated with the SoMat data, they are compared with the ground reaction forces measured by the forceplate.
Because the X_F and Y_F directions of the foot clamp change during stance phase with respect to the global reference system (GRS), a comparison between forces acting at the clamp of the foot and the ground reaction force cannot directly be made. First the forces acting at the clamp need to be rotated using angle theta (Figure 5.3.3.1). Theta is measured for every 10 percent of the contact phase of the step within the in the high-speed video footage using Kinovea. The measured angles used for the validation of some of the runs can be found in Table 5.3.3.1. Per athlete only the data of some of the runs contain both forceplate information and SoMat information and therefore can be validated. For the Runner cat. 4 there is no data available for accomplishing a validation at all.

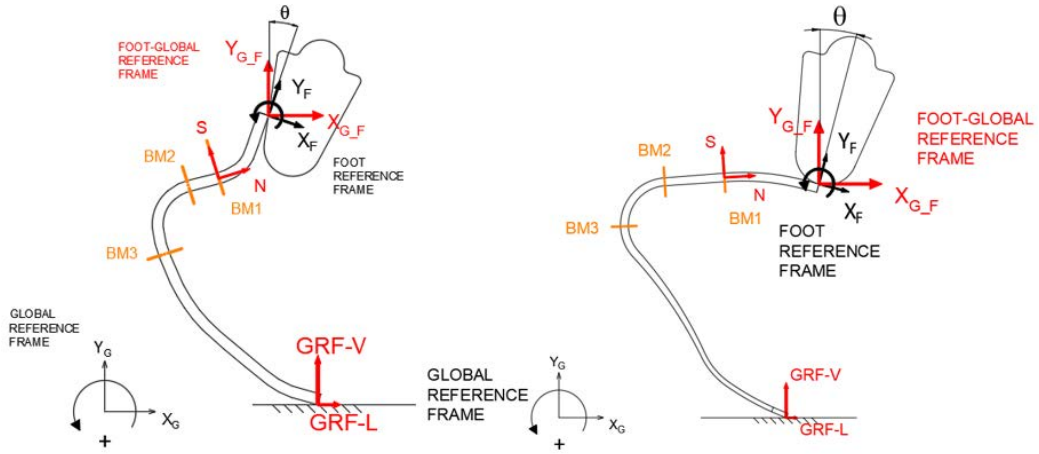

Figure 5.3.3.1: Reference frames and angle theta. Left= J-shaped Cheetah Xtreme(Össur), Right= C-shaped Runner(Ottobock).

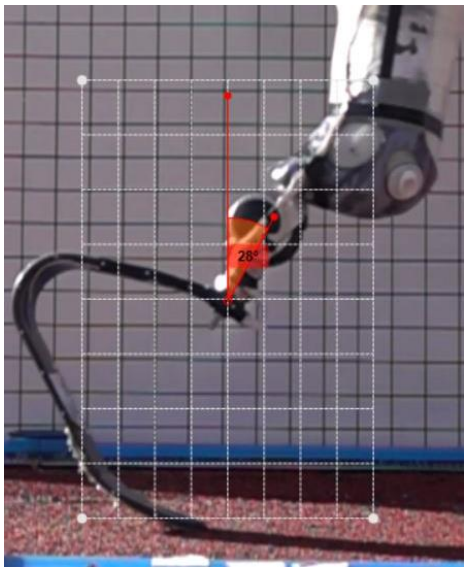

Figure 5.3.3.2: Measurement of the angle alpha at 80 percent of the contact phase

Table 5.3.3.1: Angle theta for every 10 % of the contact phase

		Angle theta										
	% of CP	**0%**	**10%**	**20%**	**30%**	**40%**	**50%**	**60%**	**70%**	**80%**	**90%**	**100%**
Manigrasso (Cheetah Xtreme cat. 5)	Run 1	-4°	4°	10°	17°	23°	29°	35°	41°	46°	48°	52°
	Run 2	-3°	5°	11°	19°	25°	31°	37°	42°	48°	49°	52°
	Run 3	-2°	8°	14°	19°	24°	33°	37°	42°	45°	48°	50°
Contrafatto (Runner cat.3)	Run 1	-20°	-10°	-9°	2°	6°	12°	18°	24°	28°	32°	36°
	Run 2	-18°	-13°	-5°	2°	6°	14°	20°	22°	24°	29°	31°

With the equations:

$$F_{Y_{G\_F}} = -F_{Y_F} * \cos\theta - F_{X_F} * \sin\theta$$

$$F_{X_{G\_F}} = F_{Y_F} * \sin\theta - F_{X_F} * \cos\theta$$

the forces acting at the clamp of the foot with respect to the global reference system are calculated for every ten percent of the contact phase. A validation can be made by overlaying the graphs of both the ground reaction force for every 10 % of the stance phase and forces acting at the foot clamp rotated to the GRS.

In Figure 5.3.3.3, 5.3.3.4, 5.3.3.5 and 5.3.3.6 the validation and the error of the validation in Y-direction, of respectively the Cheetah cat.5 and Runner cat.3, are shown. The first 10 percent and final 10 percent of the contact phase represent respectively the landing and taking of the athlete on the ground. During these events many force fluctuations occur, which makes a reliable comparison impossible. Therefore, the calculated mean error for these phases is removed.

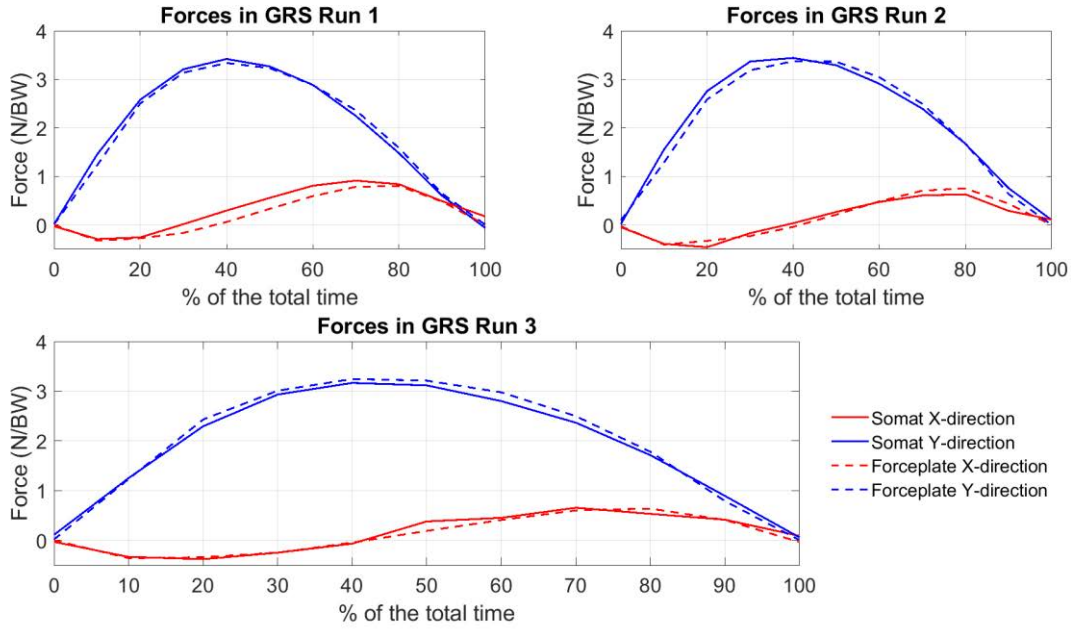

Figure 5.3.3.3: Dynamic validations of Cheetah cat.5, realized by using data acquired during the in vivo tests with Manigrasso

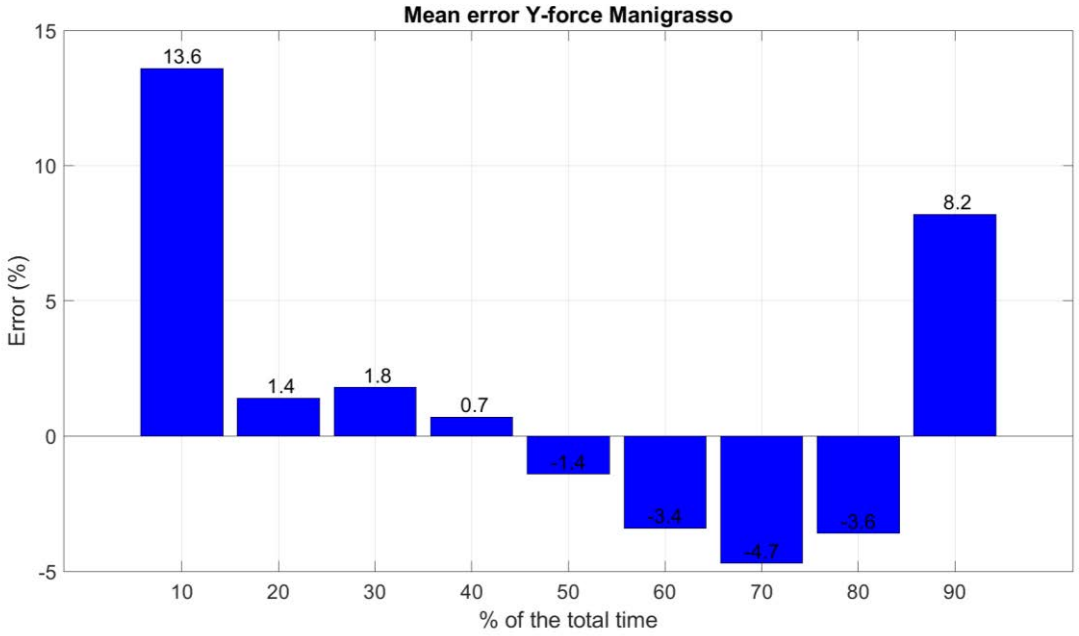

Figure 5.3.3.4: Mean error validation y-direction, Manigrasso

In Figure 5.3.3.3 it is possible to see three different runs for the athlete Manigrasso, with the Cheetah Xtreme cat. 5 prosthetic foot. As mentioned before, Manigrasso has a transtibial amputation.
All the three plots are normalized by the Body Weight of the athlete, but they refer to different prosthetic foot configuration. Run1 refer to configuration 0, where the foot is in the same configuration which the athlete runs in his competition, instead Run2 and Run3 refer to configuration 1, where the foot is moved forward of 2.5 [cm] respect to the previous adjustment.

In both case, it is possible to see that the trend of the SoMat curves is close to the trend of the Forceplate, and the error that occurs is shown in Figure 5.3.3.4. It is less than 5% in the middle time percentage of the stance phase, but in the landing and taking, first and last 10% of time, the error reaches its peaks and that is due to the force fluctuations.

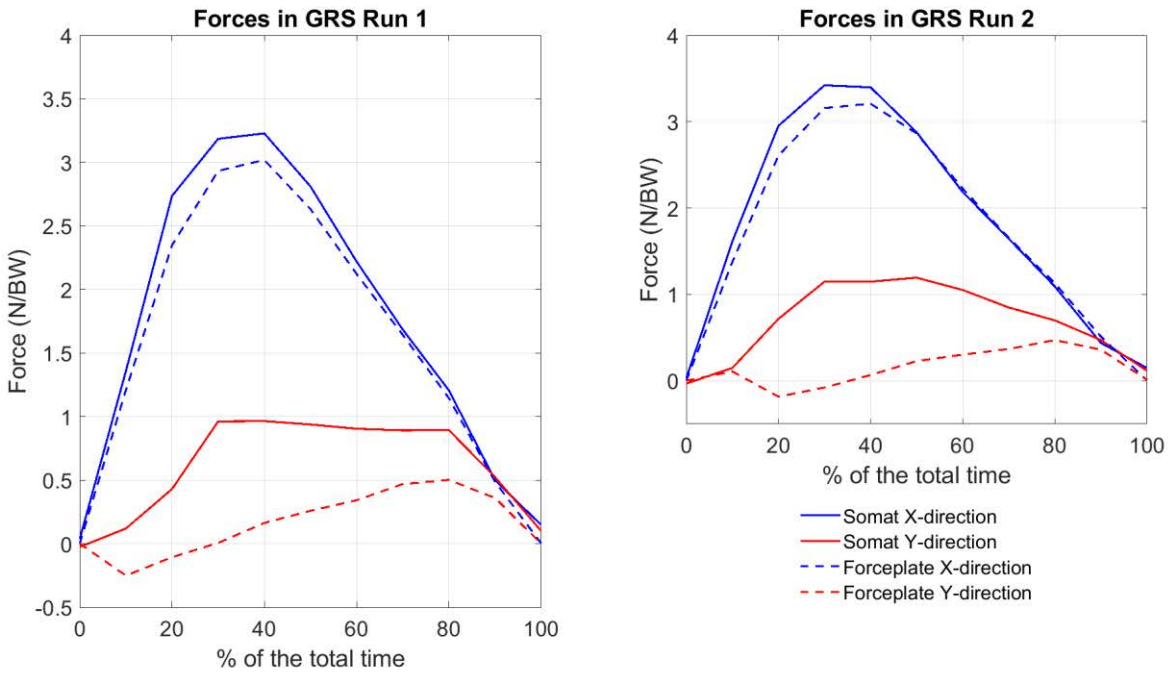

Figure 5.3.3.5: Dynamic validations of Runner cat. 3, realized by using data acquired during the in vivo tests with Contraffatto.

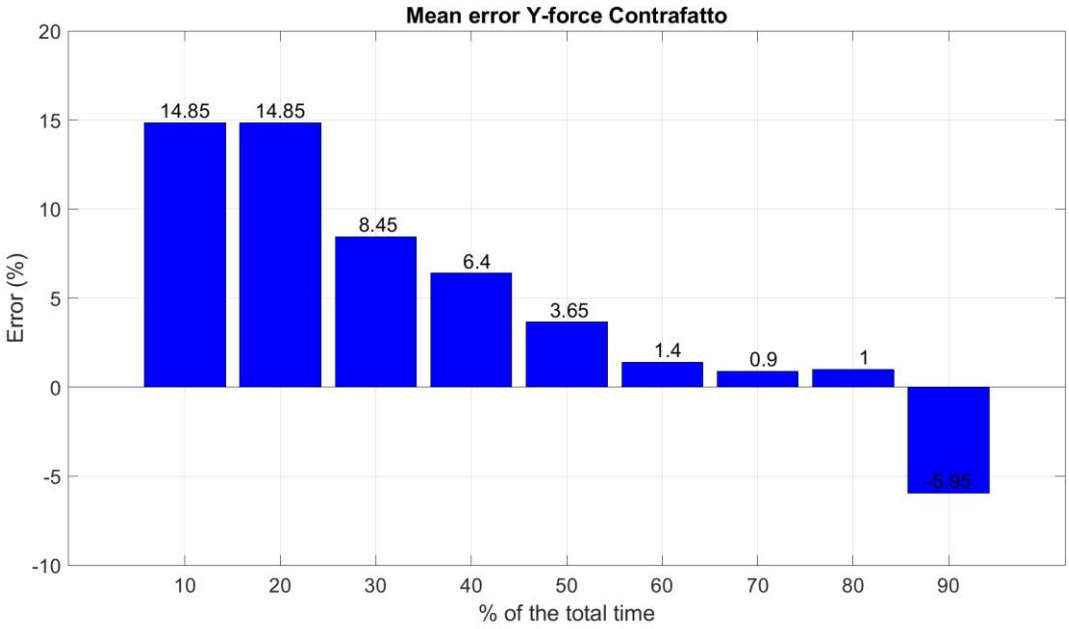

Figure 5.3.3.6: Mean error validation y-direction, Contraffatto

In Figure 5.3.3.5 it is possible to see two different runs for the athlete Contraffatto, which runs with the Runner cat.3 prosthetic foot. She is a transfemoral amputee, so she uses a mechanic knee with one rotation axis.

In her case, the two plots refer to the same configuration of the prosthetic foot.

There is a considerable difference in the first 40% of time, between the forces read by the SoMat and by the Forceplate. This could be due to the calibration procedure, because

already in the validation, the error was about 13% for the maximum load.
In the first and last 10% of the stance phase, the error is due to the force fluctuation during landing and taking.

About the longitudinal force, drawed with the red line, the error isn't calculated, but it is possible to see the huge difference between the force of the SoMat and of the Forceplate during all the stance phase. Also here, it could be possible that the big error that occurred in the validation procedure influence the SoMat data.

5.4: Result of the in-vivo tests

Using the calculations explained before, forces during every step of the run can be calculated from the SoMat data. Figure 5.4.1 and 5.4.2 show the forces acting on the socket in different reference systems. In addition, the moment acting at the foot clamp during the contact phase is plotted. These plots and calculations can be made for every run when using a RSP with strain gauge bridges.

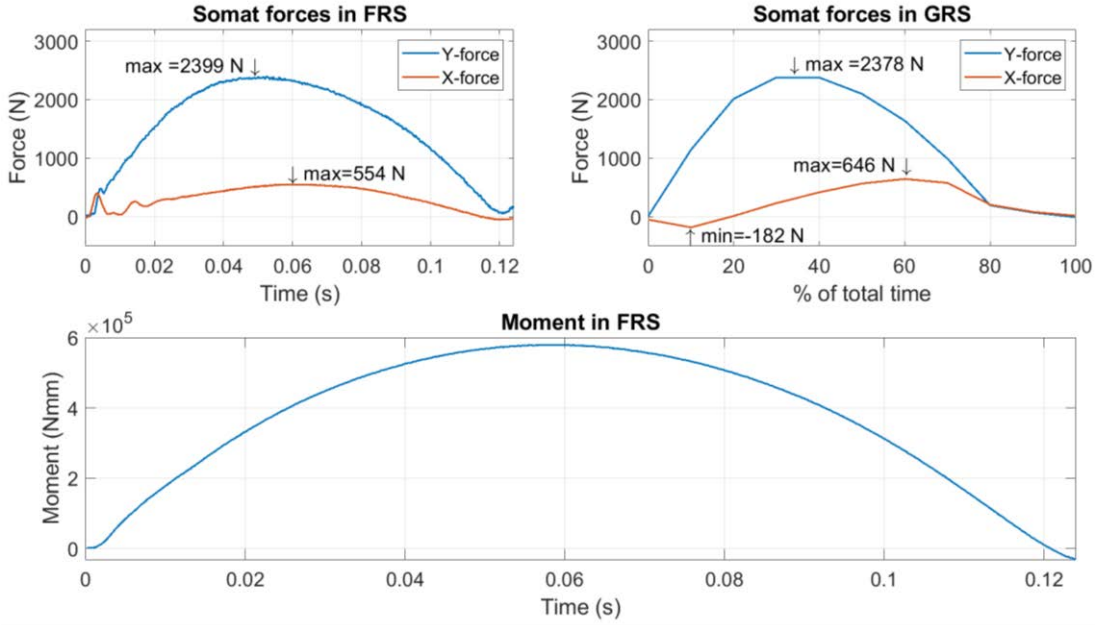

*Figure 5.4.1: Analysis of the SoMat data of **configuration 1, trial 1, Manigrasso's** in vivo test. Upper left: Forces on the foot clamp in the reference system of the foot clamp. Upper right: The forces on the foot clamp rotated to the global reference frame for every 10% of the contact phase. Below: Moment acting on the foot clamp related to the reference system of the foot clamp.*

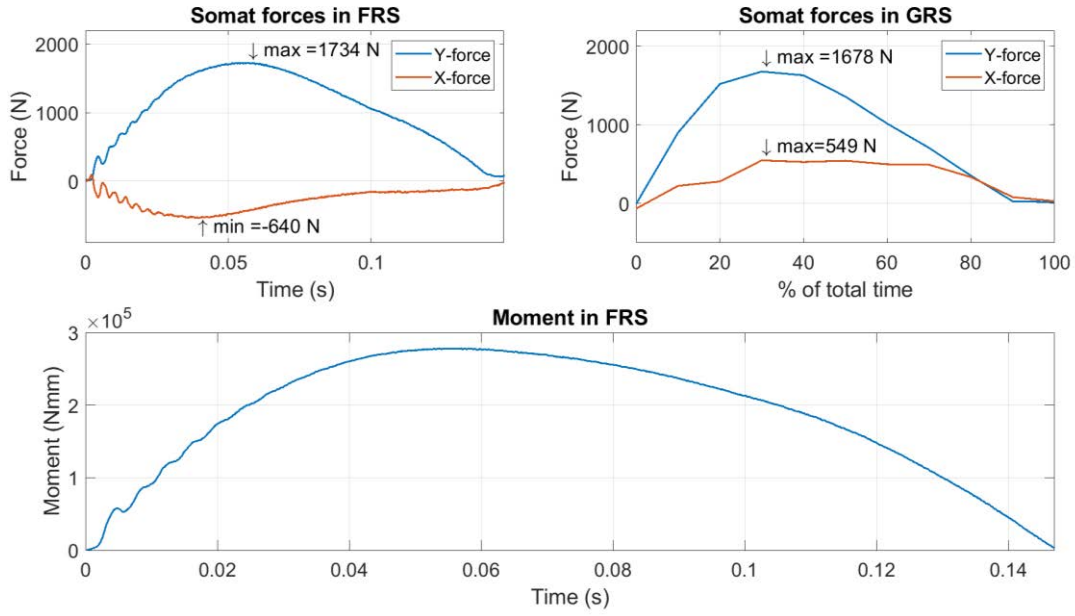

*Figure 5.4.2: Analysis of the SoMat data of **configuration 3, trial 2** of **Contraffatto's** in vivo test. Upperleft: Forces on the foot clamp in the reference system of the foot clamp. Upperright: The forces on the foot clamp rotated to the global reference frame for every 10% of the contact phase. Below: Moment acting on the foot clamp related to the reference system of the foot clamp.*

In Figure 5.4.1. it is shown the forces read by the SoMat in the two different reference system, Foot reference system (**FRS**) and Global reference system (**GRS**), and it is also reported the maximum and minimum values of force for Manigrasso step. For both forces in the **FRS**, the trend is always positive, that isn't surprise for the vertical load, but isn't usual for the longitudinal force, that in the Global Reference system has a first negative trend and after it changes the sign.
The positive value means that the athlete is always press his stump against the backward section of the stump, so he is pushing the prosthesis backward, so that the RSP gives him a forward reaction because it can't slide on the ground.

In the third graph, it is plotted the moment acting at the foot clamp, in the Foot Reference System. It is always positive, except in the last few milliseconds.
The almost always positive value is due to the configuration, because the vertical force is forward respect to the foot clamp reference point for the majority of time during the stance phase. When it moves backward, during stance, it generate a negative moment, but there is the positive longitudinal force (Pushing) that create a positive moment, bigger than the negative one, so the moment at the foot clamp stay positive.

In Figure 5.4.2 it is shown the forces and moment at the foot clamp in two reference systems, the Foot Reference System (**FRS**) and the Global Reference System (**GRS**) for Contraffatto step.

For the longitudinal force in the **FRS**, it is possible to see a different trend compared with the Manigrasso's result. For her the force is always negative and has a peak in the first phase of the stance and after tend to zero.

Speak about the moment at the foot clamp, for a transfemoral amputee, like Contraffatto, that has to wear a mechanical knee, it must be always positive. That means that the knee has the tendency to extend, otherwise, if the moment is negative, the knee close and the athlete fall down.

5.5: Comparison between Affected and Unaffected Leg

From the datasets of Contraffatto is possible to compare the steps of the affected leg (AL) with the unaffected leg (UL), the results are show in Figure 5.5.1 for the vertical force and in Figure 5.5.2 for the longitudinal, where both are normalized by the Body Weight (BW) of the athlete:

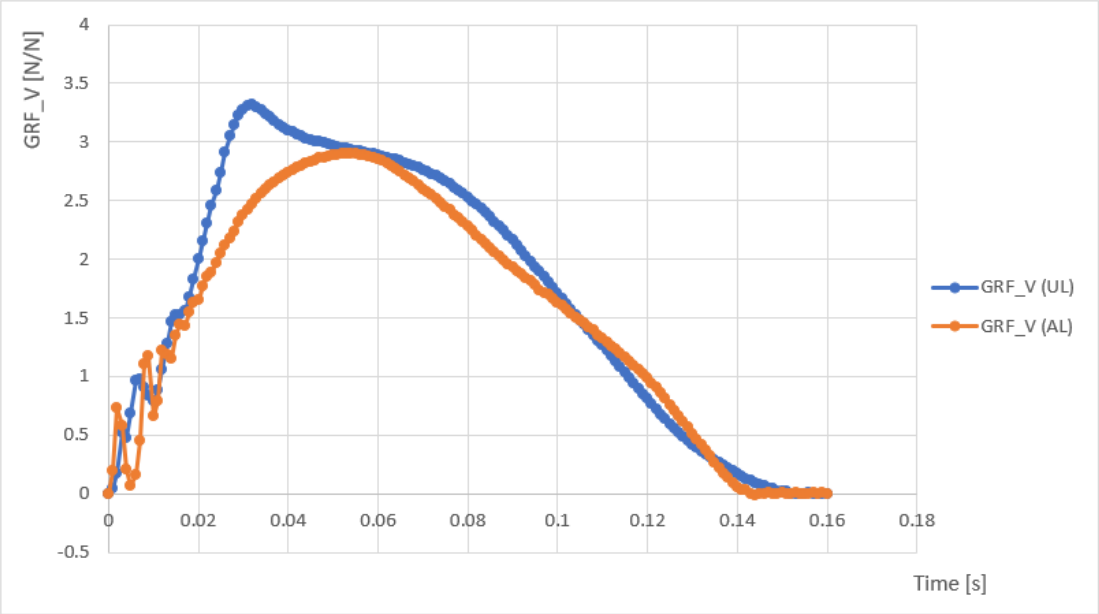

Figure 5.5.1: Comparison between vertical forces of UL and AL

As is possible to see in Figure 5.5.1 for the vertical force, the Unaffected Leg reach a peak of value bigger than the Affected Leg and the difference is about 14%. This data suggests that the RSP or muscle weakness/impairment due to the prosthesis, could limit force production.

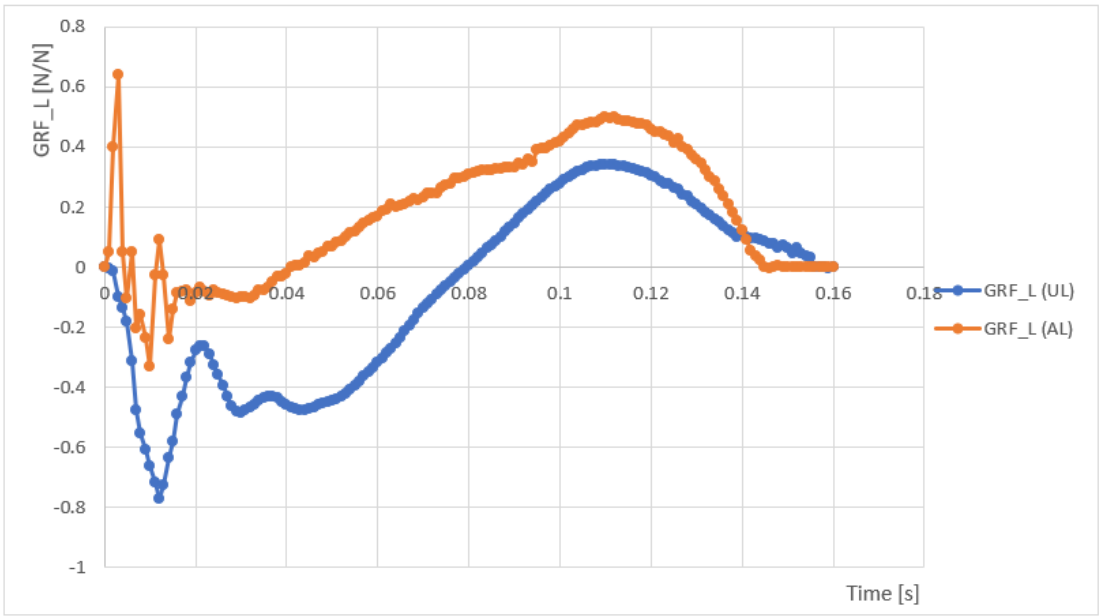

Figure 5.5.2: Comparison between longitudinal forces of UL and AL

For the longitudinal loads, it is possible to see, in Figure 5.5.2, that the prosthetic foot generates less breaking than the unaffected foot, and this is in according with the Makimoto's studies [19]. For the AL, the breaking phase during landing goes from 0 to 0.04 [ms], instead for the UL, it goes from 0 to 0.08 [ms], so the UL employs the double time of breaking compared to the AL.
Conversely compared to the Makimoto's studies [paragraph 1.2], the propulsive impulse is higher for the Prosthetic limb than the Intact limb.

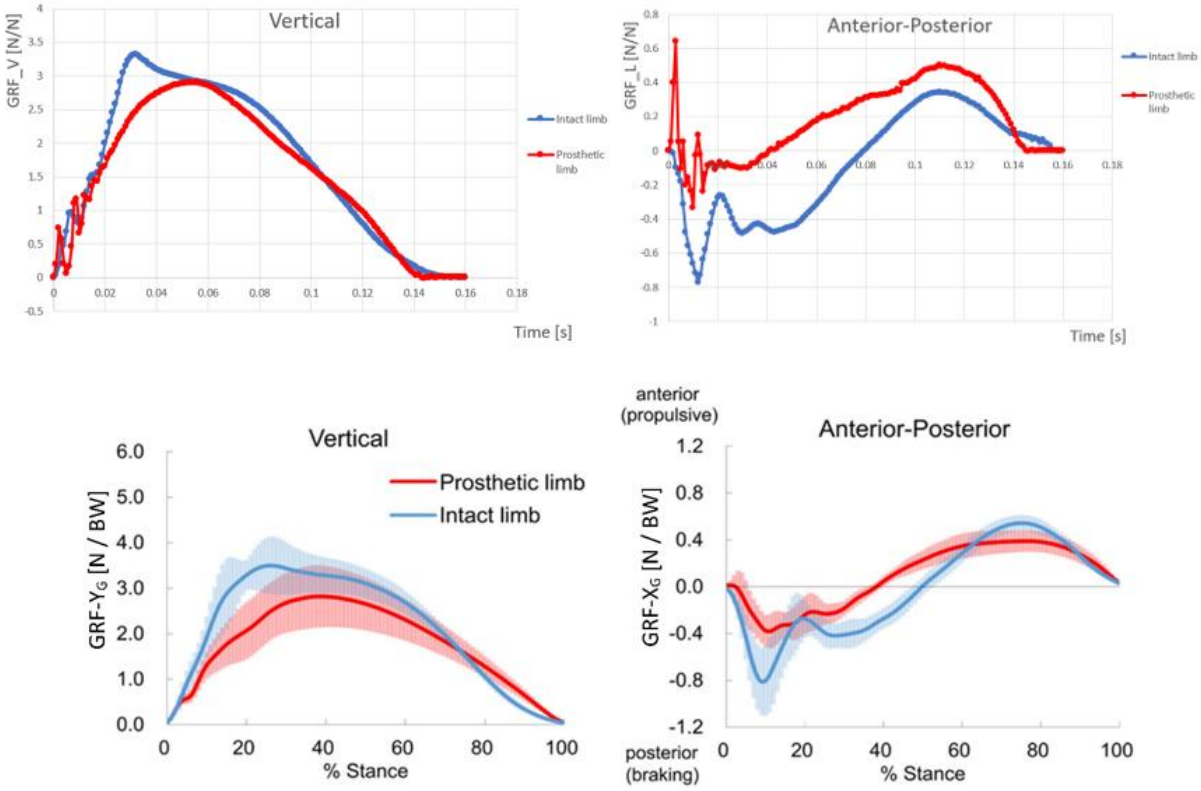

Figure 5.5.3: Comparison between the forces read by the forceplate at the Contraffatto's step (Upward plot) and Makimoto's studies (Downward plot).

In both the pictures is possible to see, for the AL, an initial dumping trend. It is due to the prosthesis vibration generate during landing.

For a comparison of the values of load applied by the Intact limb (UL) and by the Prosthetic limb (AL), in Figure 5.5.4 are shown the vertical step loads in [N], and in Figure 5.5.5 are shown the longitudinal step loads, in [N].

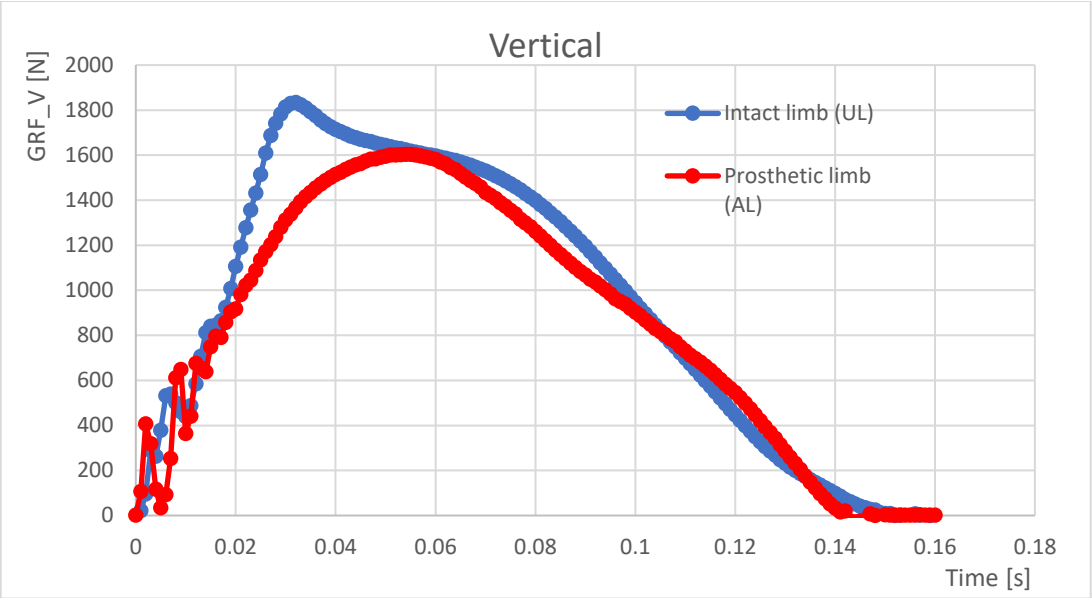

Figure 5.5.4: Values of load for the Affected leg (AL) and for the Unaffected leg (UL)

An important difference of force values could be seen between the unaffected leg and the affected leg, where the intact limb reaches a peak about 1830 [N], instead the prosthetic limb reaches a peak about 1600 [N].

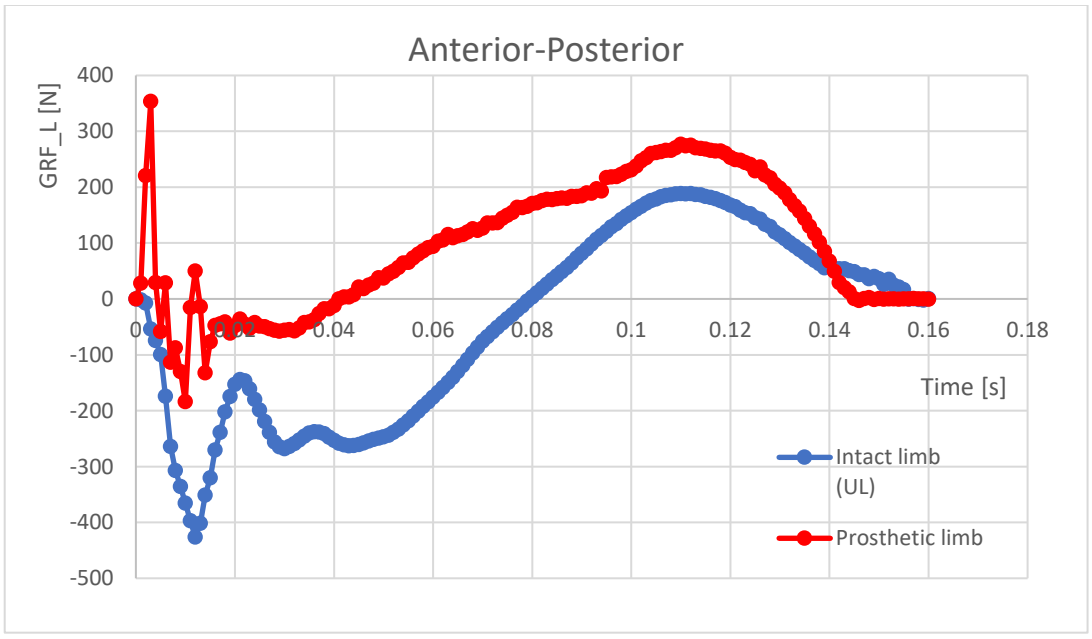

Figure 5.5.5: Values of load for the Affected Leg (AL) and for the Unaffected leg (UL)

About the longitudinal forces is possible to see a higher peak in the breaking phase for the unaffected leg, about -430 [N], instead for the affected leg, the mean values in the landing zone are under -100 [N]. Concerning the pushing phase, the peak for the Prosthetic limb is about 275 [N], and for the Intact limb, it is about 200 [N].

CHAPTER 6:

IN-VITRO DROP TEST

6.1: Drop test method

In order to evaluate the energy absorption of the RSP during different phase of running, a pilot drop test was performed. The prosthesis that was used is the Cheetah cat. 5. The sledge, where the RSP was fixed, was lifted at 0.226 [m] from the ground and its weight is of 18.5 [kg]. The tip impacted on a 3-axes load cell covered with a layer of tartan. The test was repeated two times for each different inclination of the α angle, that is the angle between the ground and the axis of fall of the prosthesis.

The α angle, during the stance phase of Manigrasso's run, with the Cheetah cat.5, was analyzed every 10% of the total time for understand how it was changing.
In this way it is possible to define a set of inclination angles for the ground of the bench test so as to simulate, as much as possible, the real condition of a run.

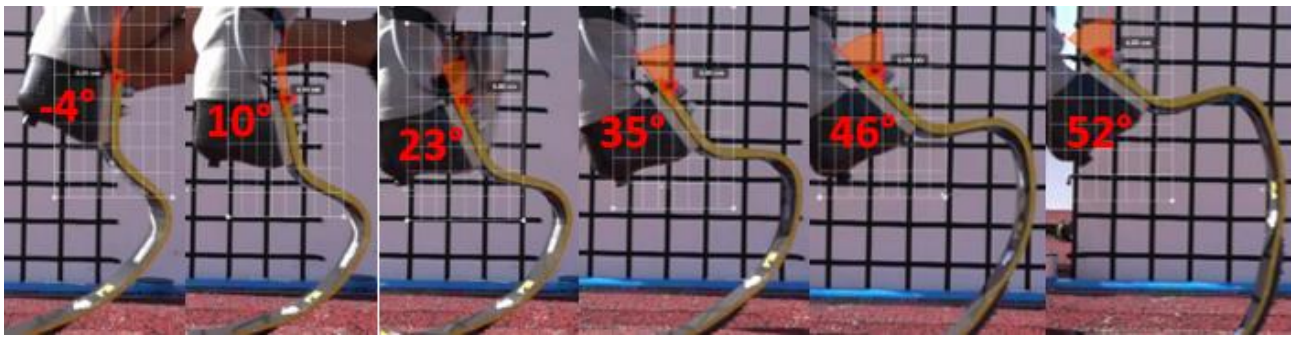

Figure 6.1.1: α angles for 0, 20%, 40%, 60%, 80% and 100% of the stance phase

The set of impact angles is defined to:

$$-10°, -5°, 0, 5°, 10°, 15°, 20°, 25°, 30°, 35°, 40°$$

And for each angle value two drops are performed and the mean values were calculated. This sequence of values gives a good representation of the rotation of the prosthesis, but the higher field angles can't be reached because the horizontal sledge rotation is limited to 40°.

For every test, the initial height of the drop, was set always to the same value, equal to 0.226 [m], so that the initial potential energy (E_i) is fixed.
The rebound potential energy (E_R) is define like the energy that the prosthesis has at the maximum height of the first rebound on the ground, and it is different from the initial cause the dissipation due to the behavior of the RSP, but also by the effect of the tartan and friction of the rails of the sledge.

The height of the rebound is measured with a ruler placed sideways to the sledge from a high speed video analysis.

6.2: Results

The difference between the initial and the rebound potential energy is the energy absorbed by the RSP, plus the effect of the tartan and friction on the rails.

$$E_a = E_i - E_f \quad [J]$$

The dissipation of the tartan depends also from the inclination angle, because bigger it is and bigger is the contact surface of the sole and it is expected that the absorption of energy increases.
However, for a first analysis, the amount of energy dissipation is compared through the different angles, without considering the effect of each component of dissipation (Figure 6.2.1). Also the energy ratio, between the energy of the first rebound and the initial energy, is plotted, with the trend along different field angles.

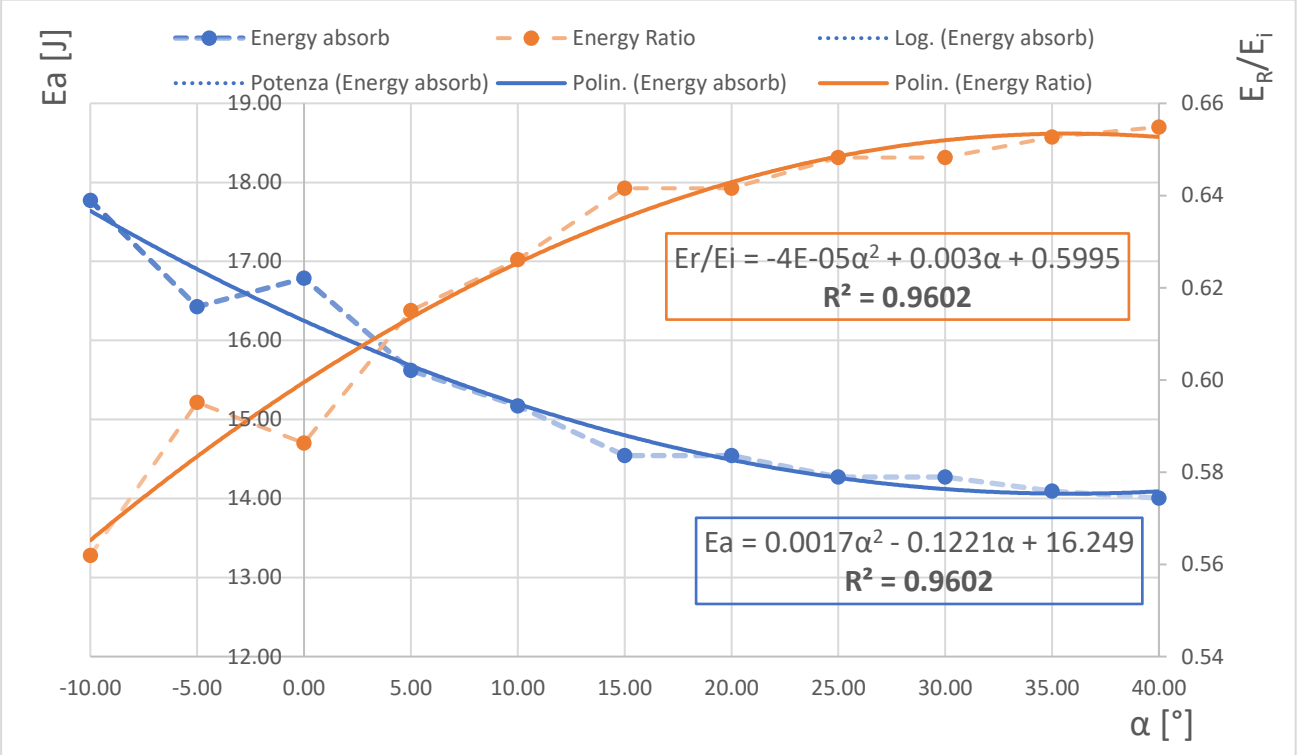

Figure 6.2.1: Energy absorbed for each angle (blue line) and energy ratio between energy of rebound and the initial energy compared with the variation of the field angles (orange line).

In Figure 6.2.1 is possible to see that the absorption of energy tends to reduce when the angle increases. This means that the prosthesis seems to release more energy and to give to the athlete more pushing force.

During the drop tests was also possible to measure the forces at the ground in the global directions, Fx (Longitudinal) and Fy (Vertical), and the ground reaction forces, all applied at the CoP of the prosthesis. In this case, the GRFs reference frame rotate with the inclination of the ground, instead the Fx and Fy force are in the fixed Global Reference system, Figure 6.2.2.

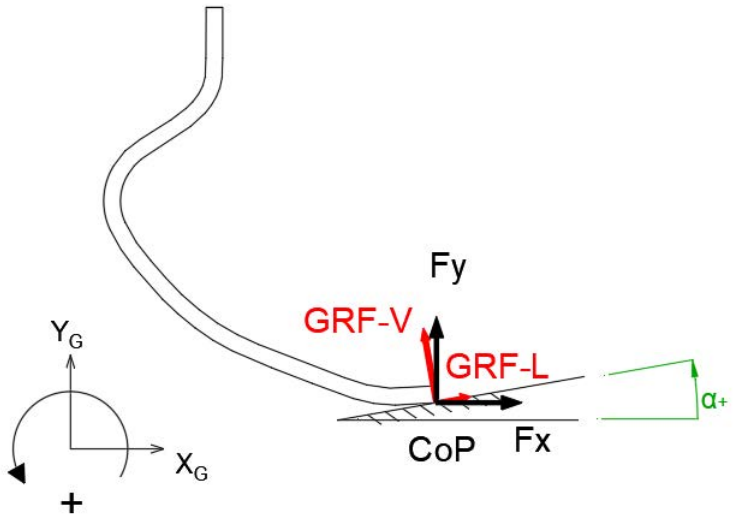

Figure 6.2.2: Forces acting at the Centre of Pressure (CoP)

In Figure 6.2.3 the trends for the Fx (blue) and Fy (orange) in correlation with the α angle are plotted:

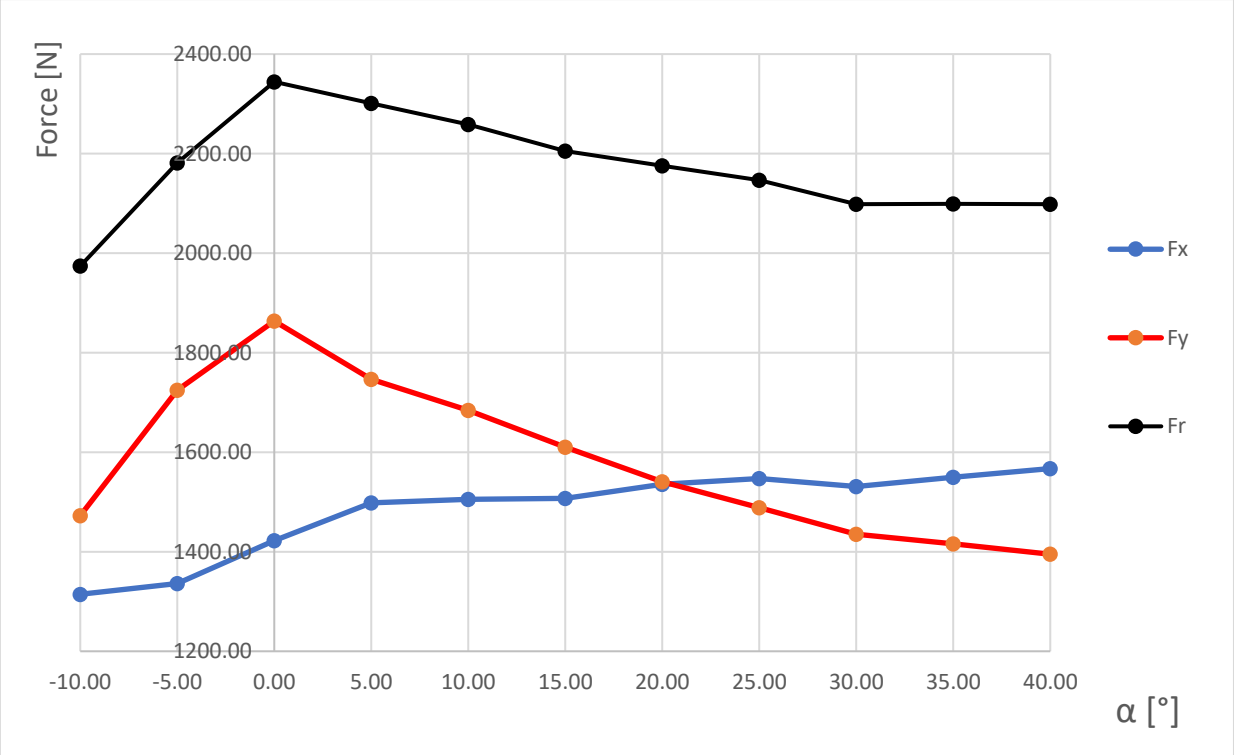

Figure 6.2.3: Trend of the Vertical, Longitudinal and Resultant forces (Fy, Fx and Fr) along the different field angles.

It is possible to see that the Fx, longitudinal force, is becoming higher when the angle is increasing, because the prosthesis tends to push longitudinally against the ground, in the Global reference system. Vice versa, from 0 to 40° and from 0 to -10°, the vertical force, Fy, is becoming softer.
These trends for the longitudinal and vertical force suggest an evaluation of the resultant force Fr, calculated in its value but not in its direction. In Figure 6.2.3, the trend of the resultant force Fr is plotted with the black curve.
It has the peak value for 0 degrees, when the direction of fall is orthogonal to the ground. When the angle increases, the force reduces until it reaches a plateau about 30°. The reduction could be due to the dissipation of energy by the tartan layer, this could be analyzed by replacing it with a steel, wood or aluminum smooth surface.

To complete the evaluation of the force component, the GRFs compared with the angles are showed in Figure 6.2.4:

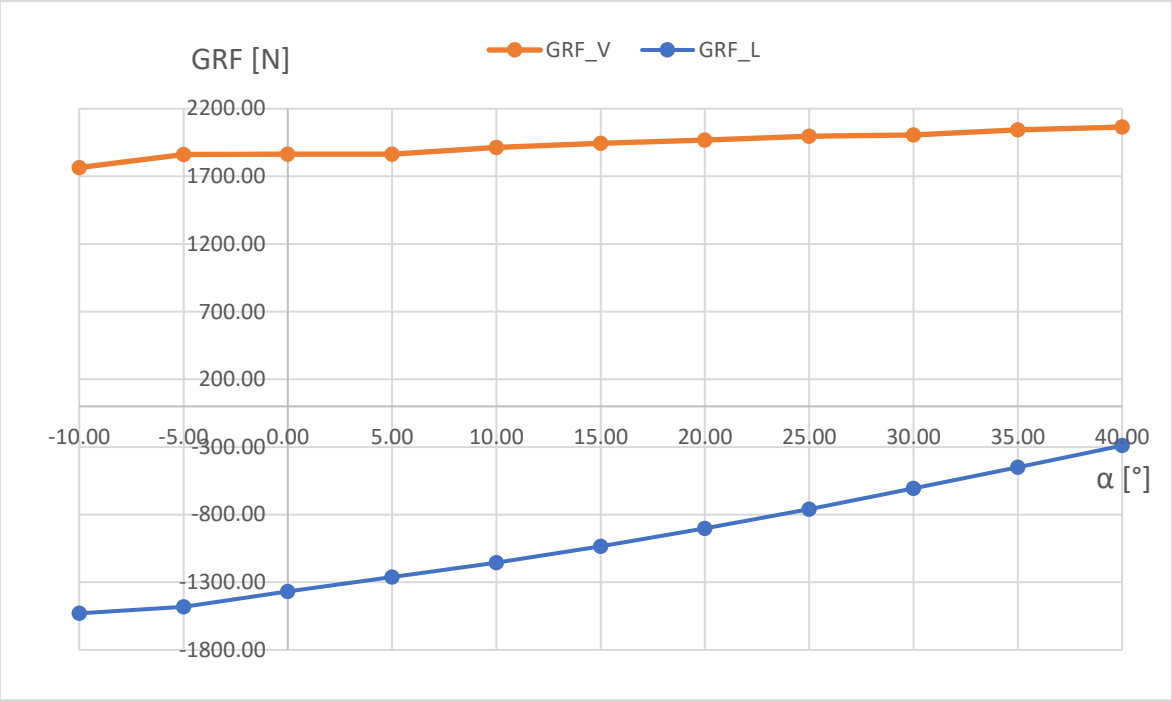

Figure 6.2.4: Relation between GRFs and angles

It is possible to see that the vertical component (GRF_V) is always increasing with the angle, instead the longitudinal component is always decreasing until almost to zero for an angle bigger than 40°.

A further analysis for this dropping test could be add more weight to the vertical sledge for simulate the body weight of the athlete and also evaluate the amount of energy dissipated only by the RSP, without the contribute of tartan and friction dissipations.
Also the evaluation of the forces acting at the foot clamp, against the socket could be interesting.

Another type of test should be a dynamic test, with a rotation of the floor while applying vertical and horizontal forces with the actuators, where forces and angles are taken from the in-vivo analysis.

BIBLIOGRAPHY

[1] VENTURA, Jonathan; SHVO, Galit. Yellow as “Non-Black”: Prosthetics, Semiotics, Hermeneutics, Freedom and Function. The Design Journal, 2017, 20.sup1: S4652-S4670.

[2] STAROS, Anthony. The SACH (solid-ankle cushion-heel) foot. Ortho Pros Appl J, 1957, 23-31.

[3] https://www.thecanadianencyclopedia.ca/en/article/terry-fox-and-the-development-of-running-prostheses/

[4] HOBARA, Hiroaki. Running-specific prostheses: The history, mechanics, and controversy. Journal of the Society of Biomechanisms, 2014, 38.2: 105-110.

[5] Grabowski, A. M., McGowan, C. P., McDermott, W. J., Beale, M. T., Kram, R. & Herr, H. M. 2010 Running-specific prostheses limit ground-force during sprinting. Biol. Lett. 6, 201–204. (doi:10.1098/rsbl.2009.0729)

[6] Weyand, P. G., Bundle, M. W., McGowan, C. P., Grabowski, A., Brown, M. B., Kram, R. & Herr, H. 2009 The fastest runner on artificial legs: different limbs, similar function? J. Appl. Physiol. 107, 903–911. (doi:10.1152/japplphysiol.00174.2009)

[7] Alexander, R. M. 1992 A model of bipedal locomotion on compliant legs. Phil. Trans. R. Soc. Lond. B 338, 189–198. (doi:10.1098/rstb.1992.0138)

[8] Blickhan, R. 1989 The spring–mass model for running and hopping. J. Biomech. 22, 1217–1227. (doi:10.1016/ 0021-9290(89)90224-8)

[9] Blickhan, R. & Full, R. J. 1993 Similarity in multilegged locomotion: bouncing like a monopode. J. Comp. Physiol. A 173, 509–517.

[10] Farley, C. T., Glasheen, J. & McMahon, T. A. 1993 Running springs: speed and animal size. J. Exp. Biol. 185, 71–86.

[11] McMahon, T. A. & Cheng, G. C. 1990 The mechanics of running: how does stiffness couple with speed? J Biomech. 23 (Suppl 1), 65–78. (doi:10.1016/0021-9290(90)90042-2)

[12] Farley, C. T., Blickhan, R., Saito, J. & Taylor, C. R. 1991 Hopping frequency in humans: a test of how springs set stride frequency in bouncing gaits. J. Appl. Physiol. 71, 2127–2132.

[13] Aruin, A. S.: Sports after amputation, Biomechanics in sport: performance enhancement and injury prevention, 637-650, (2000).

[14] ALEXANDER, R. McNeil. Energy-saving mechanisms in walking and running. Journal of Experimental Biology, 1991, 160.1: 55-69.

[15] SAIBENE, F. P.; MARGARIA, R. Mechanical work in running. J. appl. Physiol, 1964, 19: 249-256.

[16] CZERNIECKI, Joseph M.; GITTER, Andrew; MUNRO, Carolyn. Joint moment and muscle power output characteristics of below knee amputees during running: the influence of energy storing prosthetic feet. Journal of biomechanics, 1991, 24.1: 67-75.

[17] NOLAN, Lee. Carbon fiber prostheses and running in amputees: a review. Foot and ankle surgery, 2008, 14.3: 125-129.

[18] BRÜGGEMANN, Gert-Peter, et al. Biomechanics of double transtibial amputee sprinting using dedicated sprinting prostheses. Sports Technology, 2008, 1.4-5: 220-227.
[19] MAKIMOTO, Atsushi, et al. Ground reaction forces during sprinting in unilateral transfemoral amputees. Journal of applied biomechanics, 2017, 33.6: 406-409.
[20] BECK, Owen N.; TABOGA, Paolo; GRABOWSKI, Alena M. Characterizing the mechanical properties of running-specific prostheses. PloS one, 2016, 11.12: e0168298.
[21] MCGOWAN, Craig P., et al. Leg stiffness of sprinters using running-specific prostheses. Journal of The Royal Society Interface, 2012, rsif20110877.
[22] DYER, Bryce TJ; SEWELL, Philip; NOROOZI, Siamak. An investigation into the measurement and prediction of mechanical stiffness of lower limb prostheses used for running. Assistive Technology, 2014, 26.3: 157-163.
[23] NISHIKAWA, Yasuhiro; HOBARA, Hiroaki. Mechanical stiffness of running-specific prostheses in consideration of clamped position. Mechanical Engineering Letters, 2018, 4: 17-00452-17-00452.
[24] ISO, ISO. 10328: Prosthetics–Structural testing of lower-limb prostheses–Requirements and test methods. 2006.
[25] Gianfabio Costa, Design and construction of a multichannel bench test for running specific prostheses, 2018

APPENDIX

Appendix “A”: RSPs calibration and validation

1E91 Runner SPR-3-S-N (ottobock)

This prosthesis was used by Contraffatto Monica

Calibration tables:

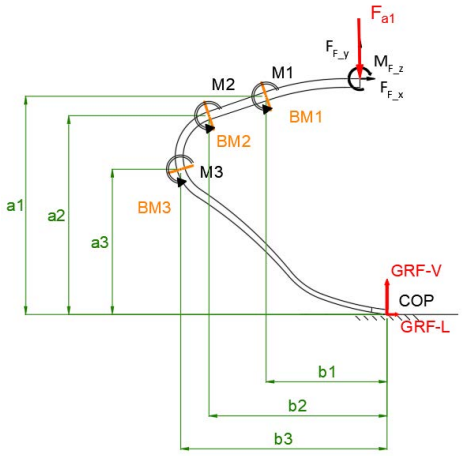

free to move_horizontal_sledge						
F_{a1}	a1	b1	a2	b2	a3	b3
(N)	(mm)	(mm)	(mm)	(mm)	(mm)	(mm)
-300	299	46	286	107	205	172
-500	290	54	278	114	196	179
-700	282	64	270	124	186	187
-900	272	75	258	134	174	196
-1100	262	86	248	147	161	204
-1300	248	98	232	157	145	212
-1460	234	109	219	168	130	221

Load_Cell_3ax		
GRF-T	GRF-L	GRF-V
(N)	(N)	(N)
0	0	0
10.3882	-20.0662	306.369
9.95993	-8.93011	506.906
8.70584	-26.613	706.569
7.75559	-20.0502	919.634
18.775	-12.3159	1110.86
16.1693	-20.2782	1313.72
7.1895	-20.9135	1475.67

Moment acting on the RSP		
M1	M2	M3
(Nmm)	(Nmm)	(Nmm)
0	0	0
20092.77	38520.42	56809.04
29962.66	60269.85	92486.48
52725.28	94800.07	137078.4
74426.2	128403.9	183737
98760.73	166350.8	228598.3
133773.6	210958.6	281449
165741.8	252492.6	328841.8

For the data acquired by the SoMat, it is only reported the average values for each step of load:

Channel output SG bridges		
BM_1	BM_2	BM_3
(mV/V)	(mV/V)	(mV/V)
0	0	0
0.352723	0.610512	1.16399
0.530877	0.973259	1.90151
0.911972	1.54106	2.82873
1.27666	2.10981	3.80335
1.70131	2.72124	4.77291
2.2686	3.48417	5.89488
2.7832	4.15488	6.84001

With the values of the moments and of the channels, it is plotting the graph for the calibration:

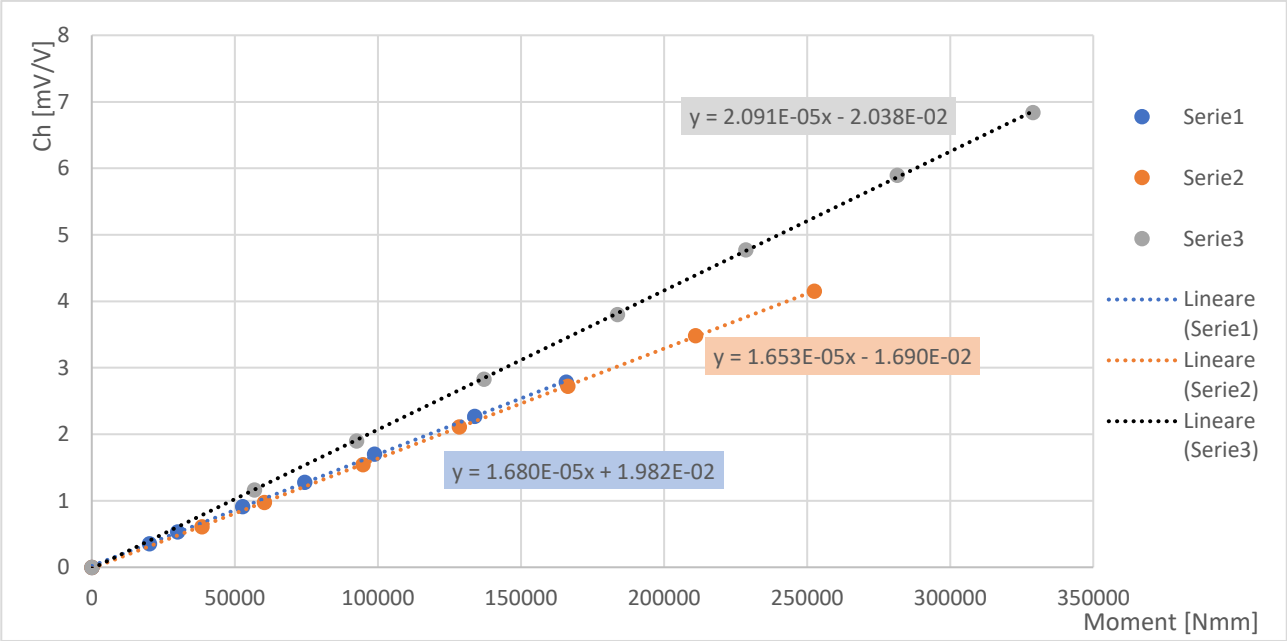

Figure 13: Relation between Moment and Channel output

From the slope of each curve it is find the sensitivity coefficient of every bridge:

- BM1: $Sensitivity\ coefficient = 1.680 * 10^{-5}$
- BM2: $Sensitivity\ coefficient = 1.653 * 10^{-5}$
- BM3: $Sensitivity\ coefficient = 2.091 * 10^{-5}$

The calibration coefficient calculated from the sensitivity values are:

- BM1: $C_1 = 5.952 * 10^4$
- BM2: $C_2 = 6.05 * 10^4$
- BM3: $C_3 = 4.782 * 10^4$

For a first evaluation of the calibration, it is calculated the forces acting at the foot clamp and its vertical component is compared with the vertical force read by the 3-axes force platform:

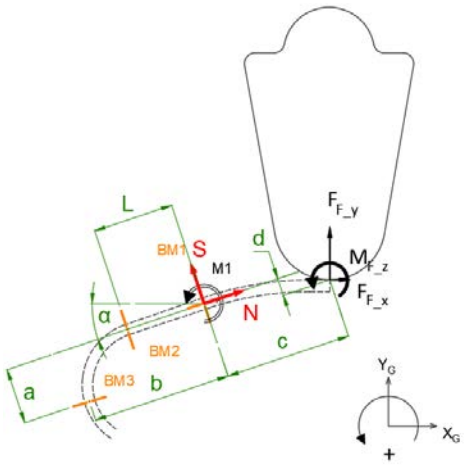

Data										
F_{a1}	M1	M2	M3	L	a	b	c	d	alpha	alpha
(N)	(Nmm)	(Nmm)	(Nmm)	(mm)	(mm)	(mm)	(mm)	(mm)	(°)	(rad)
0	0	0	0	60	73	148	69	8	11.8	0.206
-300	20092.77	38520.42	56809.04	60	73	148	69	8	11.8	0.206
-500	29962.66	60269.85	92486.48	60	73	148	69	8	12	0.209
-700	52725.28	94800.07	137078.4	60	73	148	69	8	11.9	0.208
-900	74426.2	128403.9	183737	60	73	148	69	8	12.4	0.216
-1100	98760.73	166350.8	228598.3	60	73	148	69	8	12.6	0.220
-1300	133773.6	210958.6	281449	60	73	148	69	8	13.1	0.229
-1460	165741.8	252492.6	328841.8	60	73	148	69	8	13.6	0.237

loadcell	shear	axial force	Forces on the foot clamp, on socket			
GRF-V	T	N	F_{F_y} (V)	F_{F_x} (L)	M_{F_z}	e%_V
(N)	(N)	(N)	(N)	(N)	(Nmm)	%
0	0	0	0	0	0	0
306.37	-307.13	-119.71	325.12	54.37	-22149.45	6.12
506.91	-505.12	-167.59	528.93	58.91	-36193.98	4.34
706.57	-701.25	-266.18	741.06	115.86	-50515.46	4.88
919.63	-899.63	-326.50	948.75	125.70	-64686.33	3.17
1110.86	-1126.50	-505.27	1209.59	247.36	-81770.68	8.89
1313.72	-1286.42	-585.13	1385.56	278.33	-93443.80	5.47
1475.67	-1445.85	-697.06	1569.22	337.54	-105339.93	6.34

Table 2: Forces acting at the foot clamp and error calculation for vertical force, during calibration

Validation tables:

For the data acquired by the SoMat, it is only reported the average values for each step of load:

Channel output SG bridges		
BM_1	BM_2	BM_3
(mV/V)	(mV/V)	(mV/V)
0.0	0.0	0.0
0.030081	0.296114	0.87428
-0.19512	0.266894	1.2843
-0.41512	0.245072	1.705
-0.63695	0.221494	2.12853
-0.87091	0.191837	2.56887
-1.09552	0.163709	3.00944
-1.29328	0.130877	3.37827

From these values, it is calculated the forces acting at the foot clamp and its vertical and longitudinal components are compared with the vertical and longitudinal ground reaction forces read by the 3-axes force platform:

Data										
F_{a1}	M1	M2	M3	L	a	b	c	d	alpha	alpha
(N)	(Nmm)	(Nmm)	(Nmm)	(mm)	(mm)	(mm)	(mm)	(mm)	(°)	(rad)
0	0	0	0	60	73	148	69	8	11.8	0.205949
-300	1790.524	17913.73	41811.57	60	73	148	69	8	11.8	0.205949
-500	-11614.5	16146.04	61420.37	60	73	148	69	8	12	0.20944
-700	-24709.6	14825.89	81539.93	60	73	148	69	8	11.9	0.207694
-900	-37913.5	13399.52	101794.8	60	73	148	69	8	12.4	0.216421
-1100	-51839.6	11605.38	122853.7	60	73	148	69	8	12.6	0.219911
-1300	-65209.5	9903.751	143923.5	60	73	148	69	8	13.1	0.228638
-1460	-76981	7917.544	161562.4	60	73	148	69	8	13.6	0.237365

Loadcell		shear	axial force	Forces at the foot clamp, on socket				
GRF-V	GRF-L	S	N	F_{F_y} (V)	F_{F_x} (L)	M_{F_z}	e%_V	e%_L
(N)	(N)	(N)	(N)	(N)	(N)	(Nmm)	%	%
0	0	0	0	0	0	0	0	0
300.2	-42.5	-268.72	3.43	262.34	-58.31	-18514.24	12.61	27.16
505.6	-126.0	-462.68	62.45	439.58	-157.28	-31425.05	13.05	19.89
709.6	-208.8	-658.92	119.57	620.11	-252.87	-44509.23	12.61	17.42
910.1	-294.6	-855.22	179.95	796.62	-359.40	-57570.32	12.47	18.03
1116.5	-385.8	-1057.42	249.26	977.58	-473.92	-70967.67	12.44	18.60
1317.6	-477.5	-1251.89	326.76	1145.25	-602.00	-83766.17	13.08	20.68
1488.9	-559.0	-1414.97	399.00	1281.48	-720.53	-94441.26	13.93	22.41

Table 3: Validation table, error calculation for vertical and longitudinal forces

1E91 Runner SPR-4-S-N (ottobock)

Calibration tables:

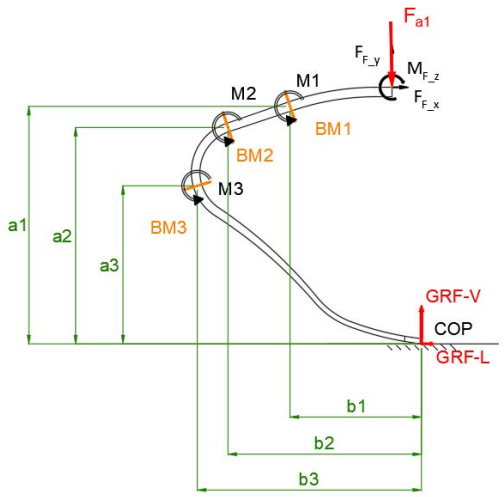

free to move_horizontal_sledge						
F_{a1}	a1	b1	a2	b2	a3	b3
(N)	(mm)	(mm)	(mm)	(mm)	(mm)	(mm)
-300	298	54	285	119	220	173
-500	295	64	280	120	214	178
-700	289	66	275	126	207	183
-900	283	68	268	132	201	189
-1100	277	74	263	140	192	195
-1300	269	81	253	147	184	202
-1500	261	91	245	155	175	208

Load_Cell_3ax		
Fz	Fx	Fy
(N)	(N)	(N)
0	0	0
-3.7	-23.0	302.7
-7.0	-25.5	500.1
-9.4	-24.9	703.6
-11.6	-29.8	899.2
-11.5	-29.3	1102.7
-10.4	-24.3	1301.8
-9.1	-27.3	1501.6

Moment acting on the RSP		
M1	M2	M3
(Nmm)	(Nmm)	(Nmm)
0	0	0
23196.1	42571.41	57421.7
39517.69	67140	94463.64
53643	95509	133917.7
69578.02	126682.8	175944
89712.54	162083.5	220655.5
111987.2	197514.1	267432.1
143780.7	239443.6	317112.5

For the data acquired by the SoMat, it is only reported the average values for each step of load:

Channel output SG bridges		
BM_1	BM_2	BM_3
(mV/V)	(mV/V)	(mV/V)
0	0	0
0.276111	0.50521	0.779331
0.429811	0.808819	1.29003
0.654974	1.18036	1.86281
0.917709	1.582	2.45734
1.2185	2.02478	3.0945
1.53477	2.47687	3.74826
1.92708	3.00015	4.45151

With the values of the moments and of the channels, it is plotting the graph for the calibration:

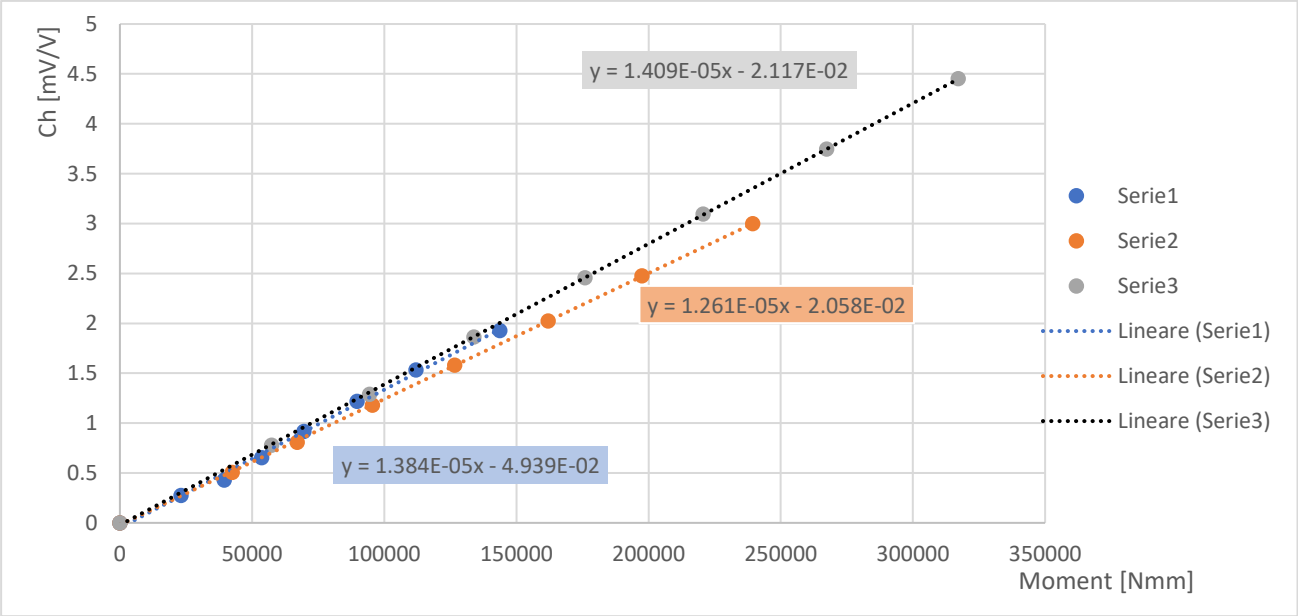

Figure 14: Relation between Moment and Channel output

From the slope of each curve it is find the sensitivity coefficient of every bridge:

- BM1: $Sensitivity\ coefficient = 1.384 * 10^{-5}$
- BM2: $Sensitivity\ coefficient = 1.261 * 10^{-5}$
- BM3: $Sensitivity\ coefficient = 1.409 * 10^{-5}$

The calibration coefficient calculated from the sensitivity values are:

- BM1: $C_1 = 7.225 * 10^4$
- BM2: $C_2 = 7.93 * 10^4$
- BM3: $C_3 = 7.097 * 10^4$

For a first evaluation of the calibration, it is calculated the forces acting on the foot clamp and its vertical component is compared with the vertical force read by the 3-axes force platform:

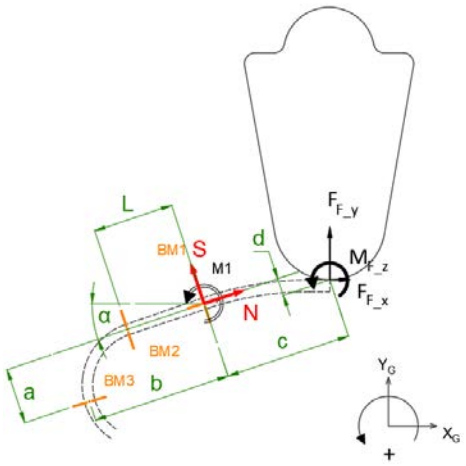

Data										
F_{a1}	M1	M2	M3	l	a	b	c	d	alpha	alpha
(N)	(Nmm)	(Nmm)	(Nmm)	(mm)	(mm)	(mm)	(mm)	(mm)	(°)	(rad)
0	0	0	0	68	60	141	65	7	11.7	0.204204
-300	19950.22	40064.23	55310.93	68	60	141	65	7	11.7	0.204204
-500	31055.71	64141.08	91556.42	68	60	141	65	7	11.9	0.207694
-700	47324.71	93605.08	132207.95	68	60	141	65	7	11.8	0.205949
-900	66308.45	125455.99	174403.12	68	60	141	65	7	12.3	0.214675
-1100	88041.91	160569.39	219623.85	68	60	141	65	7	12.5	0.218166
-1300	110893.79	196421.09	266022.71	68	60	141	65	7	13	0.226893
-1500	139239.88	237918.32	315934.00	68	60	141	65	7	13.5	0.235619

loadcell	shear	axial force	Forces at the foot clamp			
GRF-V	T	N	F_{F_y} (V)	F_{F_x} (L)	M_{F_z}	e%_V
(N)	(N)	(N)	(N)	(N)	(Nmm)	%
302.68	-295.79	-105.77	311.10	43.59	-19967.04	2.78
500.077	-486.55	-135.05	503.94	31.82	-32571.05	0.77
703.585	-680.59	-184.67	703.98	41.59	-45531.30	0.06
899.243	-869.82	-242.49	901.51	51.63	-58235.52	0.25
1102.74	-1066.58	-313.43	1109.14	75.15	-71521.76	0.58
1301.76	-1257.75	-370.24	1308.80	77.82	-84345.73	0.54
1501.57	-1451.15	-465.31	1519.68	113.69	-97582.14	1.21

Table 4: Forces acting at the foot clamp and error calculation for vertical force, during calibration

Validation tables:

For the data acquired by the SoMat, it is only reported the average values for each step of load:

Channel output SG bridges		
BM_1	BM_2	BM_3
(mV/V)	(mV/V)	(mV/V)
0.00	0.00	0.00
0.007	0.255	0.566
-0.124	0.305	0.866
-0.207	0.400	1.212
-0.281	0.501	1.563
-0.417	0.540	1.858
-0.562	0.581	2.172
-0.687	0.637	2.493

From these values, it is calculated the forces acting on the foot clamp and its vertical and longitudinal components are compared with the vertical and longitudinal ground reaction forces read by the 3-axes force platform:

Data										
F_{a1}	M1	M2	M3	l	a	b	c	d	alpha	alpha
(N)	(Nmm)	(Nmm)	(Nmm)	(mm)	(mm)	(mm)	(mm)	(mm)	(°)	(rad)
300	498.11	20201.27	40169.84	68	60	141	65	7	11.4	0.198968
500	-8990.82	24170.26	61444.71	68	60	141	65	7	10.9	0.190241
700	-14946.53	31704.52	86029.10	68	60	141	65	7	10.3	0.179769
900	-20308.09	39734.58	110911.99	68	60	141	65	7	9.8	0.171042
1100	-30113.66	42831.72	131850.25	68	60	141	65	7	9.4	0.164061
1300	-40619.80	46050.91	154161.11	68	60	141	65	7	8.8	0.153589
1500	-49624.93	50521.57	176938.25	68	60	141	65	7	8.4	0.146608

Loadcell		shear	axial force	Forces at the foot clamp, on the socket				
GRF-V	GRF-L	T	N	F_{F_y} (V)	F_{F_x} (L)	M_{F_z}	e%_V	e%_L
(N)	(N)	(N)	(N)	(N)	(N)	(Nmm)	%	%
302.17	47.70	-289.75	-19.72	287.93	-37.94	-18971.96	4.71	20.46
506.31	118.11	-487.66	27.92	473.59	-119.63	-31502.67	6.46	1.28
714.21	179.34	-686.04	70.72	662.34	-192.25	-44097.87	7.26	7.20
917.04	236.81	-882.98	112.00	851.03	-260.65	-56609.74	7.20	10.07
1115.08	312.94	-1072.73	178.49	1029.17	-351.30	-68477.75	7.70	12.26
1326.19	396.54	-1274.57	251.11	1221.15	-443.15	-81089.23	7.92	11.75
1529.20	475.56	-1472.74	315.11	1410.91	-526.87	-93522.51	7.74	10.79

Table 5: Validation table, error calculation for the vertical and longitudinal forces

Appendix “B”: MATLAB script

Forceplate data analysis

MATLAB script used for the forceplate data analysis of the in-vivo tests:

```
%% Import data
F=char(filename);
data_raw= load_data(F);
n=length(data_raw);

%Zero adjustment
for i=1:n
   data_fp(i,:)=data_raw(i,:)-mean(data_raw(1:100,:));
end
%Raw cut of the data
x=find(data_fp(:,4)>1.5);
xx=[1;x];
y_force=data_fp(xx,4);
x_force=data_fp(xx,3)*-1;
z_force=data_fp(xx,2);

%% Locations for validation
Loc_fp_cal=[round(0.010*length(y_force)),
round(0.10*length(y_force)),round(0.20*length(y_force)),round(0.30*length(y_force)),ro
und(0.40*length(y_force)),round(0.50*length(y_force)),round(0.60*length(y_force)),roun
d(0.70*length(y_force)),round(0.80*length(y_force)),round(0.90*length(y_force)),round(l
ength(y_force))] ;

% Forces for every 10% (for the validation)
n=11;
for i=1:n
Fy_cal(i,:)=y_force(Loc_fp_cal(:,i));
Fx_cal(i,:)=x_force(Loc_fp_cal(:,i));
end

%% Time axis
Fs_fp=1000; %sample frequency
dt_fp=1/Fs_fp;
t_fp=dt_fp*(0:length(y_force)-1);
```

Somat data analysis

```
%% Dataselection
x=find(BM_3>max(BM_3)*0.5); %Treshold, all data below x is removed
 %Selecting only the sprint part and zero adjustment
BM_1x=BM_1(x(1):x(end))-bias(:,1);
BM_2x=BM_2(x(1):x(end))-bias(:,2);
BM_3x=BM_3(x(1):x(end))-bias(:,3);
 %% Calibration coefficients
p1=5.92*10^4;
p2=6.04*10^4;
p3=4.81*10^4;

%% Calculations of Moments
M1=BM_1x*p1;
M2=BM_2x*p2;
M3=BM_3x*p3;
%% Calculations force at BM1
l=60;
a=73;
b=148;
c=69;
d=8;
alfa=8;
S=-(M2-M1)/l; %Orthogonal, shearforce
N=(M3+S *b-M1)/a; %Angular force
%% Forces acting at the foot clamp
Fy_F=-S*cosd(alfa)-N*sind(alfa);
Fx_F=-S*sind(alfa)+N*cosd(alfa);

%% Filter data to select 8th step
Fs=5000; %sample frequency
f_co=30; %cut-off frequency
[B, A] = butter(2, (2 * f_co / Fs)); %2nd order low-pass butterworth filter
data_filt_y = filtfilt(B, A, Fy_s);
data_filt_y_inv = 1.01*max(data_filt_y) - data_filt_y;

%% Select location of the peaks
max_value_y=max(data_filt_y);
[~,locsy]=findpeaks(data_filt_y,'MinPeakHeight',(max_value_y/2)); %location max peak
[~,MinIdx_1] =findpeaks(data_filt_y_inv); %location min peak

point_start=find(MinIdx_1<locsy(FP_hit),1,'last');
point_end=find(MinIdx_1>locsy(FP_hit),1,'first');
t_start=MinIdx_1(:,point_start);
t_end=MinIdx_1(:,point_end);

%% Full forces one step
Fy_som=Fy_s(t_start:t_end);
Fx_som=Fx_s(t_start:t_end);
F_som=[Fy_som;Fx_som];
```

Appendix “C”: Vocabulary

abduction: Motion of a limb or body part away from the median plane of the body. The resulting effect can cause problems with proper gait and/or ambulation and may prolong the rehabilitation process, especially in cases of lower extremity limb loss—adduction is its opposite.

AK (above-the-knee): A specific level of amputation—also known as **transfemoral**.

alignment: The position of the prosthetic socket in relation to the foot and knee.

amputation: The cutting off of a limb or part of a limb.

anterior: The front portion of a shoe or foot.

bilateral amputee: A person who is missing or has had amputated both arms or both legs. For example, a person that is missing both legs below-the knee is considered a bilateral BK.

biomechanics: Applying mechanical principles to the study of human movement; or the science concerned with the action of forces on the living body.

BK (below-the-knee): A specific level of amputation—also known as transtibial.

bumper: Rubber like, polymer based devices that are available in varying degrees of density, depending on an amputee’s desired level of stiffness in a prosthetic knee or heel. As with other prosthetic componentry, basic maintenance or replacement may be required as a result of wear and tear.

C-Leg: The Otto Bock C-Leg features a swing and stance phase control system that senses weight bearing and positioning to provide the knee’s microprocessor information about the amputee’s gait, thus promoting smoother ambulation. The outer shell houses a hydraulic cylinder, microchip, and rechargeable battery.

check or test socket: A temporary socket, often transparent, made over the plaster model to aid in obtaining proper fit and function of the prosthesis.

contralateral: Originating in or affecting the opposite side of the body.

definitive, or **permanent prosthesis**: The definitive prosthetic replacement for the missing limb or part of a limb, meeting standards for comfort, fit, alignment, function, appearance and durability.

distal: (1) The end of the residual limb. (2) The end that is farthest from the central portion of the body. Distal is the opposite of **proximal**.

donning and doffing: Putting on and taking off a prosthesis, respectively.

dorsiflexion: An upward movement or extension of the foot/toes or the hand/fingers.

functional prosthesis: Designed with the primary goal of controlling an individual’s anatomical function, such as providing support or stability or assisting ambulation.

gait: A manner of walking that is specific to each individual.

kinesiology: The study of muscles and human movement.

lateral: To the side, away from the median plane of the body.

Liner (roll-on liner): Suspension systems used to hold the prosthesis to the residual limb and to provide additional comfort and protection for the residual limb. Roll-on liners can also accommodate volumetric changes in the residual limb. These liners may be made of silicon, pelite, or gel substances.

gait: A manner of walking that is specific to each individual.

kinesiology: The study of muscles and human movement.

lateral: To the side, away from the median plane of the body.

Liner (roll-on liner): Suspension systems used to hold the prosthesis to the residual limb and to provide additional comfort and protection for the residual limb. Roll-on liners can also accommodate volumetric changes in the residual limb. These liners may be made of silicon, pelite, or gel substances.

neuroma: When a nerve is severed during amputation, the nerve endings form a mass (neuroma) reminiscent of a cauliflower shape. Neuromas can be troublesome, especially when they are in places that are subject to pressure from the socket. They can also cause an amputee to experience sensory phenomena in or around the residual limb, which can be aggravating and/or painful.

nylon sheath: A sock interface worn close to the skin on the residual limb to add comfort and deter perspiration.

pistoning: Refers to the residual limb slipping up and down inside the prosthetic socket while walking.

plantarflexion: When the toe/foot is pointing down, away from the median plane of the body.

ply: In this context, it refers to the thickness of stump sock material. The higher the ply number, the thicker the sock.

prosthesis: An artificial limb, usually an arm or a leg, that provides a replacement for the amputated or missing limb. Prostheses is plural.

prosthetics: The profession of providing those with limb loss or with a limb difference (congenital anomaly) a functional and/or cosmetic restoration of missing or underdeveloped human parts.

pylon: A rigid member, usually tubular, between the socket or knee unit and the foot that provides a weight bearing, shock-absorbing support shaft for the prosthesis.

quad socket: A socket designed for an AK amputee that has four distinctive sides. The design allows the muscles to function as much as possible as it works to improve the AK

amputee's ability to control knee function. The distal end of the socket should match the shape and size of the residual limb and should provide secure contact, alleviating edema and other skin problems.

residual limb: The portion of the arm or leg remaining after an amputation, sometimes referred to as a stump or residuum.

SACH foot (Solid-Ankle Cushion Heel): The foot is made of wood with a flexible rubber shell that surrounds the wooden core. The SACH foot is usually prescribed to moderately active or less active amputees, but can be prescribed to amputees of all activity levels. SACH feet are also used in the design of foreshortened prostheses, or stubbies.

socket: The portion of the prosthesis that fits around and envelopes the residual limb and to which the prosthetic components are attached.

stance control knee: These prosthetic knee joints typically offer a weight-activating friction brake that locks the knee into place during pivotal points of ambulation, offering stability and balance where needed.

stump: A word commonly used to refer to the residual limb.

suction socket: Mainly for use by AK level amputees, this socket is designed to provide suspension by means of negative pressure vacuuming. This is achieved by forcing air out of the socket through a one-way valve when donning and using the prosthesis. In order for this type of socket to work properly, the soft tissues of the residual limb must precisely fit the contours of the socket. Suction sockets work very well for those whose residual limbs maintain a constant shape and size.

swing phase: This is when the prosthesis moves from full flexion to full extension. The term is usually used in reference to prosthetic knee units.

transmetatarsal amputation: An amputation through the metatarsal section of the foot bone. (see partial foot amputation)

unilateral: An amputation that affects only one side of the body (opposite of bilateral).